ETC-DI Report 2024/4

Specification for calculating landscape fragmentation

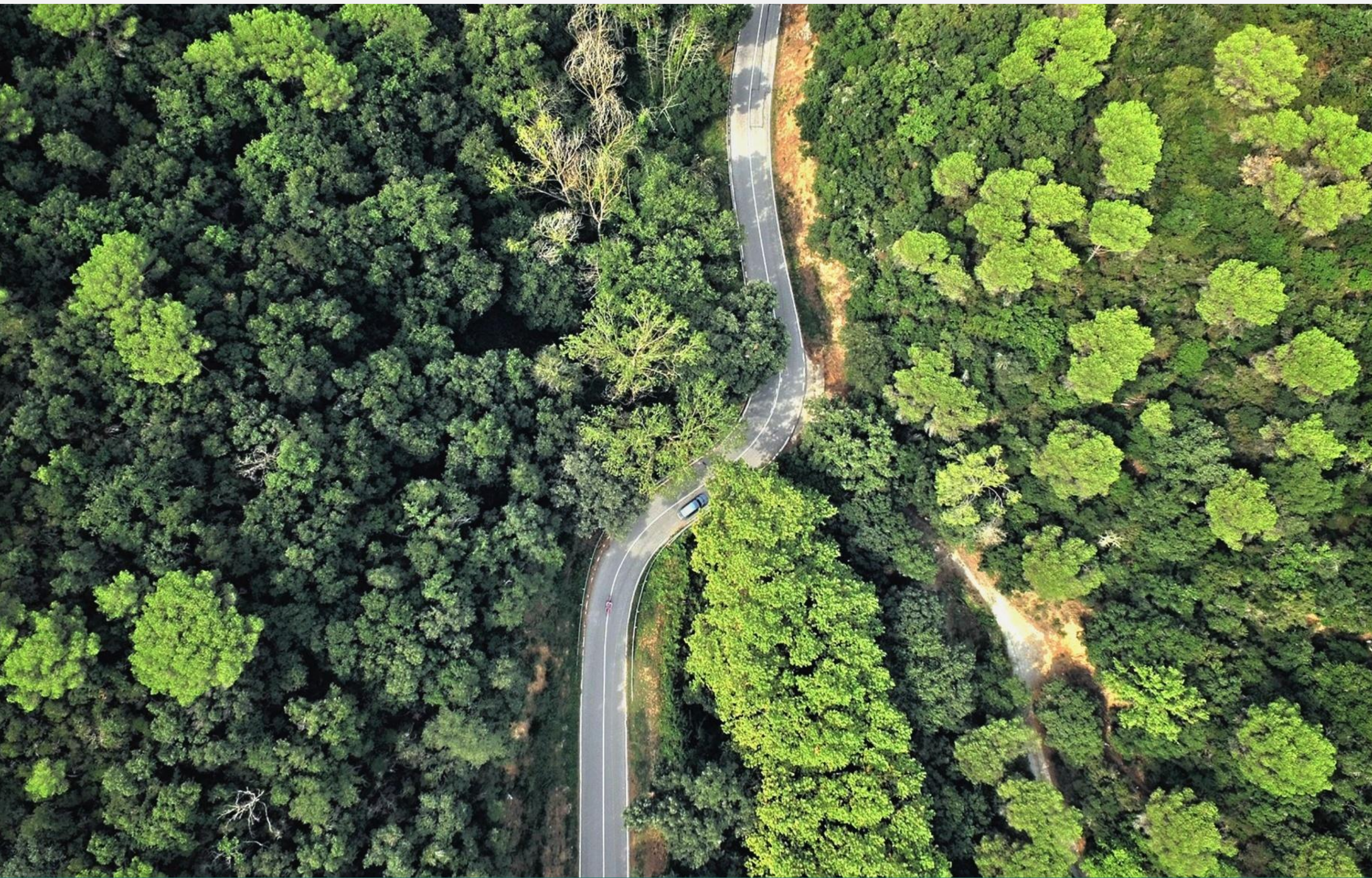

Authors:

Jaroslav Dufek (GISAT), Eva Ivits (EEA)

European Environment Agency
European Topic Centre
Data integration and digitalisation

Cover design: EEA

Cover image © https://treesforlife.org.uk/

Layout: ETC DI

Version: 1.0

Publication Date: 02.04.2025

ETC-DI coordinator: Umweltbundesamt GmbH (UBA) / Environmental Agency Austria (EAA)

ETC-DI partners: University of Malaga, Space4Environment Sarl, Universitat Autonoma de Barcelona, GISAT S.R.O., Epsilon-I, Sinergie, Lechner, Stiftelsen Norsk Institutt fof Luftforskning (NILU), Stichting Wageningen Research – Wageningen Environmental Research (WENR).

doi: 10.5281/zenodo.15124179

European Topic Centre on
Data integration and digitalisation (ETC-DI)
https://www.eionet.europa.eu/etcs/etc-di

Contents

Acknowledgments

The completion of this work was provided within Negotiated procedure N° EEA/DIS/R0/23/003 between the European Environment Agency (EEA) and European Topic Centre on Data Integration and Digitalisation (ETC DI) thanks to the financial support of the Service Level Agreement (SLA) between the Directorate-General for Regional and Urban Policy of the Commission (DG REGIO) and the EEA.

Summary

This report presents a detailed analysis of the spatial dynamics and temporal trends of landscape fragmentation across Europe, using the effective mesh size (meff) index alongside a non-cross boundary method in 1 km output grid.

Landscape fragmentation is primarily driven by human activities that alter land, dividing large, contiguous natural habitats into smaller, isolated patches. These drivers can vary widely depending on the region and the specific context. This study focuses on the expansion of built-up areas and transportation infrastructure development drivers. The spread of built-up areas into natural or semi-natural landscapes leads to the direct loss of habitats.

Transportation infrastructures dissect and fragment landscapes, creating barriers to wildlife movement and altering the integrity of ecological networks. The study confirms the increasing trend in landscape fragmentation driven by the expansion of the built-up areas and transportation infrastructure development and provides a detailed Europe-wide spatial-temporal assessment for the years 2012-2018.

Utilizing harmonized imperviousness data provided by EEA, and time series of the commercial TomTom® (previously known as TeleAtlas) MultiNet® data, the analysis provides a nuanced view of fragmentation patterns across the continent. Despite some inconsistencies in archived data, the results reveal a pronounced spatial heterogeneity, with Western European countries exhibiting higher fragmentation levels compared to the relatively intact landscapes of Northern Europe. Furthermore, landscape fragmentation is considered regarding the population at different spatial units (NUTS0, NUTS3, LAU) and different urbanization types (DEGURBA). The highly fragmented and densely populated regions like the Netherlands or Malta are characterized by low fragmentation per capita as a large population shares the fragmented landscape.

The analysis offers valuable insights into the geospatial distribution of landscape fragmentation, emphasizing the need for standardized spatial units in landscape analyses and the importance of addressing data inconsistencies for more accurate interpretation.

Background, scope and objectives

This document is deliverable report of task 2, called “Landscape fragmentation” under the REGIND project concluded between the EEA and ETC DI based on the Negotiated procedure N° EEA/DIS/R0/23/003. The work that is covered by this contract was executed within the overall framework of a Service Level Agreement (SLA) which has been signed end of 2021 between the Directorate-General for Regional and Urban Policy of the Commission (DG REGIO) and the EEA. The overall aim of the SLA is the support of DG REGIO by the EEA in implementing “Regional and urban environmental indicators and analysis” by addressing regional and urban land use, and various aspects of air pollution in Europe.

Landscape fragmentation, a significant issue addressed in the European Green Deal, involves the disruption of continuous land, primarily caused by the expansion of built-up areas and transportation networks. This process has profound effects on the environment, leading to reduced resilience of habitats, a decline in their ability to support diverse ecosystems and provide ecosystem services, and contributing to biodiversity loss. It's a critical aspect of environmental challenges in the European Union, particularly under the Biodiversity Strategy for 2030 (BDS 2030). Fragmentation not only impacts biodiversity but also alters land use patterns, affecting natural and agricultural lands and potentially influencing their carbon sequestration capacity.

To measure and analyse landscape fragmentation, a variety of metrics exist. However, there's a lack of consistency in addressing different phases of fragmentation. The European Environment Agency (EEA) has developed operational indices to measure 'Landscape fragmentation pressure from built-up and transport infrastructure expansion' (identified as LSI 004 and CSI 054). These indices are based on methodologies developed at ETH Zurich by Jaeger in the early 2000s, focusing on the effective mesh size (meff) and effective mesh density (seff). This approach utilizes data from the Copernicus Land Monitoring Service (CLMS), which provides built-up area information, and integrates it with commercial data from the TomTom® MultiNet® on European transport networks. The quality and coherence of both spatial and temporal data are crucial for accurate measurement.

The indices meff and seff allow for the comparison of landscape fragmentation across Europe and provide the ability to track trends and dynamics over time. The methodologies underwent revisions in line with suggestions from DG REGIO. These revisions involved calculating effective mesh size values without the Cross-Boundary Calculation (CBC) to reduce the influence of large unfragmented areas and focusing solely on the Meff measure to avoid issues with infinite values in seff (Moser et al., 2007).

1 Introduction

Fragmentation of the landscape is a process in which an originally integral part of the landscape - large, contiguous habitats - is divided into smaller segments that are bounded by impermeable anthropogenic barriers such as transport infrastructure or buildings (Jaeger, 2000; Figure 1). Fragmentation of the landscape is a serious problem for nature conservation, as it reduces biodiversity and, by limiting the size and connectivity of natural habitats, leads to an overall reduction in the ecological stability of the landscape. The effects of small and isolated patches on ecological stability and habitat connectivity are frequently discussed environmental issues and are described in detail in the Theory of Island Biogeography and Metapopulation Theory (MacArthur and Wilson, 1967; Hanski, 1999). Supporting the ecological stability of the landscape, monitoring changes over time, and reducing the negative impacts of landscape fragmentation are therefore frequent goals of studies and environmental policies. Efforts aimed at reducing the negative ecological impacts of landscape fragmentation and protecting biogeographically valuable localities at the pan-European level include elements of green infrastructure in the form of bio-centers and bio-corridors, particularly within the NATURA2000 protected areas system.

Landscape fragmentation is primarily driven by human activities, but these drivers can vary widely depending on the region and the specific socioeconomic and environmental contexts. This study focuses on the expansion of built-up areas and transportation infrastructure development drivers. The spread of built-up areas into natural or semi-natural landscapes leads to the direct loss of habitats. The expansion of built-up areas often results in permanent changes to land cover, transforming ecosystems into built environments. Roads, highways, railways, and other transportation infrastructures dissect and fragment landscapes, creating barriers to wildlife movement and altering the integrity of ecological networks. These infrastructures can also facilitate further development and urban sprawl.

Addressing landscape fragmentation requires comprehensive analysis and monitoring using suitable indices that have been developed to measure and understand the extent and impact of landscape fragmentation. Effective mesh size (meff) is one such index that quantifies the degree of landscape connectivity by calculating the probability that two randomly chosen points within an area are connected without encountering a barrier. Utilizing the harmonized imperviousness time series developed in the REGIND project and time series of the TomTom MultiNet[1] data, this analysis provides a nuanced view of fragmentation patterns across the continent. This assessment aims to identify trends and patterns in landscape fragmentation, understand the underlying drivers, and support the development of strategies to mitigate fragmentation's negative effects. By highlighting areas of significant fragmentation and providing insights into regional differences, this study contributes to the broader goal of promoting ecological connectivity and landscape sustainability across Europe.

This task aims to perform a Europe-wide spatial-temporal assessment of landscape fragmentation using the meff index calculated by the non-CBC method with a 1 km output grid resolution in the territory of the EEA38+UK for the years 2012, 2015, and 2018.

[1] TomTom. MultiNet Product Documentation. www.tomtom.com/licensing

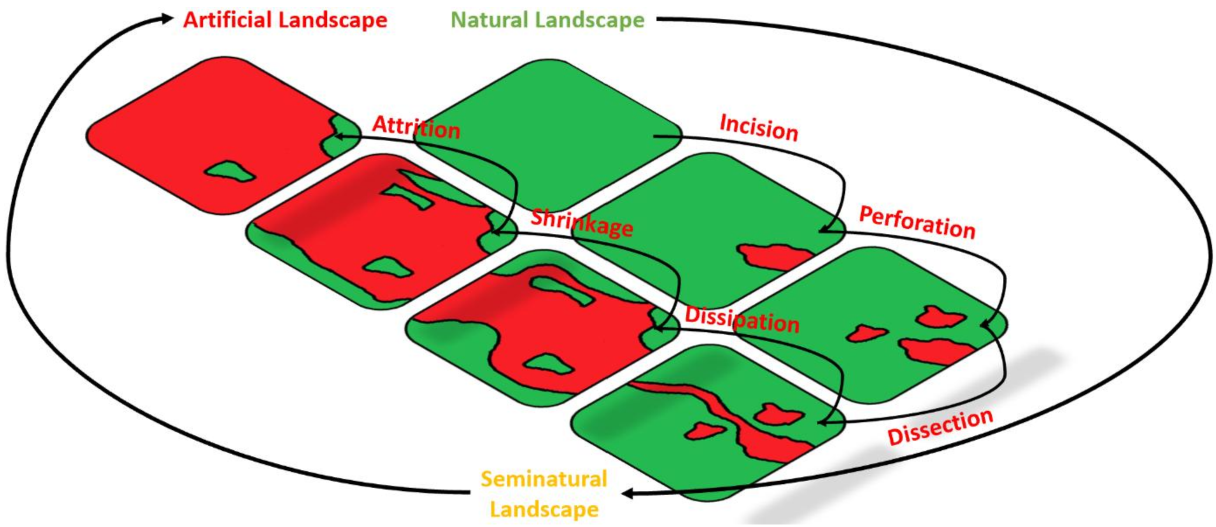

Figure 1: Phases of the fragmentation process, distinguished according to geometric characteristics, represent the transition from natural to artificial landscape by loss of habitats (based on Forman, 1995, modified).

2 Overview of selected landscape fragmentation indices

There is a variety of indices available for assessing landscape fragmentation. Commonly used tools include the Effective Mesh Size (meff), Effective Mesh Density (seff), and Average Patch Size (APS) indices (Gustafson, 1998; Jaeger, 2000; Moser et al., 2007; Table 1).

2.1 Effective Mesh Size (meff)

The meff measure is based on the probability that two points chosen randomly in an area are connected. This means that two randomly selected points must not be completely separated by the barriers of a fragmentation geometry such as transport routes or built-up areas. The more barriers in the landscape, the lower the probability that the two points can be connected, and the lower the effective mesh size. Hence, meff is a measure of landscape connectivity, i.e. the degree to which movements between different parts of the landscape are possible. The probability is converted into the size of a patch (meff) by multiplying it by the total size of the region investigated. Thus, the unit of meff is that of an area (e.g. km^2) and it can also be interpreted as the size of a continuous patch a point will be located in that is chosen randomly anywhere in the region, or as the ability of two randomly placed animals of the same species to find each other. The value of meff is between 0 (entirely fragmented or developed landscape) and the size of the entire region investigated (unfragmented). In addition, the meff index can be computed using cross-boundary (CBC) and non-cross-boundary (non-CBC) methods. The difference between these two calculation approaches (non-CBC and CBC) lies in how they account for fragmentation geometry and how these elements influence the fragmentation of the landscape calculation for analytical units.

The CBC approach is used to measure landscape fragmentation considering landscape patches extending beyond the boundaries of the reporting unit (e.g. a grid cell). This method is designed to account for connections within unfragmented patches that cross the boundaries of the unit being analyzed. For example, when calculating fragmentation for a specific region (e.g. NUTS0), the non-CBC approach focuses only on the fragmentation within the specified reference analytical unit without considering the influence of external boundaries or barriers. While the CBC method provides a more holistic measure of landscape connectivity for larger contiguous landmasses by including cross-boundary patches, it can overestimate fragmentation on small islands surrounded by sea or inland water bodies. This overestimation of the amount of fragmentation related to small islands occurs because of several factors. One reason is the specific boundary effects when small islands have more edges relative to their area (i.e. high perimeter-to-area ratio) where the CBC method includes the area outside the island's boundary as part of the calculation, treating the surrounding water as part of the landscape. The CBC method treats the edges (coastlines) as fragmentation barriers, even when they are not actual barriers to ecological connectivity within the island. For small islands, this disproportionately inflates the fragmentation metric and causes very high fragmentation values because the external boundary (coastline) artificially inflates the number of patches considered fragmented.

The non-CBC approach measures the fragmentation resulting from elements entirely contained within the area of interest, and the borders of selected reference analytical units have the same effect as other barriers (roads, railways, and buildings). For this reason, maximum meff non-CBC values can only reach the size of the selected reference unit, as opposed to the CBC procedure where the maximum value is potentially very large, e.g. an entire country. Furthermore, another difficulty with the CBC procedure is mathematical interpretability where the sun of the effective mesh size within e.g. a NUTS region may well be large than the NUTS region itself. While ecologically it is correct to state that species can travel through a NUTS region and enter another region without boundaries, the interpretation becomes difficult when summing these areas as the result can be larger than the region itself. For the above reasons the non-CBC calculation method for the meff is used in this work and thus is further described in the following methodology chapter in *3.4 Calculation and interpretation of the meff*.

2.2 Effective Mesh Density (seff)

While meff represents the size of an area that remains connected in terms of ecological continuity, seff represents the measure of the density of these connected areas or meshes (Figure 2). It indicates how fragmented a landscape is, with higher values showing higher fragmentation. Thus, seff represents the degree to which movement between different parts of the landscape is interrupted by a fragmentation geometry. Its values are represented by a number of meshes per selected area or reference unit (i.e., density). It is calculated as the inverse of the meff:

$$seff = \frac{1}{meff}$$

Because seff is calculated as the inverse of meff, any small value of meff will lead to a large value of seff. If meff is zero (or approaches zero), seff becomes infinite (or approaches infinity). This situation can arise in landscapes that are entirely developed (i.e., tiles without significant green areas), such as heavily urbanized areas or regions with extensive infrastructure development. Extremely high or even infinite values of seff can be illustrated by the following example below (Figure 2).

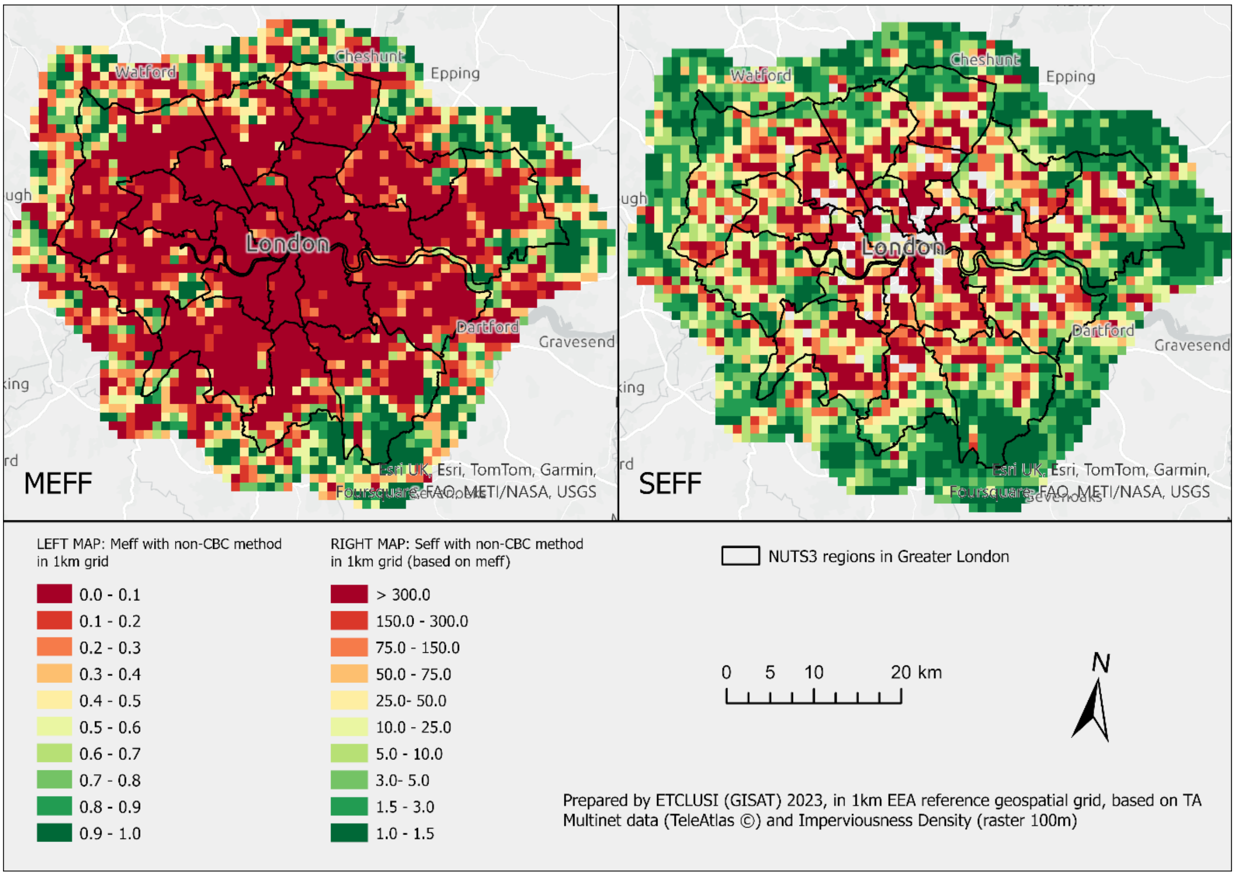

Figure 2: Comparison of different indices of landscape fragmentation - meff and seff, calculated using the non-CBC method - in the Greater London area. White (or empty pixels) in seff (map on the right) refer to pixels with very high fragmentation where meff=0 (central part of the city). The different visual output is caused by the different calculation methodology and especially the different classification of values.

The above example is from the region of Greater London, which represents an entirely developed landscape. In regions like this, the meff index calculated by the non-CBC method usually reaches very low values leading to extremely high values of seff or even values of seff equal to zero (infinity values). While the lowest possible seff values can be in this case equal to 1, there is no upper limit, and thus the only limiting factor is the number of decimal spaces in the computed meff values. For example, if the meff is equal to 0.00001, then the seff is 100000 meshes per km² (see the equations below):

$$seff = \frac{1}{meff} = \frac{1}{1} = 1\ mesh\ per\ km^2$$

$$seff = \frac{1}{meff} = \frac{1}{0.00001} = 100000\ meshes\ per\ km^2$$

$$seff = \frac{1}{meff} = \frac{1}{0} = \infty\ (infinity\ value)$$

2.3 Average Patch Size (APS)

The APS index is a straightforward metric that quantifies the distribution of patches according to their size. The APS is calculated by dividing the total area of all patches by the number of patches. However, APS does not consider the shape or configuration of patches, focusing solely on their size. More importantly, APS doesn’t behave consistently in all phases of landscape fragmentation, providing misleading signals for shrinkage and attrition (Figure 3). Shrinkage occurs when individual patches decrease in size due to factors like habitat degradation or land use change, reducing the overall area of patches without altering their number, while attrition happens when patches shrink and some disappear entirely, reducing both the number and total area of patches. This leads to significant habitat loss and fragmentation.

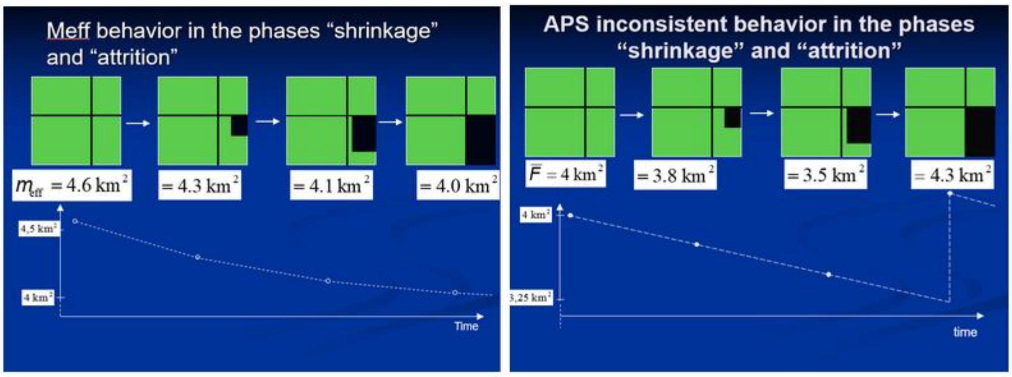

Figure 3: Meff and APS behaviour during the different phases of fragmentation (Jaeger, 2000).

Table 1: Comparison of basic characteristics of selected landscape fragmentation indices.

Index	Description	Key advantage	Key disadvantage
meff	Measures landscape connectivity based on probability of connection between points.	Clear connectivity measure on scale from 0 to 1.	No serious disadvantages.
seff	Measure landscape fragmentation. Inverse of meff, indicating patch density.	Complements meff, identifies highly fragmented areas	Infinite values in highly fragmented areas
APS	Measures average size of landscape patches.	Simple computation, size distribution insight.	Ignores shape/connectivity, potential misleading signals.

3 Methodology

3.1 Defining the area of interest

The area of interest of this study is the EEA38 (including 32 members and 6 cooperative countries) plus the United Kingdom (EEA38+UK) with an overall extent of approximately 5835060 km^2. To spatially cover the area of interest with all necessary inputs, the harmonized Imperviousness Density [2](IMD) 100m raster mask and reference overlapping 1 km tiles defined by the official EEA 1km tilling grid were used. The official EEA (European Environment Agency) gridding system is a reference spatial grid used for environmental data collection, reporting, and analysis across Europe. This grid system is designed to standardize the spatial representation of environmental data, making it easier to compare and integrate information across different European countries and regions.

Defining the area of interest that geometrically and spatially corresponds to the IMD extent was a logical step as the IMD raster was later used as one of the two main inputs to the fragmentation calculation process. The mask defined by the IMD extent contains the EEA38+UK territory. Additionally, the defined area of interest was covered by 250 km tiles which were used as working units for the optimized calculation process. This step ensured the maximum size of each tile which was processed at the same time in the computation to 62500 km^2.

3.2 Data Sources

The input data used for the calculation of landscape fragmentation using the meff index with the non-cross-boundary method can be divided into two groups according to what barrier to landscape fragmentation they represent. Therefore, these features can be referred to as fragmentation geometry.

The first group of input data includes Impervious Density Level (IMD) 100m rasters (Figure 4, Figure 5). These data are derived products from aggregation of the finer original CLMS High-Resolution Layer (HRL) IMD rasters, that provide detailed information on the human-made, artificial surfaces covered by impermeable materials across Europe. However, an inconsistency was detected in the original HRL IMD datasets regarding the continuity of time-series data due to an upgrade in the resolution of the HRL IMD data, from 20m to 10m observable between HRL IMD 2015 and 2018. This necessitated establishing new baselines for the years 2018 and 2021. Before a Europe-wide implementation, test productions were conducted in two selected areas. The choice of final input IMD data was influenced by the results of Task 1 ('Analysis of usability of Imperviousness vs. CLC+ backbone data for mapping sealed areas') in this contract. Thus, the European roll-out of landscape fragmentation and the extension of the meff time-series depended on the statistical harmonization activities conducted in Task 1. The input harmonized IMD 100m rasters were further tested and verified by statistical analysis and the calculation of landscape fragmentation in three selected areas on a total area of 187500 km^2 (southern Sweden, western Germany and central Spain; Maucha et al. 2024, Sannier et al. 2024). As an input, the TomTom MultiNet data from the same year was used to filter out the influence of the growing transport network and highlight the clear evolution of IMD.

The results of these tests confirmed that the evolution of newly harmonized IMD is consistent spatially and between all years and the evolution of meff responded adequately to the observed evolution in the harmonized IMD rasters (Appendix J, Appendix K). The set parameters for meff calculation brought a result which was visually identical to the previously provided test results on 10m IMD input data with fine and detailed fragmentation pattern with captured barrier effect of the roads. In addition, using

[2] EEA. Harmonized imperviousness time series. https://sdi.eea.europa.eu/catalogue/srv/eng/catalog.search#/metadata/b7a037c5-4c0a-47df-8d5d-17d0ce8e1fee

100m IMD showed a good cost-benefit ratio with a similar performance in fragmentation mapping as using 10m HRL IMD rasters with fine detail of fragmentation pattern across Europe with clearly captured barrier effects of the roads.

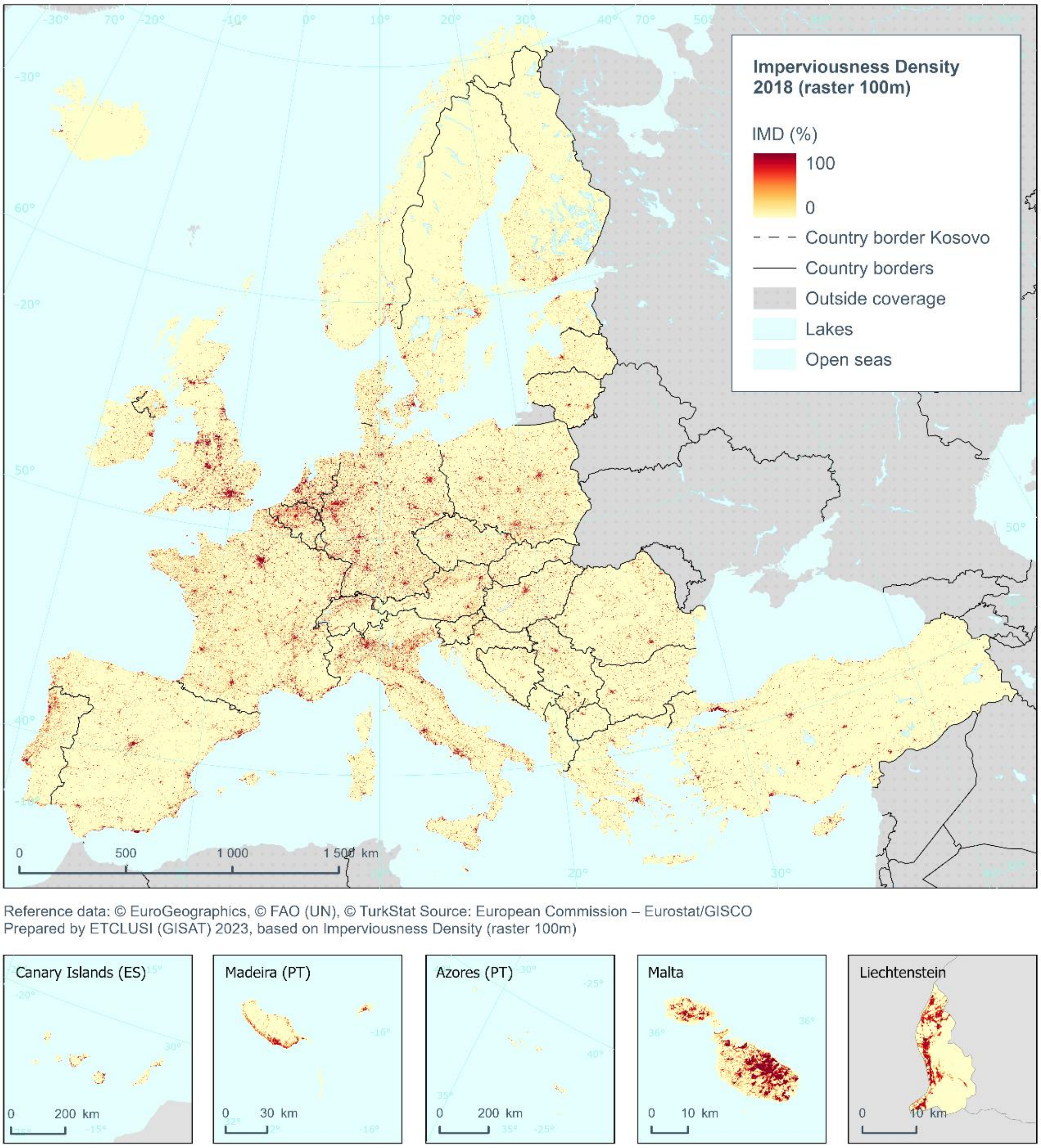

Figure 4: Distribution of imperviousness density over EEA38+UK countries expressed by harmonized IMD 100m.

The second group of input data includes the commercial vector datasets TomTom MultiNet (2012, 2015 and 2018) provided by Eurostat (Figure 5). The TomTom MultiNet is a comprehensive digital map database developed by TeleAtlas, now part of TomTom, a leading global provider of navigation and location-based services. MultiNet database is known for its detailed and accurate geographic information, covering road networks, routing attributes, points of interest (POIs), and various other layers that are essential for navigation, geographic information systems (GIS), and location-based services (LBS). From this dataset, two main types of linear transport networks were used - roads and railways. While the railway is considered a homogeneous linear layer with no further classification regardless of the importance of individual rails, the road layer is further divided into five categories according to importance - motorways, freeways, major roads less important than a motorway, other major roads, secondary roads, and local connecting roads (or tertiary roads). In addition, information on existing tunnels in these transportation segments is used for complementing fragmentation geometry creation.

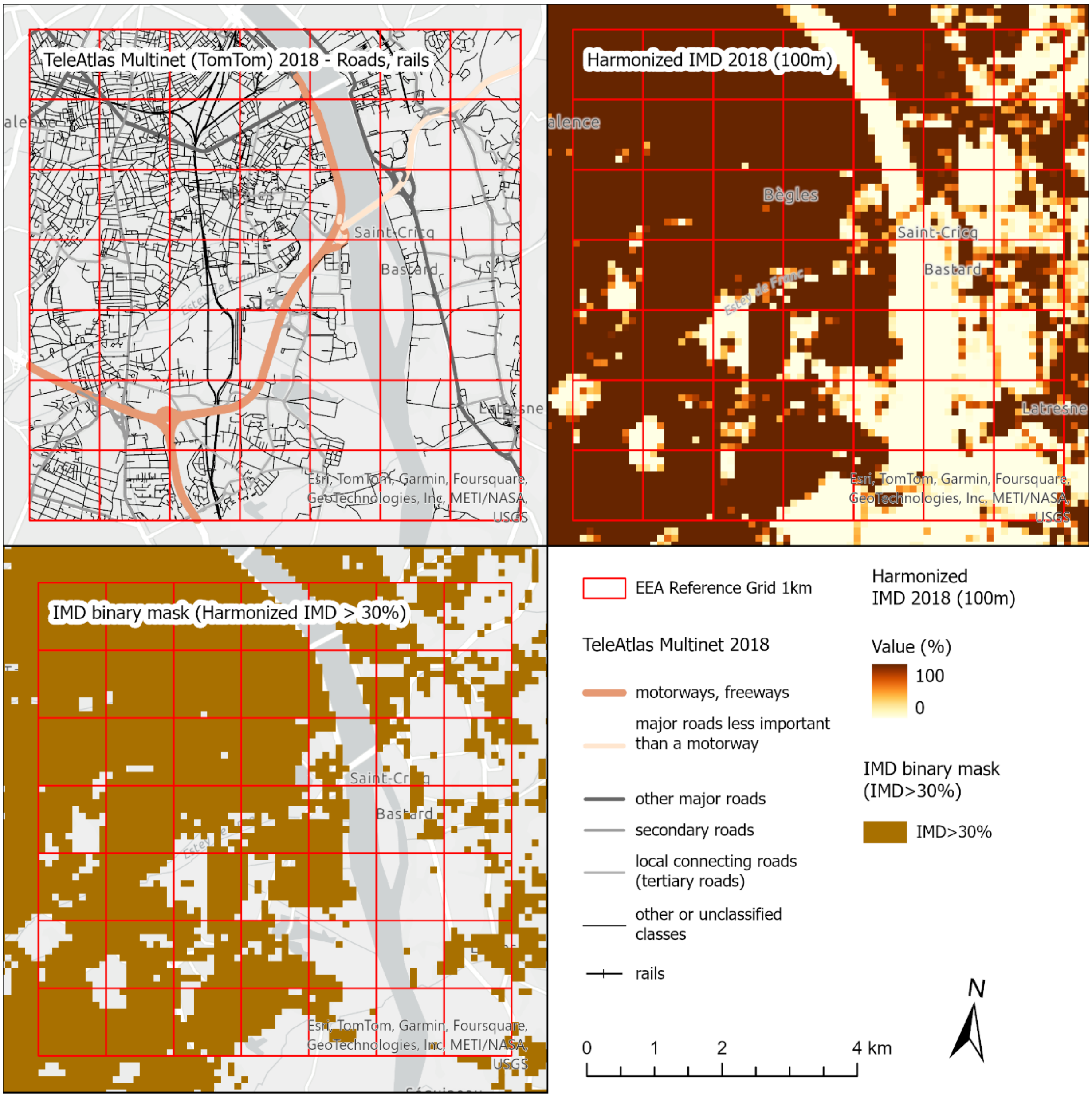

Figure 5: An example showing a detailed view of input datasets within a 1km EEA reference grid. Upper left: Vector dataset of the TomTom MultiNet 2018 (roads and rails), class 'other or unclassified classes' represents all classes not used as input to the calculation. This includes classes -1 = unclassified, 5, 6, 7 and 8 = less important road classes). Upper right: Harmonized IMD raster with 100m pixel resolution. Lower left: Binary mask representing IMD>30% used as the second input to calculation. An example is from Bordeaux, France. EPSG: 3035, XY = 3488800E, 2466800N m.

Setting the IMD threshold value above 30% leads to a reduction of the total area of impervious surfaces from 678241 km^2 (all non-zero IMD values) to 189157 km^2 and also to a significant reduction in the percentage of pixels in sparsely built-up areas within the degree of urbanisation (DEGURBA)[3] classes such as "Mostly uninhabited areas", "Dispersed rural areas", "Villages" and "Suburbs" (Table 2).

Table 2: Comparison of the impact of setting a threshold value for IMD > 30% for estimating the total area of IMD.

	Total area	Mostly uninhabited areas	Dispersed rural areas	Villages	Suburbs	Towns	Cities
IMD > 1% (km^2)	**678241**	294600	193741	62140	49245	40809	37706
Share on DEGURBA classes (%)	**13.29**	6.88	34.76	65.33	63.84	80.60	87.37
IMD > 30% (km^2)	**189157**	26344	43225	33091	25663	29831	31003
Share on DEGURBA classes (%)	**3.71**	0.62	7.75	34.79	33.27	58.92	71.84

3.3 Fragmentation geometry

The fragmentation geometry contains built-up areas extracted from the IMD raster and linear elements of the transport infrastructure from the TomTom MultiNet. The creation of fragmentation geometry can be divided into two steps. Application of these steps was necessary to compute landscape patches from which the meff index can subsequently be calculated.

The first step was to extract the polygon layer of built-up areas. Inputs for this step were IMD rasters for the reference years 2012, 2015 and 2018. From this layer, a binary mask was created with a 30% IMD threshold, i.e. only pixels with a value lower than 30 were classified as non-built up and pixels with values over the defined threshold were classified as built-up. The last part of the first step included clipping the non-build-up raster by 250x250 km tiles and converting them to vector format. Vectors were then merged into a seamless layer.

The second step required editing the line dataset of roads and railways available in the TomTom MultiNet provided by Eurostat. The line vectors were buffered according to the road class they represent, creating a new polygon layer (Table 3). Buffering was also applied to prevent small topological inconsistencies (e.g. double lines or gaps) in data. In addition, a specific procedure has been developed to deal with small erroneous gaps between line segments. The procedure to handle small erroneous gaps between line segments involves creating buffers around line endpoints (vertices) and then generating bounding boxes around these buffers. This method ensures that small gaps between line segments are closed, resulting in a seamless, contiguous polygon layer. This approach is crucial for preventing topological inconsistencies such as double lines or gaps in the data, thereby improving the overall quality and reliability of the geospatial dataset.

The result of these steps is the fragmentation geometry layer which contains landscape patches. The landscape patches represent polygons with the remaining non-fragmented areas and gaps (i.e. no values), in locations of the barriers fragmenting the landscape, i.e. the IMD and road network fragmentation geometries. If any of the selected areas (e.g. administrative unit, reference tile etc.) do not contain any features of fragmentation geometry (i.e. no roads, railways or IMD pixels with a value above the defined threshold), then the area of this unit would be the same as the area of landscape patch. However, in the opposite situation, if the reference unit is located in the central part of the city, which is covered only by IMD pixels above the value defined by the threshold, then it would be a sample of an entirely developed landscape. Thus, there would be no landscape patches. However, the situation

[3] Eurostat. Degree of urbanisation. https://ec.europa.eu/eurostat/web/gisco/geodata/population-distribution/degree-urbanisation

when no landscape patches are detected within the reference units (concerning the size of the reference unit) is rather exceptional, because even in densely built-up areas there are often, for example, rivers, water bodies or city parks.

Table 3: Parameters of the buffer set-up for the line layer of the fragmentation geometry.

Tele Atlas road class	Buffer size [m]	Buffer width [m]
motorways, freeways	15	30
major roads less important than a motorway	10	20
other major roads	7.5	15
secondary roads	5	10
local connecting roads (tertiary roads)	2.5	5
railroads	2	4

3.4 Calculation and interpretation of the meff

At the final step, the meff values are calculated for the intersection of landscape patches with selected reference units which are 1 km^2 cells defined by the EEA reference grid for Europe (1km, Figure 7). For this Europe-wide calculation of landscape fragmentation and previous testing, only the non-CBC meff calculation methodology option was suggested by DG REGIO. This method also known as the cutting-out (CUT) procedure was originally used for meff calculation (Jaeger, 2000). The selected method requires only patches included in the reference unit, which means the boundaries of the reporting units are considered to be additional barriers. The meff index with non-CBC method can be calculated as the following formula (Figure 6):

$$Meff^{non\text{-}CBC} = \frac{\sum_{i=1}^{n}\left(A_i * A_i\right)}{A_{total}}, \; i = 1, \ldots, n,$$

Where:

n = number of landscape patches, A_i = the fraction of the patch i that falls inside the reporting unit, A_{total} = the area of the reporting unit (e.g. 1km^2 tile)

Figure 6: Formula for calculating the value of meff with non-CBC method, measuring landscape fragmentation (Jaeger, 2000)

On the other hand, the non-CBC method is less computationally demanding. On the contrary, the CBC method considers not only the area of the landscape patch which falls inside the reporting unit but the whole area of that given landscape patch is accounted for (Moser et al., 2007).

The meff values are positive real numbers including 0 for grid cells completely covered by built-up areas and infrastructure. The lowest values where meff is zero indicate the landscape which is completely fragmented and thus no landscape patches exist there. Those localities might also be described as completely disconnected regarding to connectivity of nature's habitat. The highest possible value of meff calculated by the non-CBC method is an area of the reference unit (i.e. 1km^2).

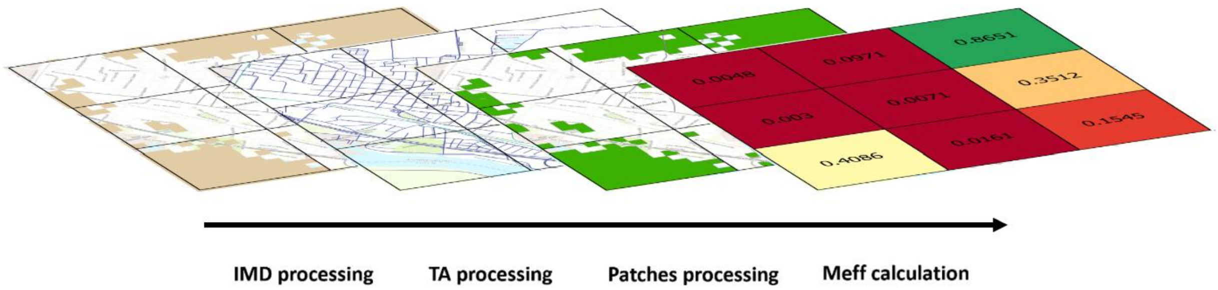

Figure 7: The individual major steps of the fragmentation calculation include preparation of fragmentation geometry and calculation of meff within 1km EEA reference grid. EPSG: 3035, XY = 4790500.00E, 2823500.00N m.

3.5 Statistical tools and outputs description

The main outputs of this task are three raster files with computed meff index prepared by non-CBC method. The output meff rasters are in tiff format with 32-bit pixel depth and float raster type in spatial resolution of 1km covering the interested area (Table 4).

Table 4: General raster information (meff non-CBC 1km), extent and spatial reference.

Columns	6374
Rows	4476
Cell Size X	1000
Cell Size Y	1000
Uncompressed Size	108.83 MB
Format	TIFF
Source Type	Generic
Pixel Type	floating point
Pixel Depth	32 bit
NoData Value	-1
Top Extent	5417000
Bottom Extent	941000
Left Extent	943000
Right Extent	7317000
Projected Coordinate System	ETRS 1989 LAEA
Projection	Lambert Azimuthal Equal Area
WKID	3035
Linear Unit	Meter (1.0)
Geographic Coordinate System	GCS ETRS 1989

The resulting rasters of landscape fragmentation expressed by the meff index computed with the non-CBC method for years 2012, 2015 and 2018 were evaluated using statistical average (weighted average, median) and statistical dispersion (standard deviation) that complement the map outputs. Meff values were also reclassified into 10 classes and visualized using histograms showing the distribution of meff values over spatial units. The provided rasters are then compared to highlight changes in the class distribution of meff values representing a fragmented landscape over time. In addition, the fragmentation pattern has been visualized at different spatial units enabling exploring this land use pattern with different levels of detail and observing variability between regions (Figure 9). The value raster inputs to the calculation of weighted averages using zonal statistics were the meff rasters with 1km spatial resolution, which are the main outputs of this work (see the output description in Table 4).

Outputs of zonal statistics (prepared in GIS) show an area-weighted average of the meff index, which may not fully reflect the overall level of fragmentation across the entire landscape. This is because the average might underrepresent localized areas with high fragmentation, thus not capturing the complete extent of fragmentation present. Data intervals in computed zonal statistics were classified according to the Quantile method to better distinguish the differences between individual regions and harmonised with other years. The Quantile algorithm distributes the observations equally across the class interval, giving unequal class widths but the same frequency of observations per class. The outputs of area weighted averages have been computed at the NUTS0 and NUTS3 levels for all processed years and maps spatially visualize them. In addition, to capture the spatial fragmentation pattern that compensates for the situation when many cells have low (or high) meff values, the amount of fragmented land per capita was computed that is much less sensitive to the variable sizes of the NUTS3 units. The fragmentation per capita refers to the amount of land impacted to fragmentation per person and it was calculated over time per NUTS0 and NUTS3 units (2012, 2015, 2018). Information about population within these regions (NUTS0 and NUTS3) was extracted from ARDECO.SNPTD dataset[4] provided by JRC / REGIO which is commonly used to compute indicators "per capita". The population for the LAU was based on the vector dataset of Local Administrative Units, 2018[5]. In the case of missing values or incomplete population in 2018, the population was estimated by zonal statistics (SUM) performed by GIS from the JRC GEOSTAT 2018[6] population grid.

Fragmentation per capita for NUTS0, NUTS3, LAU and DEGURBA classes levels 1 and 2 was calculated using the following formula:

$$\textit{Fragmentation per capita} = \frac{\sum_{n=1}^{i}((1-meff)*land)}{total\ population},\ i=1, \ldots, n$$

n = the number of reference units (i.e. the number of pixels), meff = the effective mesh size value for each pixel, land = the area of the reporting unit (1km^2 pixels), total population = total population of the spatial unit (e.g., NUTS-3 region).

In addition, differences in mean values of meff between different DEGURBA classes were analyzed. As the distribution of calculated meff values does not correspond with the normal distribution, non-parametric Kruskal-Wallis test was selected (Figure 8). The Kruskal-Wallis test was subsequently supplemented with a post-hoc Dunn's test to find out which pairs of groups have statistically significant differences in meff values ($p<0.05$ for both tests). The distribution of meff values according to DEGURBA classes was visualized by box diagrams.

---

[4] JRC / REGIO. Total Population (annual average). https://urban.jrc.ec.europa.eu/dataset/ARDECO-SNPTD/metadata?lng=en

[5] Eurostat / GISCO. Local administrative units (LAU). https://ec.europa.eu/eurostat/web/gisco/geodata/statistical-units/local-administrative-units

[6] JRC / GEOSTAT. 2018 POPULATION. https://ec.europa.eu/eurostat/web/gisco/geodata/population-distribution/geostat

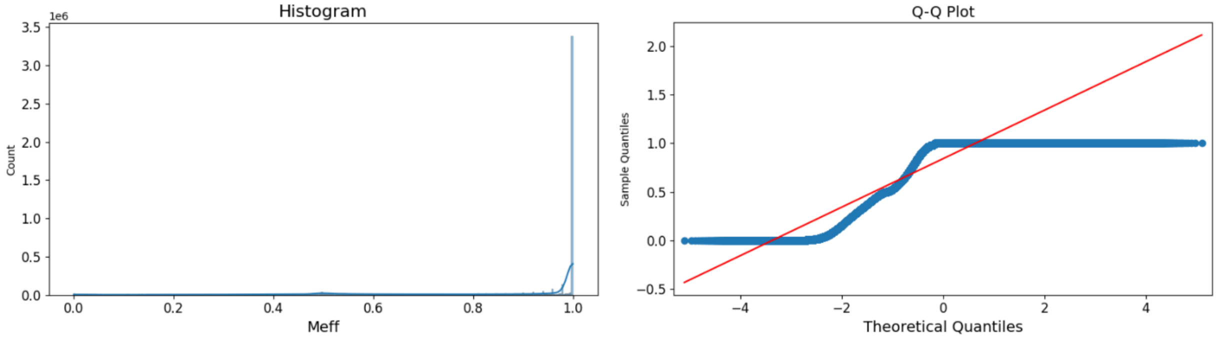

Figure 8: Statistical distribution of meff values. Visual outputs of normality tests (histogram and Q-Q plot) reject normality as the histogram shows a value distribution that is extremely skewed to the right with values concentrated mainly around the meff value of 1 and Q-Q plot shows points significantly deviated out of the line.

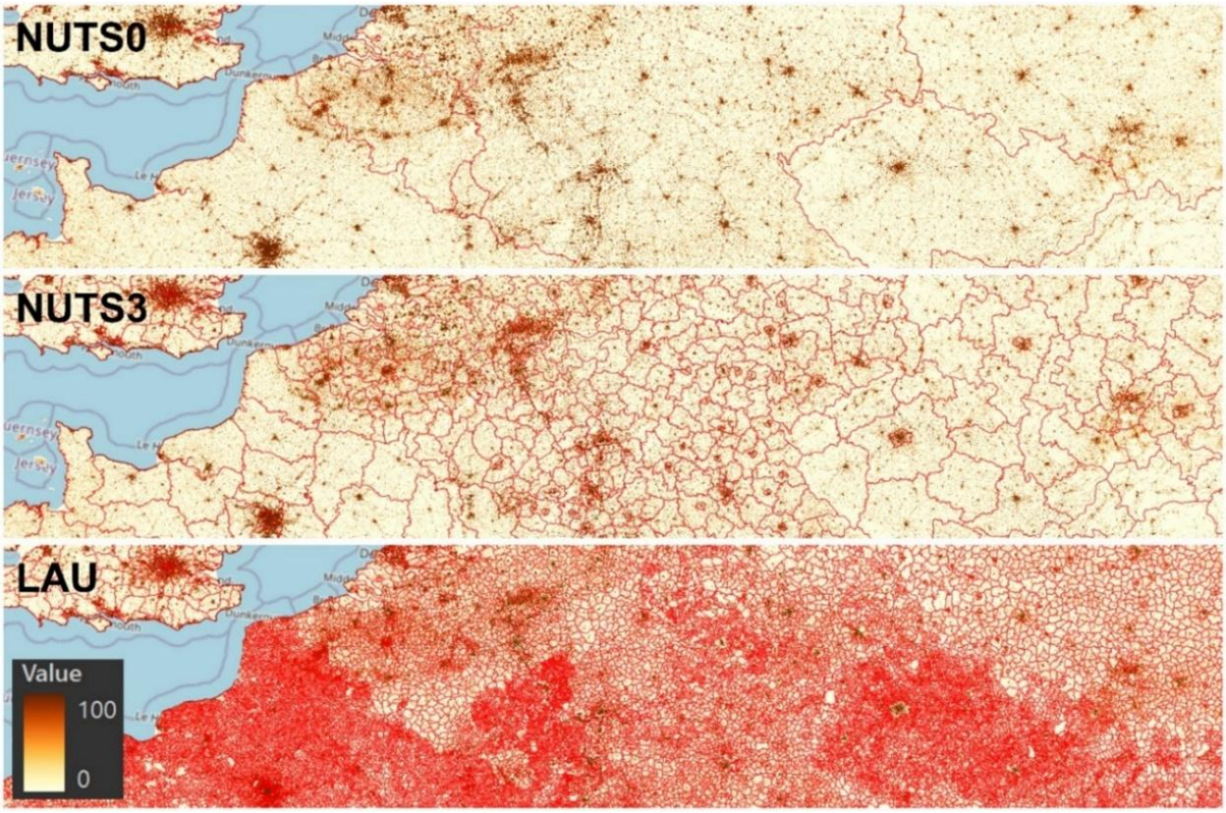

Figure 9: An example of the different levels of spatial administrative units (red polygons) in the part of Central and West Europe for which different zonal statistics of the fragmentation expressed by meff non-CBC index was prepared. The background raster layer is harmonized IMD 2018 100m which was used as one of the inputs to compute meff.

4 Results

4.1 Spatial pattern of landscape fragmentation expressed by meff index

The analysis of landscape fragmentation based on the meff index for the EEA38+UK provides insightful information on the connectivity and integrity of habitats across Europe (Figure 10, Figure 13, Appendix G). These results, derived from the described methods, provide insights into the spatial and temporal dynamics of fragmentation. The following sections detail the observed trends across Europe.

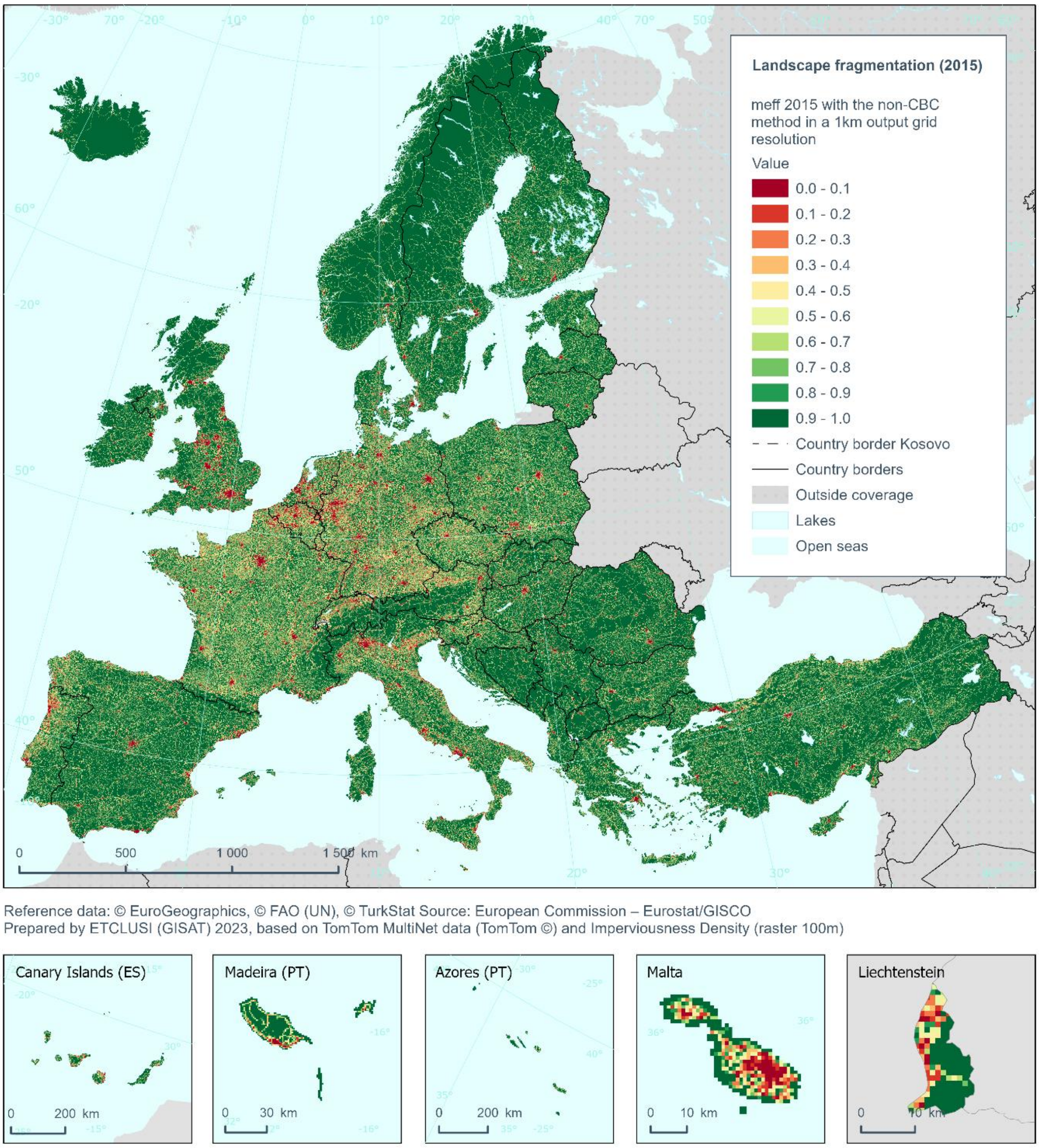

Figure 10: Landscape fragmentation represented by meff index in EEA38+UK in 2015. Low values indicate high fragmentation whereas high values indicate high connectivity of landscape elements.

Looking at the general statistics for 2012, 2015, and 2018 for the entire area of interest, it is evident that the overall landscape fragmentation trend shows an increase over time as the connectivity of the landscape is decreasing. This trend is observable through a slight decrease in the meff index and an increase in standard deviation (Table 5).

Table 5: Basic statistics describing the landscape fragmentation expressed by meff index in EEA38+UK over the selected years (2012, 2015 and 2018).

year	area [km^2]	min	max	mean	median	std
2012	5835060	0	1	0.8445	1	0.2482
2015	5835060	0	1	0.8400	1	0.2501
2018	5835060	0	1	0.8391	1	0.2507

Landscape fragmentation in Europe exhibits a complex pattern that varies significantly across regions (Figure 10, Figure 11).

Western Europe is characterized by its dense urban centers and extensive road networks, which contribute to the highest degree of fragmentation in this part of the continent. Regions such as the Netherlands, Belgium, and West Germany are particularly affected, where urban sprawl and the development of transportation infrastructure have significantly altered the landscape. These areas show lower meff values due to the high density of impermeable barriers.

Central European countries, including Poland and Czechia, also display notable fragmentation. However, there is considerable variation within these countries, with urban-industrial regions exhibiting higher levels of fragmentation compared to more preserved rural areas. Austria and Slovakia, on the other hand, are characterized by lower levels of fragmentation due to the presence of extensive mountainous regions such as the Alps and the Carpathians, which act as natural barriers to development and urban sprawl.

Southern Europe presents a diverse mix of fragmentation patterns influenced by its varied geography, which includes mountain ranges, agricultural lands, and densely populated coastal zones. Mediterranean countries like Spain, Greece and Italy can be characterized by higher fragmentation in coastal regions, driven largely by urbanization and tourism development. Inland areas, particularly those with significant agricultural activity, are usually less fragmented but degrees of fragmentation may vary.

Eastern Europe, including the Balkan countries, generally has a lower proportion of fragmented landscapes due to lower population densities, and reduced size of transportation network. This is attributed to the extensive natural forests and lower levels of urbanization that characterize these regions. Countries such as Romania and Bulgaria maintain large contiguous areas of natural habitats, contributing to higher meff values and lower fragmentation.

In contrast, Northern Europe, particularly Iceland, Sweden, Norway, and Finland, exhibits the lowest levels of fragmentation. These countries benefit from vast natural landscapes, conservative approaches against built-up expansion and urban sprawl, and lower population densities. The presence of extensive forested areas and minimal urban development contributes to higher connectivity and larger patches of unfragmented land.

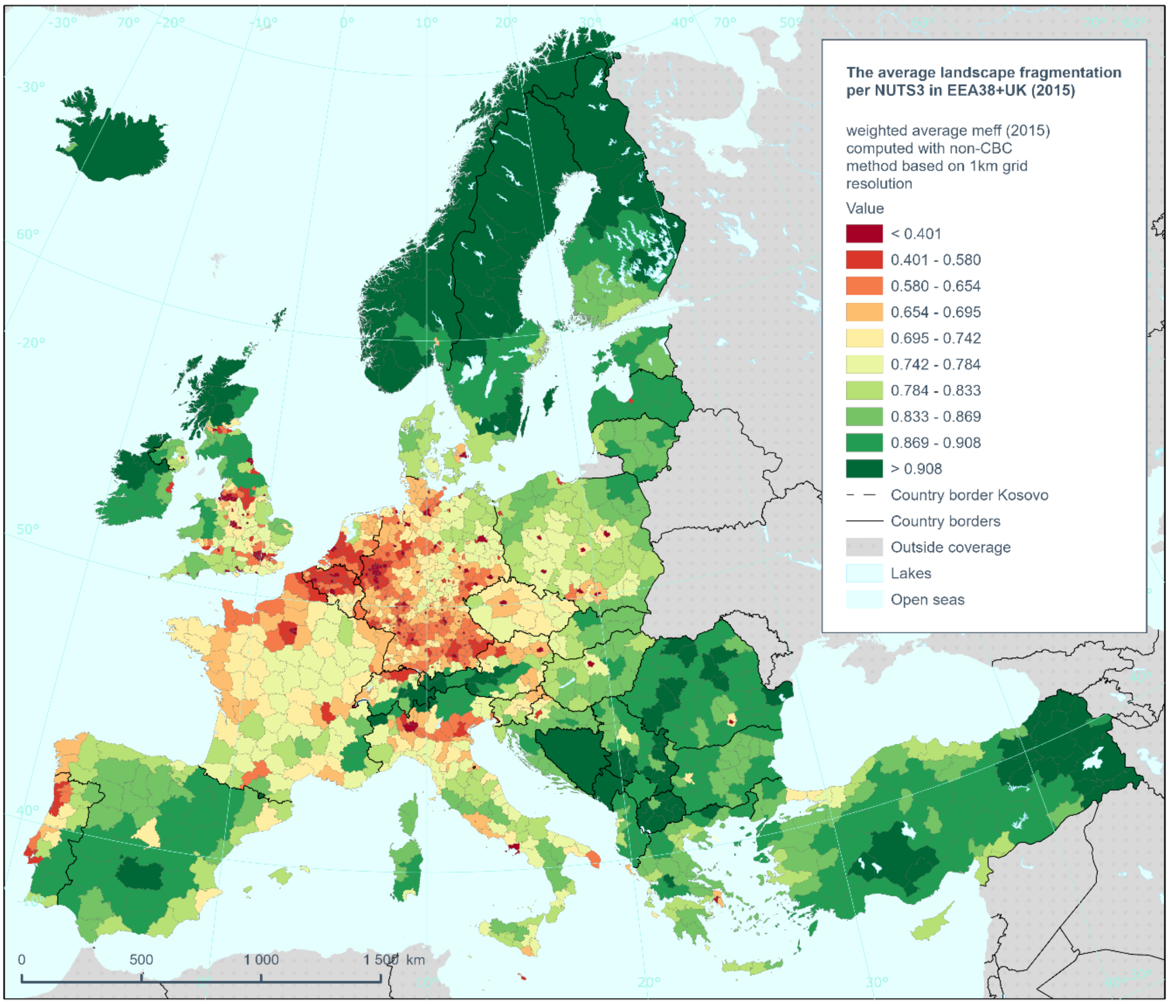

Reference data: © EuroGeographics, © FAO (UN), © TurkStat Source: European Commission – Eurostat/GISCO
Prepared by ETCLUSI (GISAT) 2023, based on TomTom MultiNet data (TomTom ©) and Imperviousness Density (raster 100m)

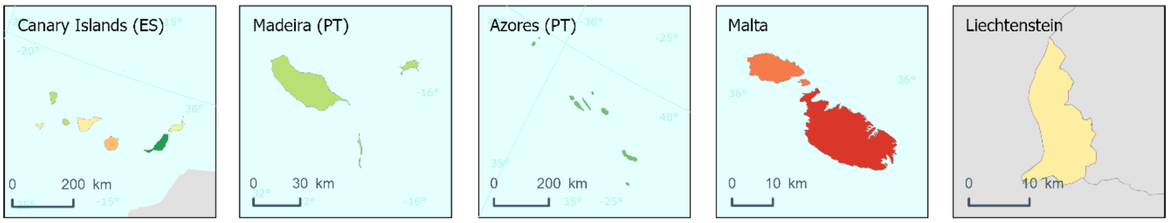

Figure 11: Weighted average meff per NUTS3 in EEA38+UK in 2015. The map legend is classified according to the Quantile method to better distinguish the differences between individual regions and harmonised with other years.

Looking at the outputs of the zonal statistics of the average landscape fragmentation in individual regions at the NUTS3 level, differences across European regions are evident (Figure 11, Figure 14, Appendix H). There are more than 1500 administrative units at the NUTS3 level. Of this number, approximately 30 units have a weighted average meff value of less than 0.1 in 2018. The 50 most fragmented NUTS3 units are cities and their upskirts in Western Europe (Table 6, Figure 12). However, the inconsistency of NUTS3 extents significantly influences the fragmentation pattern. While some countries completely miss further divisions into finer administrative units (e.g. Bosnia and Herzegovina, Montenegro or Kosovo) others contain detailed NUTS3 patterns with small unit sizes (Germany, England). A similar discrepancy comes also from non-equal defining NUTS3 around large cities which are usually the same or similar to the city itself (e.g. Berlin, Vienna, Budapest) while sometimes representing further division of the core city into smaller units (e.g. London) or including larger surroundings (e.g. Madrid, Barcelona, Stockholm, Instanbul). For this reason, Spain does not have highly fragmented NUTS3 units, although Madrid or Barcelona belong to the most fragmented built-up areas in Europe with very high built-up density.

Table 6: Examples of NUTS3 regions with the largest (London) and smallest (Norway and Iceland) average meff value.

NUTS3 name	Average meff (2018)	NUTS3 name	Average meff (2018)
Lambeth	0.013	Troms og Finnmark	0.976
Tower Hamlets	0.024	Norrbottens län	0.977
Haringey & Islington	0.024	Landsbyggð	0.978

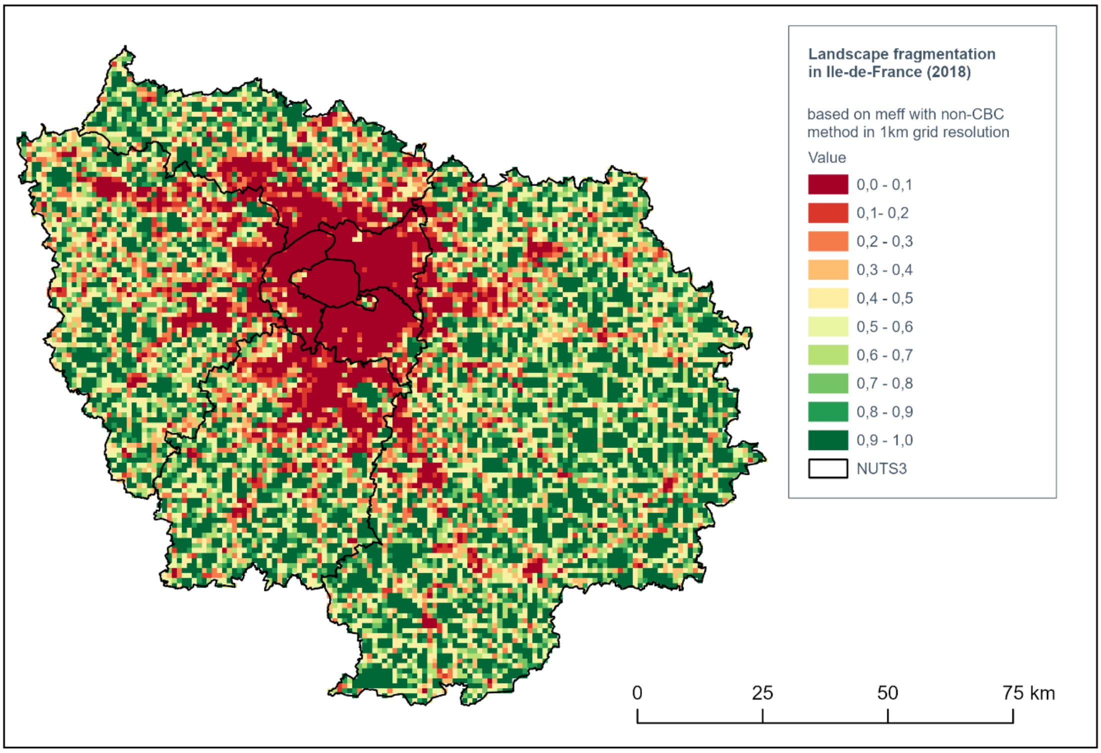

Reference data: © EuroGeographics, © FAO (UN), © TurkStat Source: European Commission – Eurostat/GISCO
Prepared by ETCLUSI (GISAT) 2023, based on Imperviousness Density (raster 100 m)

Figure 12: A detailed look at fragmentation in the Île-de-France, representing an example of one of the most fragmented city landscapes in Europe.

Overall, looking at the presented maps, it is obvious that only minor visual changes in fragmentation patterns are expected (Figure 10, Figure 13). In general, a 3-year period, with exceptions, is usually not a long enough period to see large-scale changes in spatial view of landscape fragmentation on a pan-European scale and at the resolution used. Thus direct visual comparison between 2015 and 2018 on a European scale does not enable the identification of changes. Therefore, to be able to observe the minor changes, a closer look supported by further elucidation through subsequent detailed statistical analyses is needed.

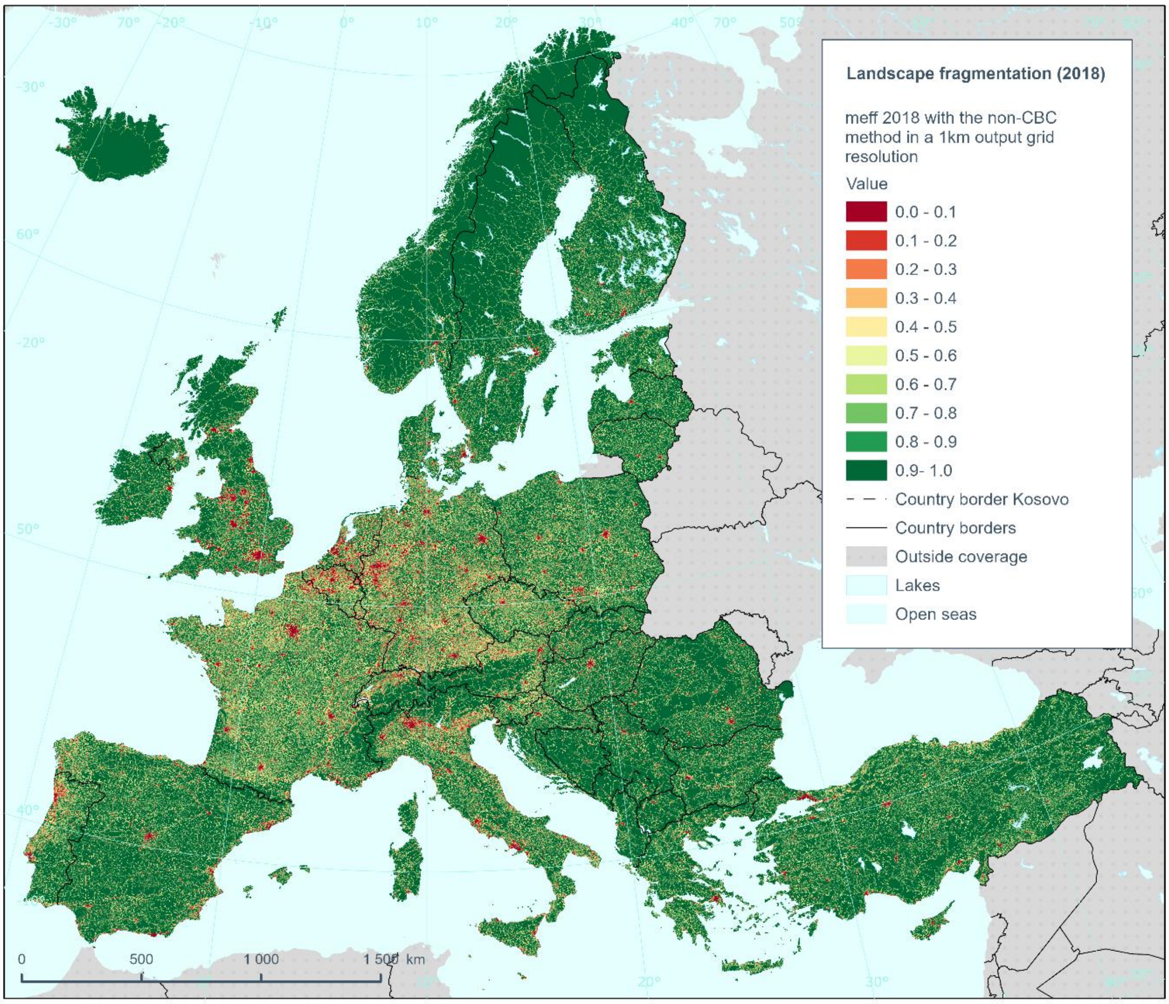

Reference data: © EuroGeographics, © FAO (UN), © TurkStat Source: European Commission – Eurostat/GISCO
Prepared by ETCLUSI (GISAT) 2023, based on TomTom MultiNet data (TomTom ©) and Imperviousness Density (raster 100m)

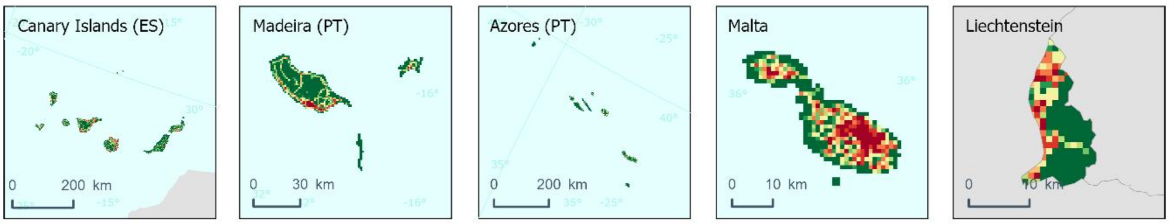

Figure 13: Landscape fragmentation represented by meff index in EEA38+UK in 2018.

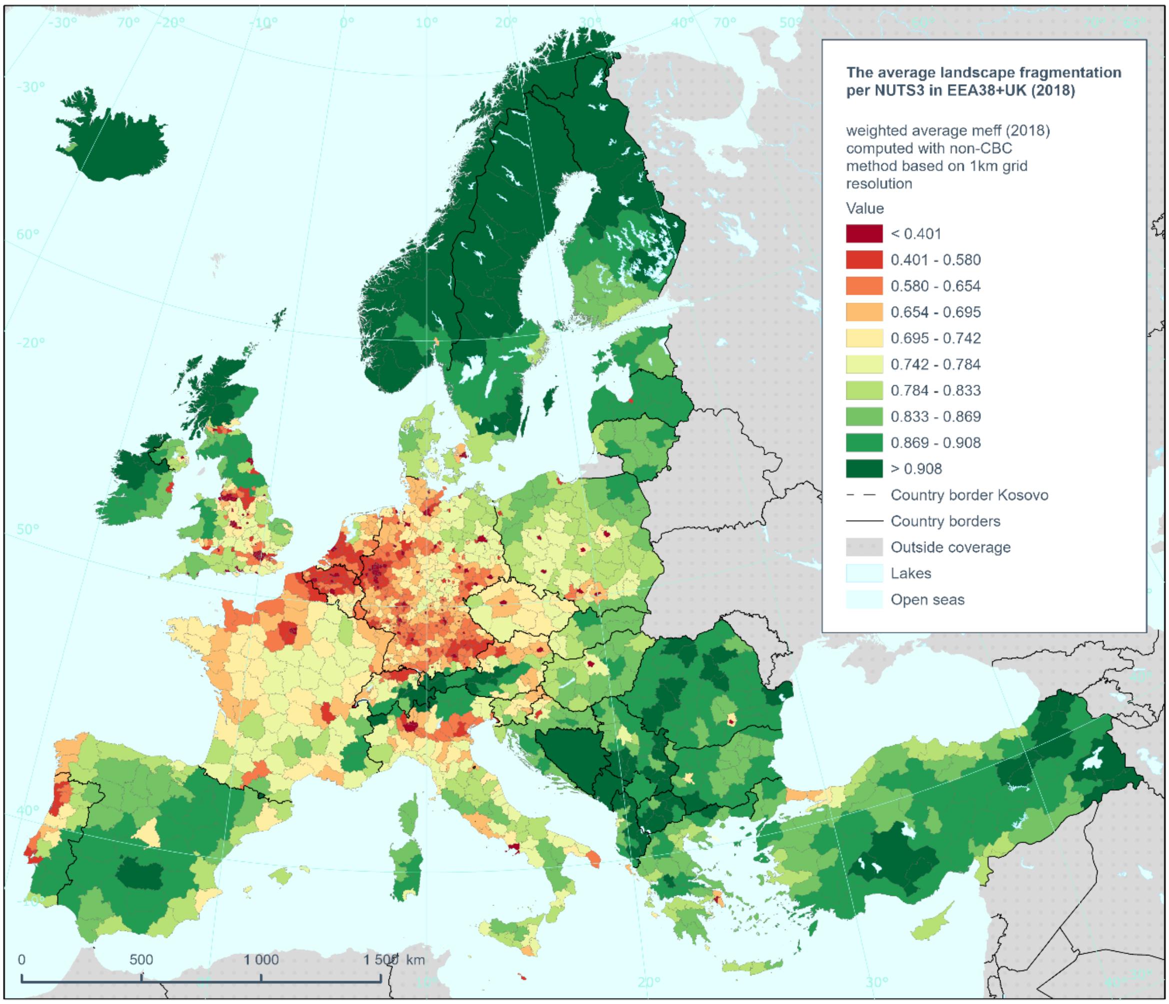

Reference data: © EuroGeographics, © FAO (UN), © TurkStat Source: European Commission – Eurostat/GISCO
Prepared by ETCLUSI (GISAT) 2023, based on TomTom MultiNet data (TomTom ©) and Imperviousness Density (raster 100m)

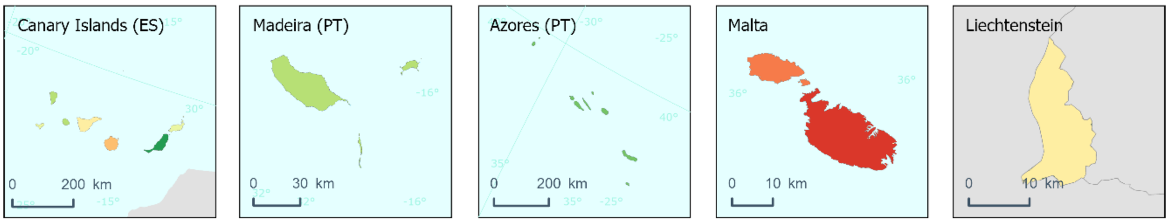

Figure 14: Average meff per NUTS3 in EEA38+UK in 2018. The map legend is classified according to the Quantile method to better distinguish the differences between individual regions and harmonized with other years.

4.2 Spatial pattern of landscape fragmentation related to population

This section presents an analysis of landscape fragmentation with a focus on fragmentation per capita across different administrative levels (NUTS0 - Figure 15, NUTS3 - Figure 16, LAU - Figure 17) and Degree of Urbanization (DEGURBA) classes. Examining fragmentation per capita provides insights into the amount of land impacted by fragmentation relative to the population size in a given region, offering a unique perspective on the effects of landscape fragmentation in both densely and sparsely populated areas. This approach highlights how fragmentation affects urban and rural populations differently, offering a unique perspective compared to traditional fragmentation metrics. While standard measures often classify sparsely populated countries with low population densities and scattered built-up areas as less fragmented, fragmentation per capita reveals that densely populated regions often have lower per capita fragmentation. This is because the extensive fragmentation in such areas is spread across a large population, typically concentrated in small compact urban centres. In contrast, in sparsely populated regions, each inhabitant's share of the fragmented landscape is larger, usually leading to higher fragmentation per capita. Even in sparsely populated countries, there might still be substantial infrastructure (e.g., highways, long roads crossing remote areas) relative to the population size. In such cases, fragmentation per capita can be higher because the few residents "absorb" the impact of a large amount of infrastructure.

NUTS0 units (countries) such as the Netherlands, Belgium, Italy, or the United Kingdom are characterized by urban centres and dense transportation networks, resulting in significant fragmentation (Figure 15). However, despite the high overall fragmentation resulting from extensive urbanization and infrastructure development, the large population in these regions dilutes the per capita impact, leading to lower fragmentation per capita. This reduction is also notable in small, densely populated countries like Malta and Liechtenstein. Conversely, countries like Iceland and Norway exhibit high fragmentation per capita. These nations have low population densities and vast areas of uninhabited or sparsely populated landscapes, where a small number of inhabitants occupies a relatively large area. Interestingly, some Balkan countries also show unexpectedly low fragmentation per capita. In Kosovo, for instance, with a relatively high population density of around 170 inhabitants per km^2, the population is largely concentrated outside the mountainous regions that cover a significant portion of the country. These extensive natural landscapes, combined with a lower density of transport infrastructure in these areas, help reduce the overall fragmentation per capita. While the availability of roads is closely tied to population size, facilitating the connection of settlements, less significant roads may not have been considered in this analysis. These less important road classes, which are common in some regions, were excluded from the dataset used. As a result, Kosovo's fragmentation per capita is comparable to that of densely populated and highly urbanized countries like the Netherlands. However, while the Netherlands achieves low fragmentation per capita due to its high population density and concentrated infrastructure, Kosovo's similar metric is primarily driven by the preservation of natural areas and lower overall infrastructure density, despite significantly different socio-economic contexts.

Analyzing the situation of amount of land (km^2) impacted to fragmentation relative to the population at the NUTS3 and LAU levels allows for the identification of spatial patterns within individual countries, distinguishing between densely populated cities, extensive rural regions, and other specific cases (Figure 16, Figure 17). At the NUTS3 level, the variation in the size of administrative units becomes evident, which can influence the resulting fragmentation per capita values. For instance, while Spain and France typically have large NUTS3 regions, Germany and the United Kingdom are characterized by smaller administrative units. The lowest fragmentation per capita values are observed in densely populated urban centres, excluding their surrounding areas. Cities such as Paris, London, Amsterdam, and other major European capitals exhibit very low fragmentation per capita. The high population in these urban areas dilutes the extent of fragmentation, resulting in lower per capita values. This trend is consistent across many European metropolitan areas, particularly in capital cities.

In contrast, remote and rural areas with sparse populations, such as Iceland and Northern Scandinavia, show very high fragmentation per capita. In these regions, even less significant infrastructure developments, such as roads or small urban settlements, can significantly increase fragmentation per capita due to the low population density. These areas often consist of large natural landscapes with minimal built-up areas, making fragmentation more pronounced per capita. On the other hand, in highly populated Western European countries like Spain and France, fragmentation per capita is generally higher across regions (excluding city areas), despite the large number of inhabitants, as the effect of population size is mitigated by the large size of the countries or their administrative units.

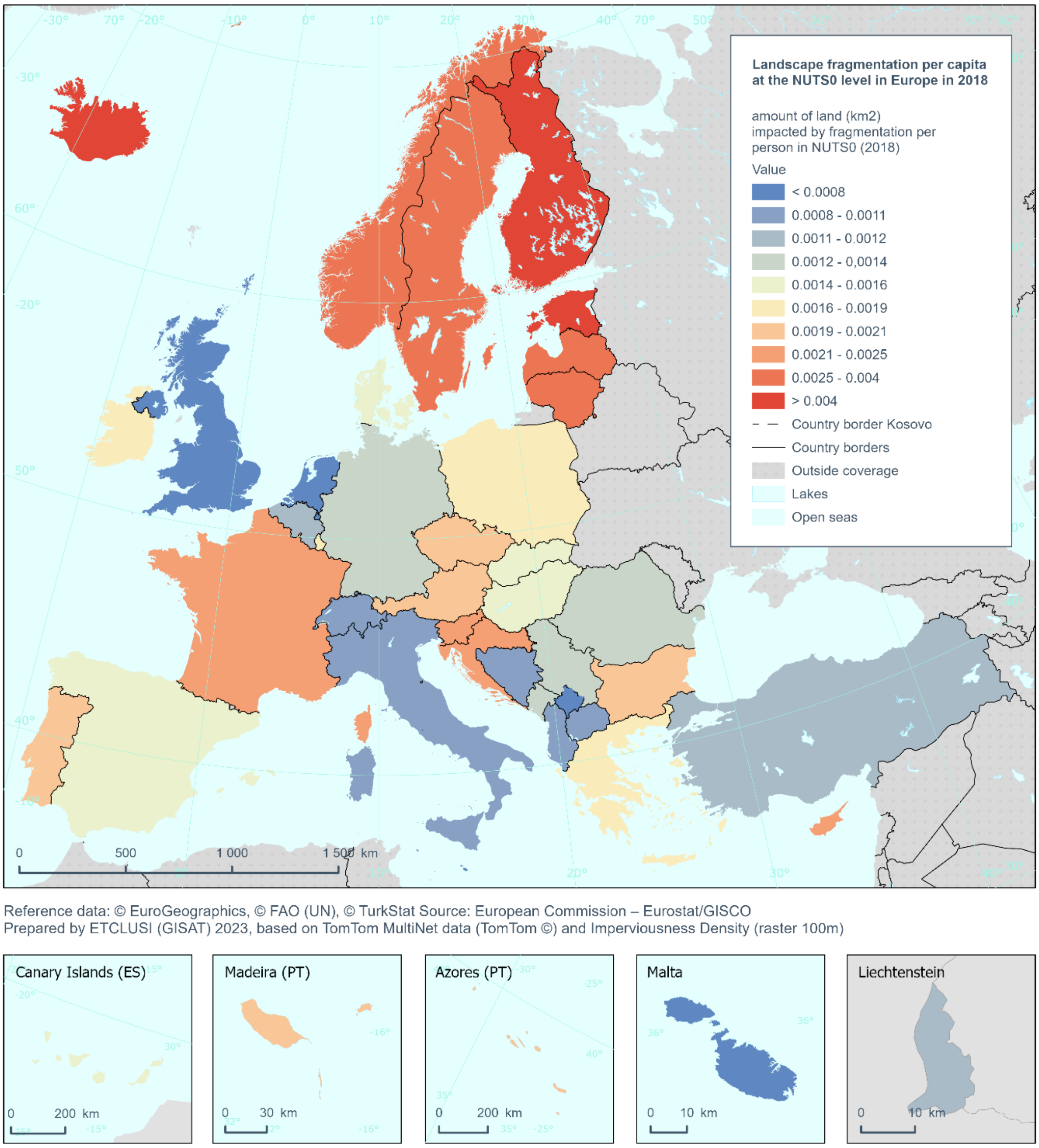

Figure 15: The map at the NUTS0 level (country level) highlights the overall fragmentation per capita across European countries (EEA38+UK) in 2018.

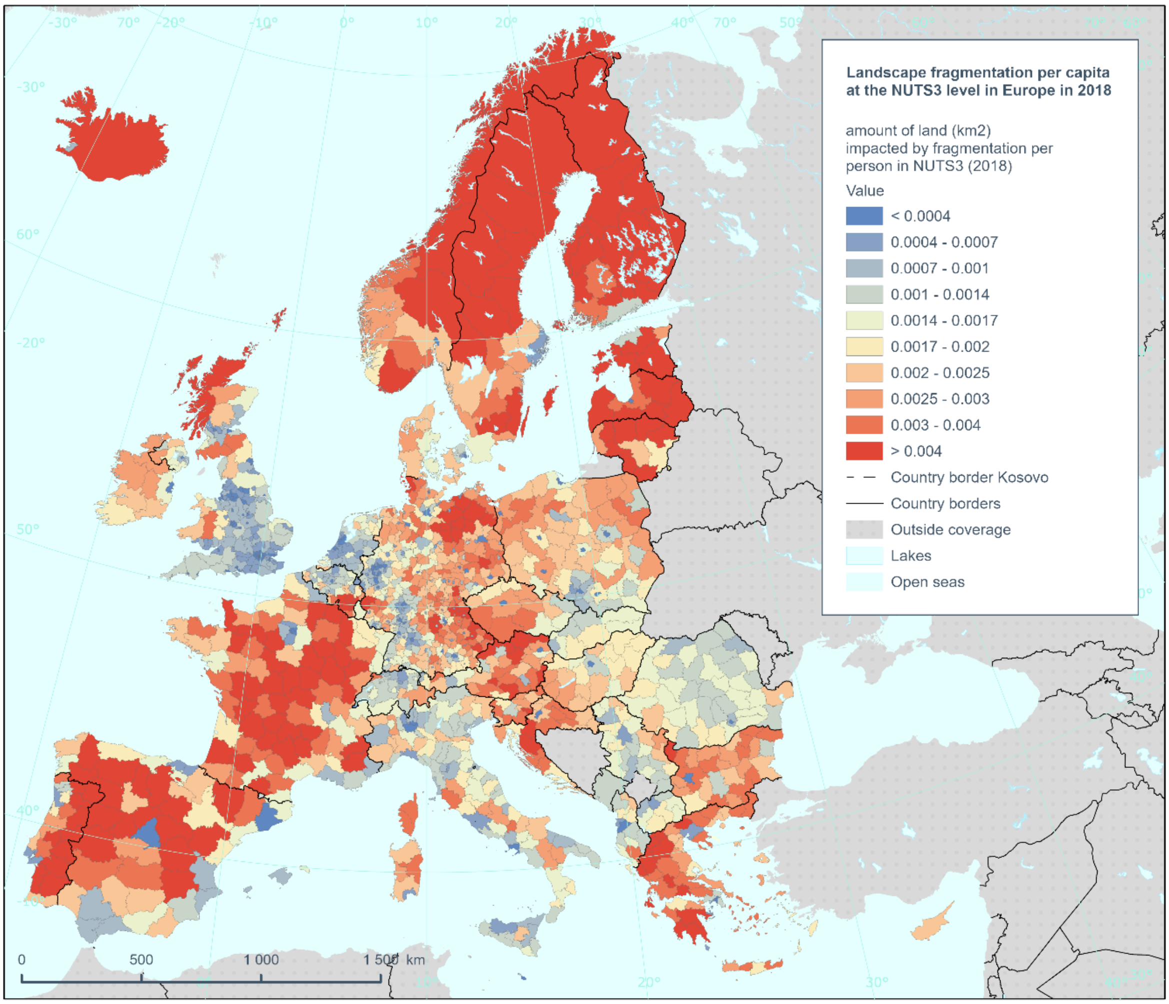

Reference data: © EuroGeographics, © FAO (UN), © TurkStat Source: European Commission – Eurostat/GISCO
Prepared by ETCLUSI (GISAT) 2023, based on TomTom MultiNet data (TomTom ©) and Imperviousness Density (raster 100m)

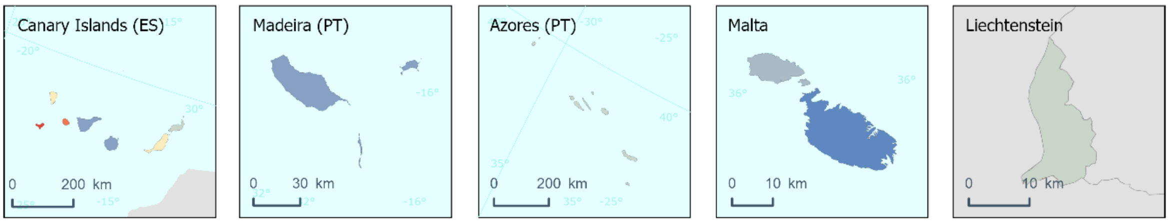

Figure 16: The map at the NUTS3 level (small regions level) highlights the fine pattern of overall fragmentation per capita across European regions in 2018. Information about fragmentation per capita over EEA38+UK is not complete compared to the NUTS0 map and some small countries (e.g. Liechtenstein) are not further divided into NUTS3 units.

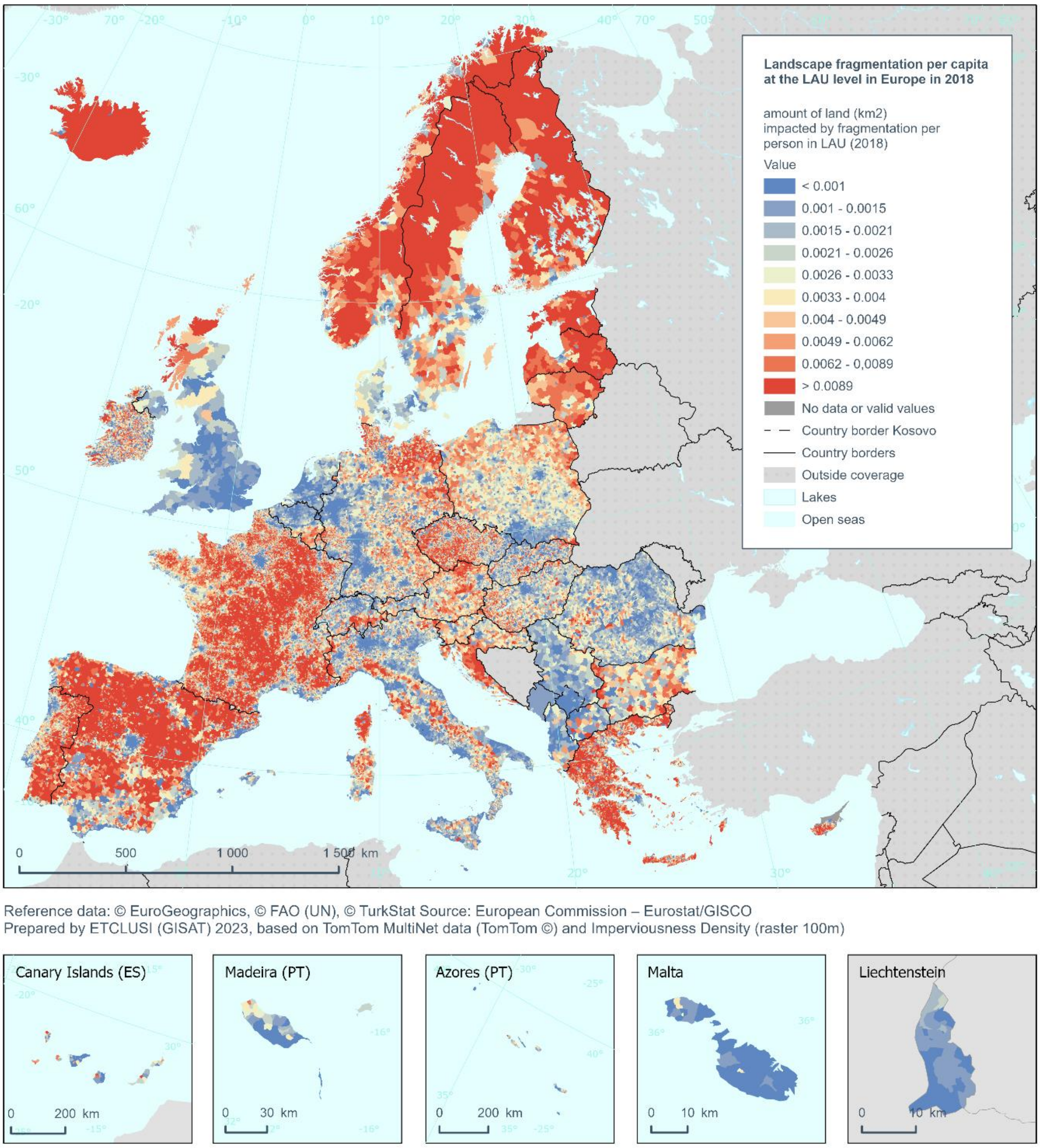

Figure 17: The map at the LAU level shows fragmentation per capita across Europe in 2018 with the finest level of administrative detail. However, the information about fragmentation per capita at LAU level over the EEA38+UK cannot be complete for every spatial unit. This is because for some of the smallest LAUs cannot be extracted any values from meff rasters even though population data is available. This limitation arises because some administrative units are significantly smaller than used 1km pixel resolution, causing the centroid of the pixel values to fall outside their boundaries. This situation is observed in approximately 650 from 102600 LAU which are available within used spatial dataset.

4.3 Landscape fragmentation over land cover classes

The distribution of meff 2018 according to CLC2018 classes was compared as additional information to the obtained results (Figure 18). Unfragmented or only very slightly fragmented landscape (meff = 1.0-0.9) has a dominant position in Europe and occupies about 66.5% of the EEA38+UK territory. This group is mainly represented by the forest cover in Scandinavia and this type of landscape represents more than 1.33 million km^2, which is 22% of the entire area. All other meff classes occupy less than 0.5 mil km^2. The most represented class from this group is the moderately fragmented landscape (meff = 0.6-0.4), which is located mainly on arable land. The vast majority of significantly fragmented landscape (meff = 0.2-0.0) is mainly in areas of urban fabric, but it also occurs partly on arable land.

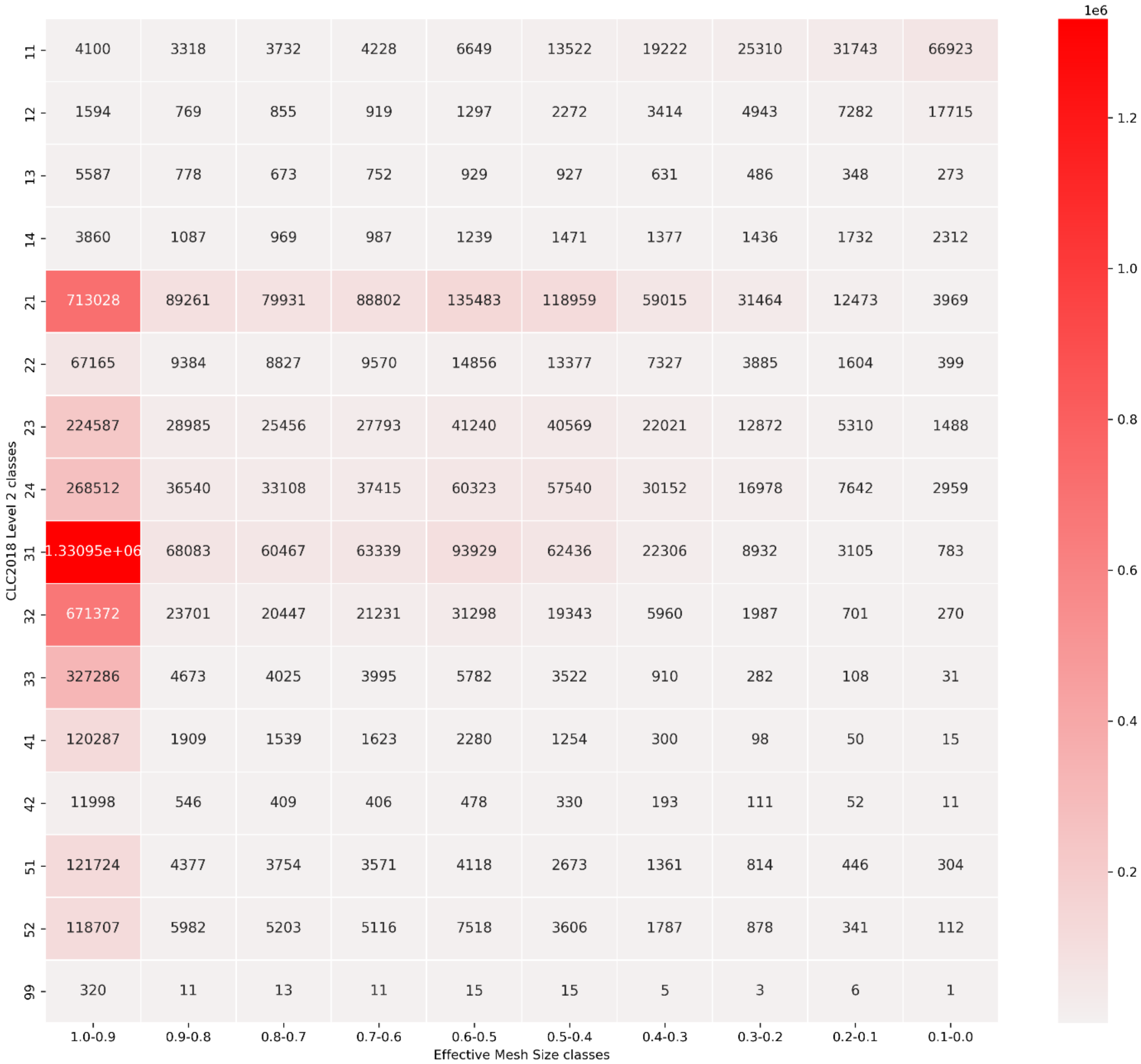

Figure 18: Heat map visualising an area distribution of meff 2018 classes over CLC2018 Level 2 classes. Class names of CLC Level 2 codes are: '11': 'Artificial surfaces', '12': 'Industrial/commercial', '13': 'Mine/dump/construction', '14': 'Artificial greenery', '21': 'Arable land', '22': 'Permanent crops', '23': 'Pastures', '24': 'Heterogeneous agricultural area', '31': 'Forests', '32': 'Shrub/herbaceous vegetation','33': 'Open spaces with little or no vegetation', '41': 'Inland wetlands', '42': 'Coastal wetlands', '51': 'Inland waters', '52': 'Marine waters', '99': 'No data'.

4.4 Statistical evaluation of landscape fragmentation

4.4.1 General descriptive statistics of meff index over European countries

The spatial pattern of landscape fragmentation described previously is further explored here. Bar charts (Figure 19) and statistical overview (Table 7) show average meff values in countries (NUTS0 units) in selected years 2012, 2015 and 2018 (Appendix I). Overall, the most fragmented countries in Europe in terms of average meff value, are from West Europe (excluding Malta), including the Netherlands, Belgium and Luxembourg. The other side of the ladder is represented by northern countries or regions from Balkan. In addition, when both years are compared, it is obvious that the overall ranking remains the same with exceptions. In general, it can be expected that landscape fragmentation is increasing over time due to the expansion of anthropogenic impervious surfaces and transport infrastructure. Although the differences between years are usually minor, this trend can be reliably confirmed. However, despite expectations and the general trend, a different development trend was detected in some countries (e.g. Albania and Luxembourg). This is explained in more detail in the chapter *0 Spatial analysis and types of the observed changes in fragmentation.*

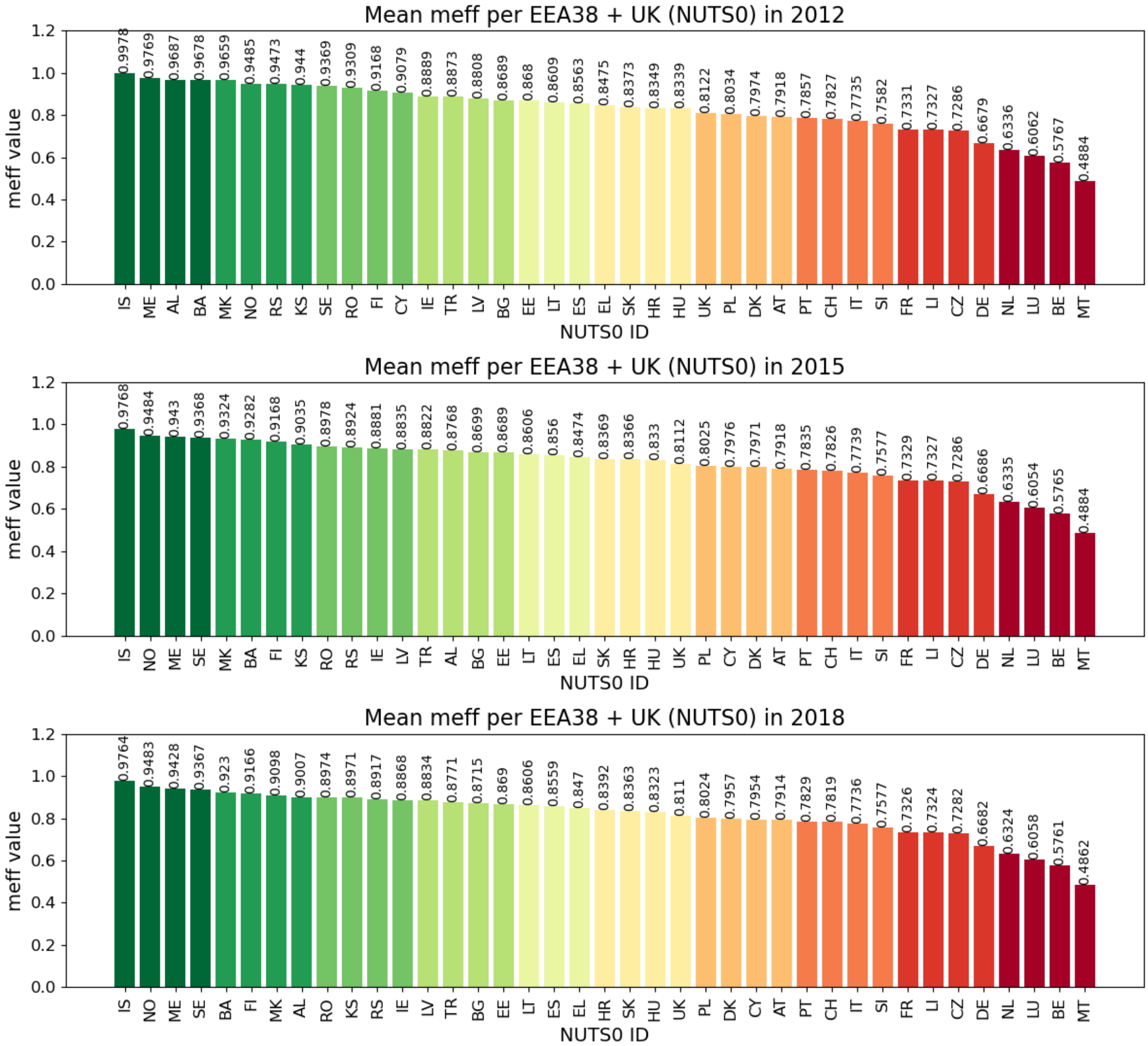

Figure 19: Bar charts with ranking of mean meff values in EEA38+UK countries in 2012, 2015 and 2018.

Table 7: General descriptive statistics of meff index in EEA38+UK countries (NUTS0 level).

		2012			2015			2018		
NUTS0	area [km²]	mean	median	std	mean	median	std	mean	median	std
AL	28780	0.9687	1.0000	0.1213	0.8768	1.0000	0.2124	0.9007	1.0000	0.1980
AT	83929	0.7918	0.9801	0.2799	0.7918	0.9801	0.2800	0.7914	0.9801	0.2803
BA	51221	0.9678	1.0000	0.1212	0.9282	1.0000	0.1722	0.9230	1.0000	0.1779
BE	30652	0.5767	0.5551	0.3166	0.5765	0.5554	0.3168	0.5761	0.5550	0.3169
BG	110999	0.8689	1.0000	0.2249	0.8699	1.0000	0.2247	0.8715	1.0000	0.2240
CY	9249	0.9079	1.0000	0.2170	0.7976	0.9801	0.2774	0.7954	0.9801	0.2797
CZ	78886	0.7286	0.8121	0.2800	0.7286	0.8123	0.2802	0.7282	0.8114	0.2806
DE	357656	0.6679	0.6997	0.3063	0.6686	0.7016	0.3065	0.6682	0.7008	0.3066
DK	43139	0.7974	0.9568	0.2710	0.7971	0.9561	0.2714	0.7957	0.9512	0.2723
EE	45328	0.8680	1.0000	0.2116	0.8689	1.0000	0.2112	0.8690	1.0000	0.2111
EL	131685	0.8475	1.0000	0.2365	0.8474	1.0000	0.2366	0.8470	1.0000	0.2369
ES	505997	0.8563	1.0000	0.2353	0.8560	1.0000	0.2357	0.8559	1.0000	0.2358
FI	337529	0.9168	1.0000	0.1797	0.9168	1.0000	0.1797	0.9166	1.0000	0.1800
FR	548901	0.7331	0.8235	0.2767	0.7329	0.8235	0.2769	0.7326	0.8229	0.2771
HR	56547	0.8349	1.0000	0.2400	0.8366	1.0000	0.2398	0.8392	1.0000	0.2396
HU	93020	0.8339	1.0000	0.2579	0.8330	1.0000	0.2586	0.8323	1.0000	0.2592
CH	41289	0.7827	1.0000	0.3015	0.7826	1.0000	0.3015	0.7819	1.0000	0.3017
IE	69949	0.8889	1.0000	0.2042	0.8881	1.0000	0.2048	0.8868	1.0000	0.2059
IS	102689	0.9978	1.0000	0.0373	0.9768	1.0000	0.0979	0.9764	1.0000	0.0988
IT	300622	0.7735	0.9567	0.2869	0.7739	0.9590	0.2871	0.7736	0.9587	0.2874
KS	10910	0.9440	1.0000	0.1552	0.9035	1.0000	0.2031	0.8971	1.0000	0.2085
LI	161	0.7327	0.9801	0.3382	0.7327	0.9801	0.3382	0.7324	0.9801	0.3385
LT	64893	0.8609	1.0000	0.2171	0.8606	1.0000	0.2174	0.8606	1.0000	0.2174
LU	2594	0.6062	0.5769	0.2943	0.6054	0.5774	0.2945	0.6058	0.5779	0.2945
LV	64578	0.8808	1.0000	0.2010	0.8835	1.0000	0.1995	0.8834	1.0000	0.1995
ME	13877	0.9769	1.0000	0.1101	0.9430	1.0000	0.1579	0.9428	1.0000	0.1584
MK	25442	0.9659	1.0000	0.1327	0.9324	1.0000	0.1761	0.9098	1.0000	0.1952
MT	321	0.4884	0.4611	0.3450	0.4884	0.4616	0.3447	0.4862	0.4566	0.3484
NL	37407	0.6336	0.6788	0.3312	0.6335	0.6784	0.3314	0.6324	0.6769	0.3319
NO	323388	0.9485	1.0000	0.1502	0.9484	1.0000	0.1504	0.9483	1.0000	0.1507
PL	311940	0.8034	0.9604	0.2521	0.8025	0.9604	0.2531	0.8024	0.9604	0.2535
PT	91885	0.7857	0.9651	0.2756	0.7835	0.9604	0.2768	0.7829	0.9604	0.2770
RO	238367	0.9309	1.0000	0.1768	0.8978	1.0000	0.2072	0.8974	1.0000	0.2077
RS	77477	0.9473	1.0000	0.1648	0.8924	1.0000	0.2157	0.8917	1.0000	0.2165
SE	449675	0.9369	1.0000	0.1652	0.9368	1.0000	0.1653	0.9367	1.0000	0.1655
SI	20273	0.7582	0.8799	0.2669	0.7577	0.8778	0.2669	0.7577	0.8790	0.2672
SK	49023	0.8373	1.0000	0.2532	0.8369	1.0000	0.2539	0.8363	1.0000	0.2545
TR	780121	0.8873	1.0000	0.2056	0.8822	1.0000	0.2098	0.8771	1.0000	0.2131
UK	244661	0.8122	0.9801	0.2827	0.8112	0.9801	0.2833	0.8110	0.9801	0.2834

Clear evidence of a trend in landscape fragmentation is provided by histograms of pixel frequencies in fragmentation classes in the entire area (Figure 20) and selected countries representing high and low-fragmented regions (Belgium - Figure 21 and Sweden - Figure 22). These example countries represent the evolution of landscape fragmentation which is completely in line with the foreseen trend. Increasing landscape fragmentation might be generally characterized by shifting class frequencies of pixels from classes with weakly fragmented landscapes to classes representing more fragmented landscapes, which is confirmed in the calculated meff index. Generally, two types of changes can be observed between 2012, 2015 and 2018, which align with the expected landscape evolution. The major change is the decrease in natural areas, represented by values from 1.0 (completely unfragmented landscape) to 0.9 (almost unfragmented landscape; Table 8). The second general change is the increase in areas in all other landscape fragmentation classes when the largest increases are observed within moderately fragmented landscapes with meff values around 0.6-0.4. The large difference in changes between 2012-2015 and 2015-2018 points to the inconsistency of some input data (Table 8). These unexpected evolution of the meff indicator in time is closely linked mainly to the inconsistent evolution of TomTom data while there are two types of observed issues. The first type represents an incomplete database of transport infrastructure in some countries, while the second issue refers to changes in classification (e.g. shifts between some road classes) and geometries. The observed problems are mentioned in the next chapter (*4.5 Spatial analysis and types of the observed changes in fragmentation*) and then further described in detail in the discussion. Detailed overview of evolution of selected statistics related to the input data for countries and selected NUTS3 regions is attached (Appendix A-F). However, overall, the relative representation of individual fragmentation classes remains almost unchanged as in all years the non-fragmented or only slightly fragmented landscape significantly dominates.

Table 8: Changes in the area of fragmentation classes provide clear evidence of the overall increase in the fragmented landscape in Europe between 2012-2015 (upper table), 2012-2018 (middle table) and 2015-2018 (lower table).

meff value	1.0-0.9	0.9-0.8	0.8-0.7	0.7-0.6	0.6-0.5	0.5-0.4	0.4-0.3	0.3-0.2	0.2-0.1	0.1-0.0
change [km^2]	**-56539**	**3731**	**5833**	**9125**	**15410**	**12360**	**4890**	**2474**	**1409**	**1307**
rel [%] 2012	67.167	4.6148	4.0792	4.3739	6.5834	5.5820	2.8991	1.8347	1.2195	1.6464
rel [%] 2015	66.198	4.6787	4.1791	4.5302	6.8475	5.7939	2.9829	1.8771	1.2437	1.6688
change [km^2]	**-66851**	**4479**	**6897**	**10426**	**17137**	**14343**	**6445**	**3313**	**1948**	**1863**
rel [%] 2012	67.167	4.6148	4.0792	4.3739	6.5834	5.5820	2.8991	1.8347	1.2195	1.6464
rel [%] 2018	66.021	4.6916	4.1974	4.5525	6.8771	5.8278	3.0095	1.8915	1.2529	1.6784
change [km^2]	**-10312**	**748**	**1064**	**1301**	**1727**	**1983**	**1555**	**839**	**539**	**556**
rel [%] 2015	66.198	4.6787	4.1791	4.5302	6.8475	5.7939	2.9829	1.8771	1.2437	1.6688
rel [%] 2018	66.021	4.6916	4.1974	4.5525	6.8771	5.8278	3.0095	1.8915	1.2529	1.6784

Another insight into changes in the fragmented landscape for different meff classes between 2012 and 2018 provides evolution in relative changes where 2012 is the starting year (Table 9). The status of all the meff classes represents 100% at the beginning of the analysed period and then increases or decreases. Changes in the meff show an expected pattern when extent of all meff classes is getting larger over time excluding unfragmented or slightly fragmented landscapes (meff class 1.0-0.9) which has been decreasing. The abrupt increase from 2012 to 2015 followed by a slight change from 2015 to 2018 is here even more evident.

Table 9: Evolution of extent of reclassified meff values expressed as relative change (in %) from 2012 within entire EEA38+UK territory.

	1.0-0.9	0.9-0.8	0.8-0.7	0.7-0.6	0.6-0.5	0.5-0.4	0.4-0.3	0.3-0.2	0.2-0.1	0.1-0.0
2012	100	100	100	100	100	100	100	100	100	100
2015	98.557	101.386	102.451	103.575	104.012	103.795	102.891	102.311	101.98	101.36
2018	98.294	101.663	102.898	104.085	104.461	104.404	103.81	103.095	102.737	101.939

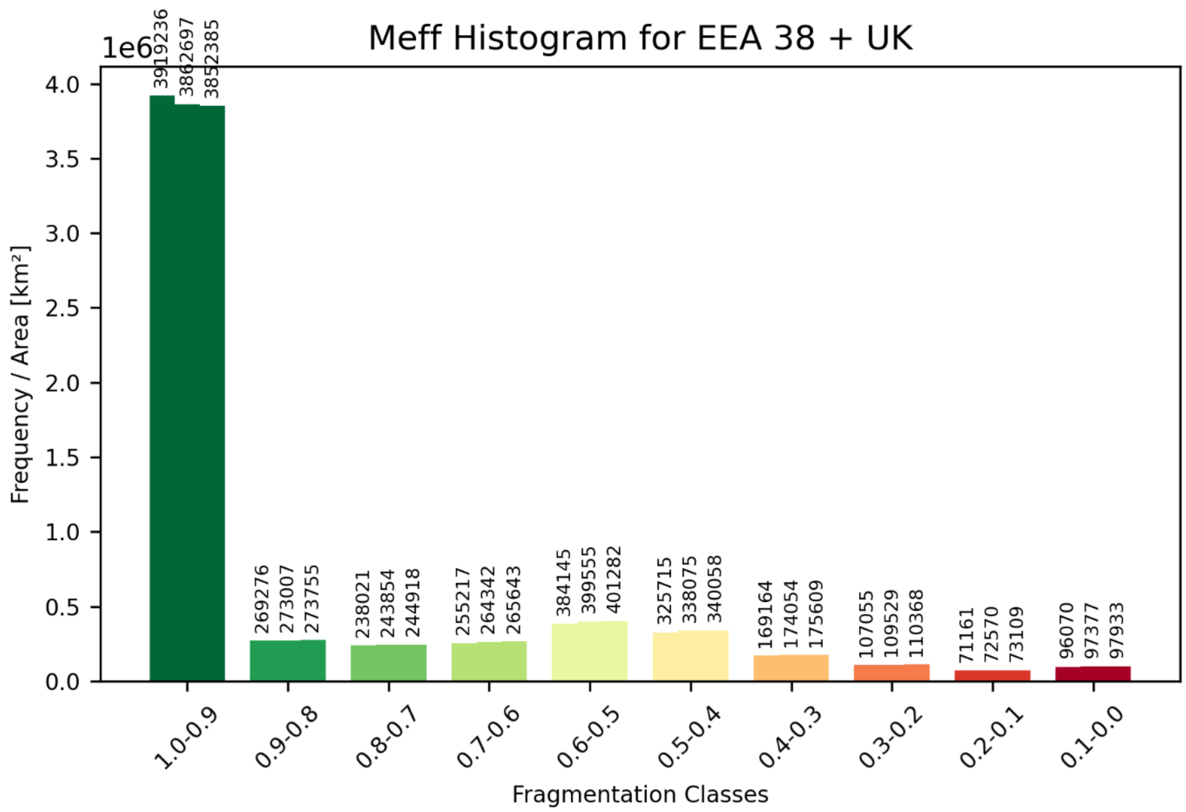

Figure 20: Histogram showing changes of distribution in class frequencies of meff values (left columns = 2012, middle columns = 2015, right columns = 2018) in the EEA38+UK.

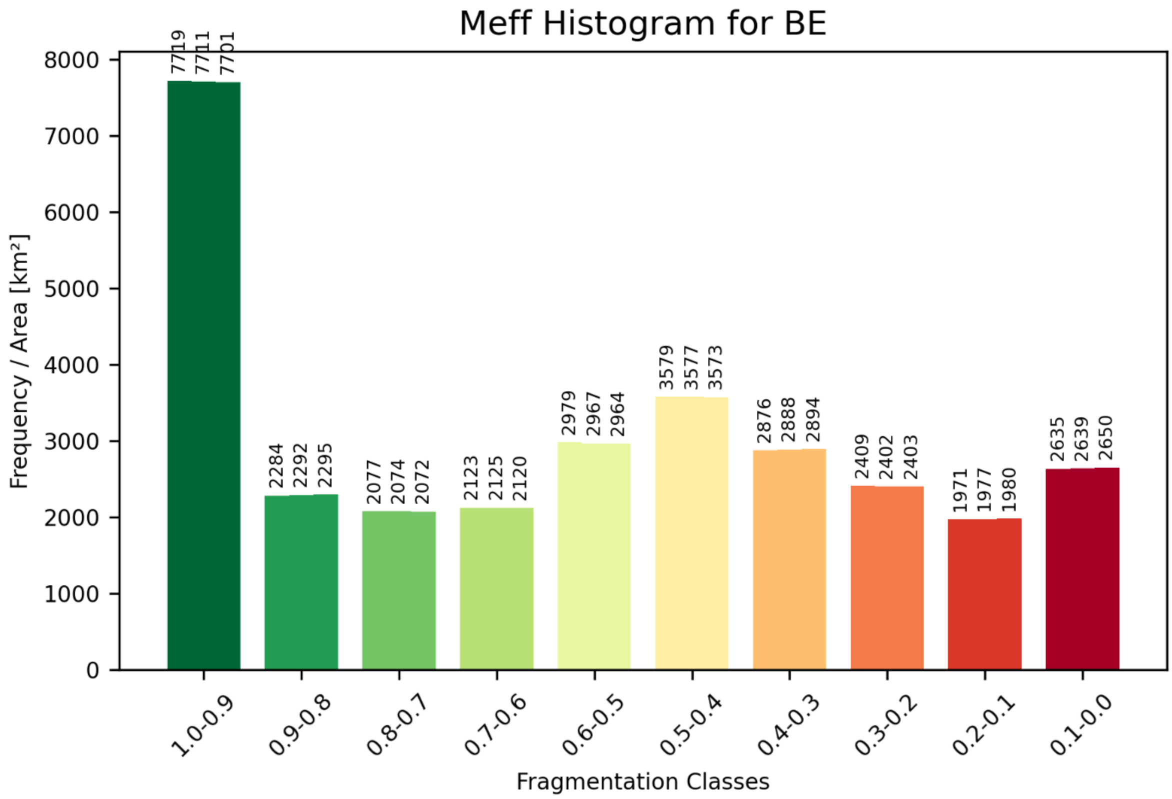

Figure 21: Histogram showing changes of distribution in class frequencies of meff values in Belgium representing a country with high population and transportation network density.

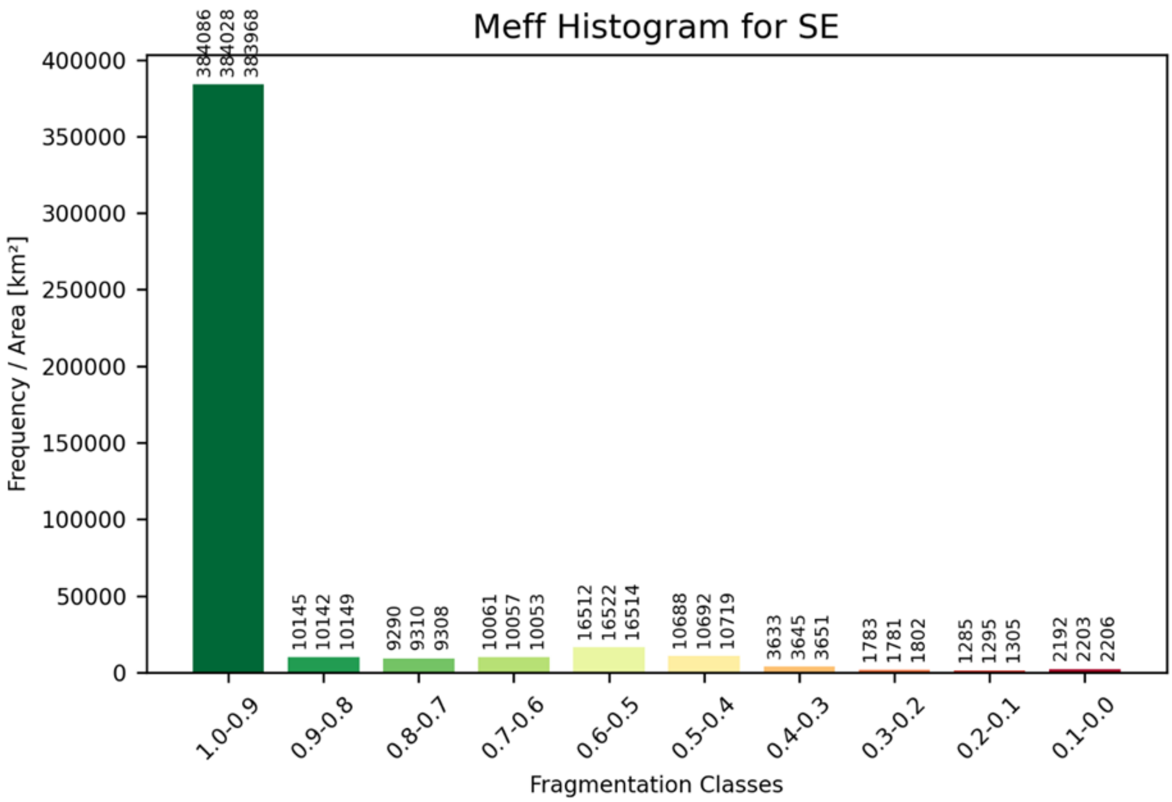

Figure 22: Histogram showing changes of distribution in class frequencies of meff values in Sweden representing a country with low population and transportation network density.

4.4.2 *Statistical evaluation of landscape fragmentation related to population*

The statistical analysis of landscape fragmentation per capita overall shows expected patterns when sparsely populated countries like Iceland, Finland, and Estonia have relatively high fragmentation per capita, reflecting the significant impact of landscape fragmentation on a per-person basis due to lower population densities whereas densely populated regions show the opposite situation (Figure 23, Table 11). However, it is crucial to also consider the density of transportation infrastructure. Regions with similar populations and areas may experience significantly different fragmentation per capita due to variations in the total length of roads and railways. This factor helps explain why some Eastern European countries with limited networks of transport infrastructure, such as Kosovo, Albania, and Macedonia, have similarly low fragmentation per capita as densely populated Western European countries like the Netherlands or the United Kingdom which was previously already described in detail in chapter *4.2 Spatial pattern of landscape fragmentation related to population*. Additionally, the presence of less important road classes, not included in this analysis, may also influence fragmentation per capita as the resulting value of fragmentation per capita might be smaller than can expected.

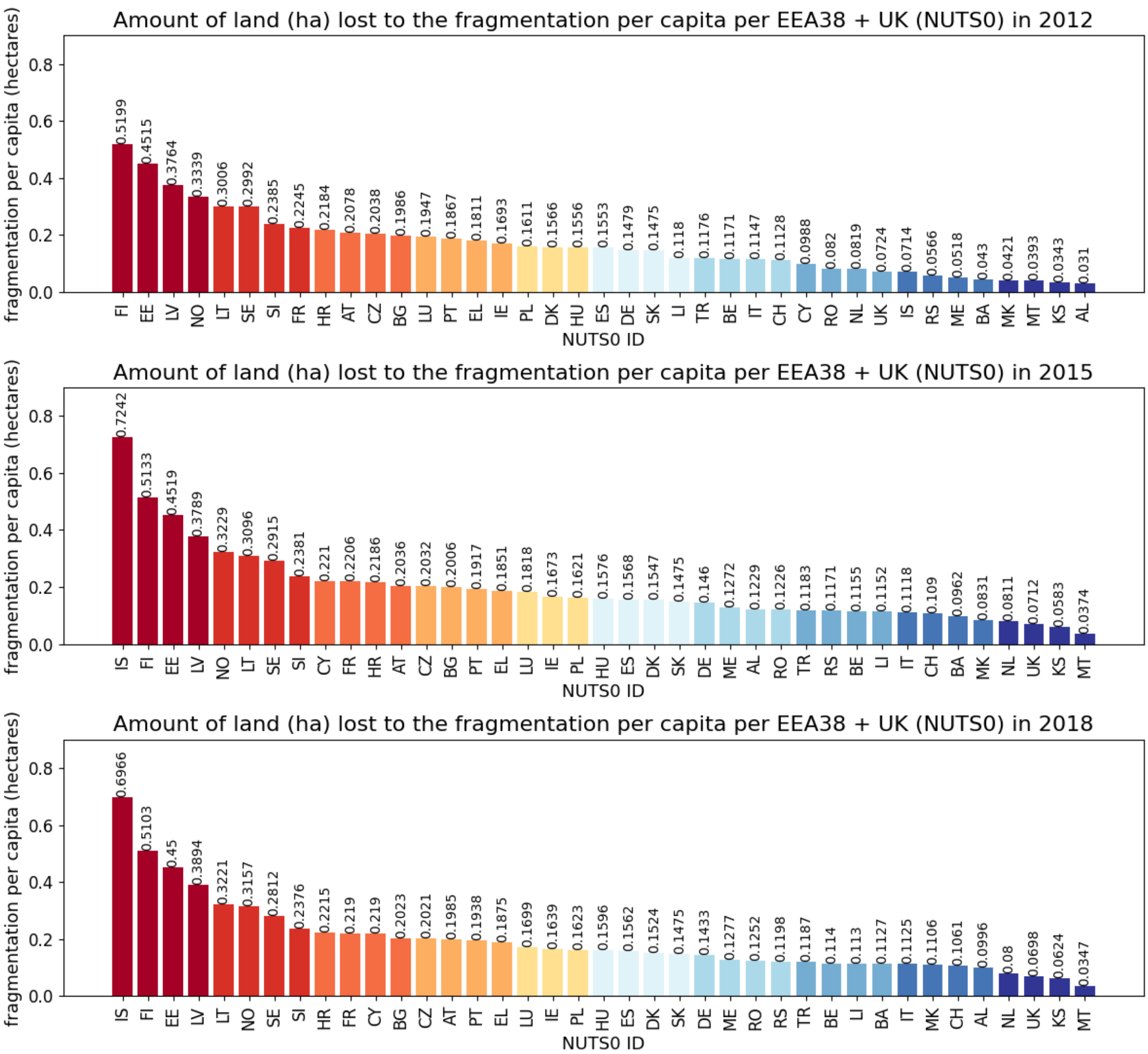

Figure 23: Bar charts with a ranking of area-weighted mean fragmentation per capita (ha) in EEA38+UK countries in 2012, 2015 and 2018. Large shift in the ranking of Iceland (IS) between 2012 and 2015 is related to the absence of TomTom data in 2012.

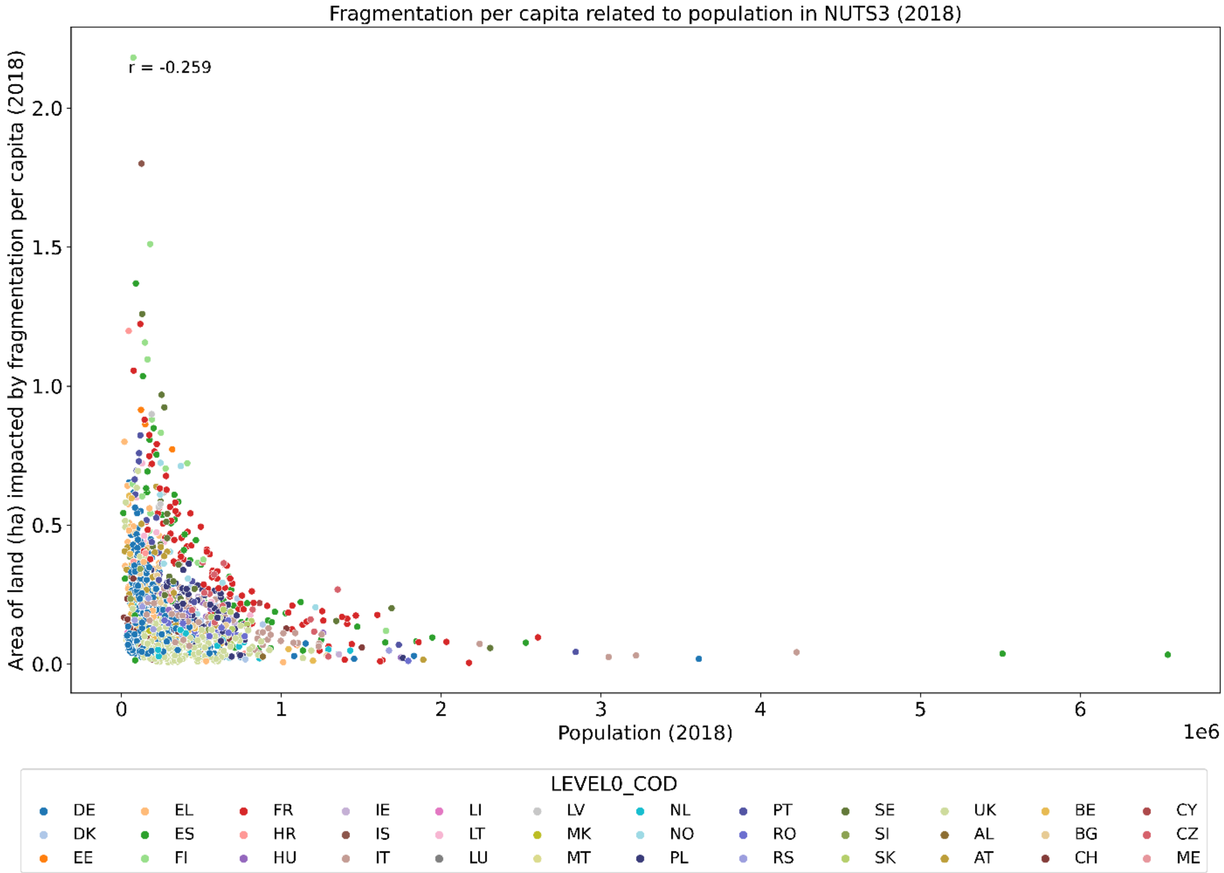

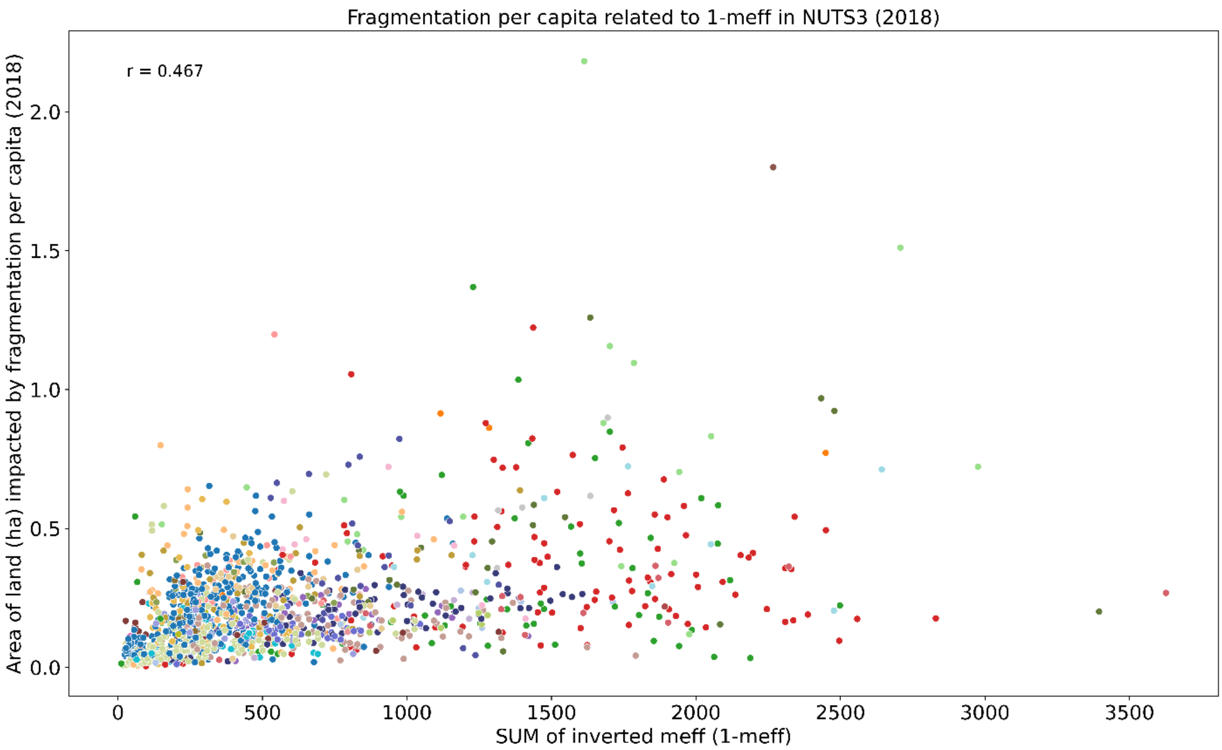

Figure 24: Scatter plots show a correlation (with Pearson correlation coefficient) between fragmentation per capita and associated input data (upper: population; lower: sum of inverted meff values) at the NUTS3 level in European countries (2018).

The correlation between landscape fragmentation per capita and population is further expressed by scatter plots (Figure 24). A weak negative correlation between population and fragmentation per capita shows that regions with higher populations tend to experience lower fragmentation per capita (r = -0.259). This is clearly visible in the most populated NUTS3 regions (e.g. with a population over 2 million) where the fragmentation is shared by a large number of inhabitants. Fragmentation per capita tends to decrease with population growth if the evolution of transport infrastructure is not considered. However, the evolution of the transport network has to be also interpreted in the spatiotemporal context of the evolution of the transportation network. Newly constructed roads in the fragmented and densely populated landscape have a smaller effect on fragmentation per capita when compared with newly built railways or roads in the previously natural landscape even though the total length of this new infrastructure is the same. The moderate positive correlation (r = 0.467) between fragmentation per capita and the sum of inverted meff values for certain regions confirms an important factor which is the density of fragmentation geometry considering also the extent of the analysed region. Administrative units with a denser fragmentation geometry tend to have lower values of fragmentation per capita.

To demonstrate the spatial aspect of fragmentation geometry (transport infrastructure and built-up areas), countries with a similar total length of roads and amount of fragmented landscape can be compared. For example, Albania and Iceland represent countries with very small overall lengths of transport infrastructure (Albania: 9559.7 km; Iceland: 7520.8 km), similar extents of fragmented landscape and, in addition, also a large proportion of natural landscape (Table 10). Although Iceland is significantly larger than Albania, its population is more than 8 times smaller. These aspects classify such countries into completely different groups of fragmentation per capita values.

Table 10: Resulting fragmentation per capita (amount of land impacted by fragmentation per person) for selected European countries with some characteristic of input variables (total length of roads, sum of inverted meff values and population, all for 2018). Selected countries represent different groups regarding the fragmentation per capita values.

NUTS0	length of roads (2018)	SUM of inverted meff (2018)	population (2018)	fragmentation per capita (ha)	ranking (EEA38+UK)	class (according to the frag. per capita)
MT	598.6	164.9	475701	0.0347	1	very low
UK	103715.1	46247.9	66273576	0.0698	3	very low
AL	9559.7	2857.5	2870324	0.0996	5	very low
CH	29978.6	9004.7	8484130	0.1061	6	low
BE	35587.4	12994.6	11398589	0.114	11	low
SK	19391.5	8027.4	5443120	0.1475	17	low
DK	21028.8	8812.9	5781190	0.1524	18	moderate
IE	20309.1	7914.8	4830392	0.1639	22	moderate
AT	55830.3	17509.2	8822267	0.1985	26	moderate
CZ	59287.4	21442.6	10610055	0.2021	27	high
FR	458859.2	146796.2	67026224	0.219	30	high
SE	78364.2	28456.4	10120242	0.2812	33	high
NO	53727.3	16719.3	5295619	0.3157	34	very high
EE	17270.7	5935.8	1319133	0.45	37	very high
IS	7520.8	2427.4	348450	0.6966	39	very high

When providing a similar comparison of population and transport infrastructure for all countries in Europe, it is evident that a similar classification can be applied. On the one side, they are countries with a relatively extensive infrastructure (regarding their population). While, on the other side, such countries where the impact of the transport network is significantly mitigated by a higher population.

Typical examples from the first group of countries are large countries with a lower population density where the transport network often passes through a natural or at least less artificially fragmented landscape (such countries cluster on the left side of the diagonal in the zoom-in scatter plot; Figure 25). The second group is represented by countries with a high population density, which corrects the fragmentation impact of the transport infrastructure (such countries are on the right side of the diagonal in the mentioned zoom-in scatter plot, Figure 25). For countries with low values fragmentation per capita can be stated, that the population is effectively connected through the transport infrastructure and via versa.

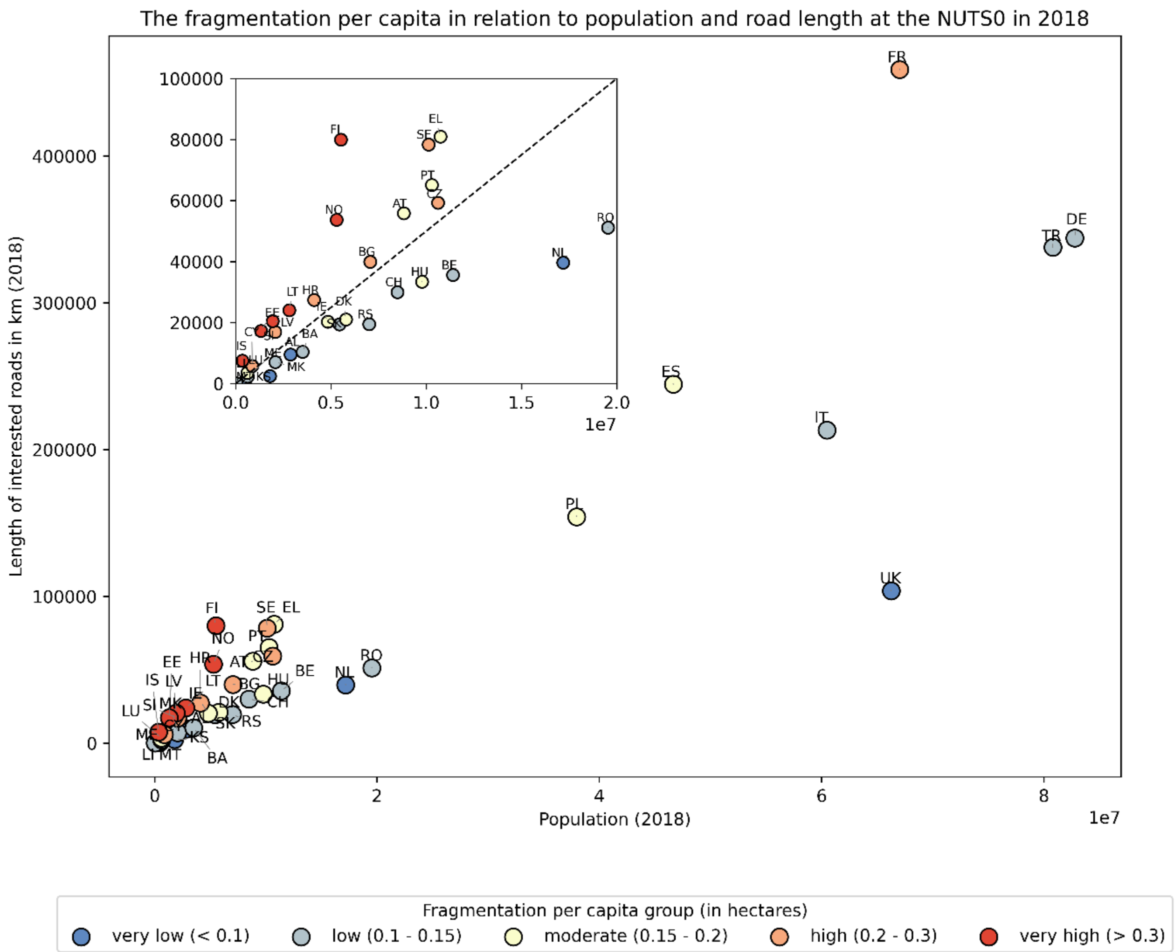

Figure 25: The scatter plot shows European countries (NUTS0 codes) classified according to computed fragmentation per capita regarding population and total length of interested road classes. The highest fragmentation per capita (in hectares) is in Iceland (0.697) while the lowest is in Malta (0.035). Zoom-in chart divided by diagonal provides a clear view for countries with populations up to 20 million and with total length of road classes up to 100 thousand km.

Table 11: Fragmentation per capita shows the average area of land impacted by fragmentation per person (ha) in EEA38+UK in 2012, 2015 and 2018. Observed discrepancies in some countries come from inconsistencies in TomTom input data further described in the following chapters.

		2012			2015			2018		
NUTS	area [km^2]	pop.	∑ (1-meff)	Frag per cap (ha)	pop.	∑(1-meff)	Frag per cap (ha)	pop.	∑(1-meff)	Frag per cap (ha)
AL	28780	2903008	900.5	0.0310	2885796	3546.1	0.1229	2870324	2857.5	0.0996
AT	83929	8408121	17470.4	0.2078	8584926	17478.0	0.2036	8822267	17509.2	0.1985
BA	51221	3839265	1649.6	0.0430	3825334	3678.6	0.0962	3500295	3945.0	0.1127
BE	30652	11075889	12974.8	0.1171	11237274	12982.4	0.1155	11398589	12994.6	0.1140
BG	110999	7327224	14553.7	0.1986	7202198	14446.0	0.2006	7050034	14260.6	0.2023
CY	9249	862011	851.7	0.0988	847008	1871.9	0.2210	864236	1892.4	0.2190
CZ	78886	10505445	21408.0	0.2038	10538275	21411.5	0.2032	10610055	21442.6	0.2021
DE	357656	80327900	118768.8	0.1479	81197537	118531.4	0.1460	82792351	118675.4	0.1433
DK	43139	5580516	8737.9	0.1566	5659715	8754.1	0.1547	5781190	8812.9	0.1524
EE	45328	1325217	5983.8	0.4515	1314870	5942.5	0.4519	1319133	5935.8	0.4500
EL	131685	11086406	20081.7	0.1811	10858018	20100.7	0.1851	10741165	20143.8	0.1875
ES	505997	46818219	72713.8	0.1553	46449565	72841.3	0.1568	46658447	72899.9	0.1562
FI	337529	5401267	28079.2	0.5199	5471753	28086.4	0.5133	5513130	28132.4	0.5103
FR	548901	65276983	146523.3	0.2245	66458153	146614.8	0.2206	67026224	146796.2	0.2190
HR	56547	4275984	9338.1	0.2184	4225316	9238.2	0.2186	4105493	9092.9	0.2215
HU	93020	9931925	15452.2	0.1556	9855571	15530.7	0.1576	9778371	15604.1	0.1596
CH	41289	7954662	8971.2	0.1128	8237666	8976.6	0.1090	8484130	9004.7	0.1061
IE	69949	4589287	7771.1	0.1693	4677627	7825.6	0.1673	4830392	7914.8	0.1639
IS	102689	319575	228.0	0.0714	329100	2383.3	0.7242	348450	2427.4	0.6966
IT	300622	59394207	68101.9	0.1147	60795612	67962.7	0.1118	60483973	68053.5	0.1125
KS	10910	1780021	611.1	0.0343	1804944	1052.3	0.0583	1798506	1122.8	0.0624
LI	161	36475	43.0	0.1180	37366	43.0	0.1152	38114	43.1	0.1130
LT	64893	3003641	9028.7	0.3006	2921262	9043.0	0.3096	2808901	9048.9	0.3221
LU	2594	524853	1021.6	0.1947	562958	1023.5	0.1818	602005	1022.6	0.1699
LV	64578	2044813	7696.3	0.3764	1986096	7526.2	0.3789	1934379	7532.7	0.3894
ME	13877	620308	321.1	0.0518	622099	791.2	0.1272	622359	794.4	0.1277
MK	25442	2059794	866.3	0.0421	2069172	1719.4	0.0831	2075301	2296.0	0.1106
MT	321	417546	164.2	0.0393	439691	164.2	0.0374	475701	164.9	0.0347
NL	37407	16730348	13705.8	0.0819	16900726	13709.9	0.0811	17181084	13750.0	0.0800
NO	323388	4985870	16649.4	0.3339	5166493	16684.0	0.3229	5295619	16719.3	0.3157
PL	311940	38063792	61335.2	0.1611	38005614	61597.7	0.1621	37976687	61646.4	0.1623
PT	91885	10542398	19687.9	0.1867	10374822	19890.3	0.1917	10291027	19948.2	0.1938
RO	238367	20095996	16477.2	0.0820	19870647	24354.2	0.1226	19533481	24447.7	0.1252
RS	77477	7216649	4084.6	0.0566	7114393	8333.0	0.1171	7001444	8388.9	0.1198
SE	449675	9482855	28376.9	0.2992	9747355	28412.6	0.2915	10120242	28456.4	0.2812
SI	20273	2055496	4901.7	0.2385	2062874	4912.0	0.2381	2066880	4911.5	0.2376
SK	49023	5404322	7973.7	0.1475	5421349	7995.5	0.1475	5443120	8027.4	0.1475
TR	780121	74724269	87903.2	0.1176	77695904	91906.0	0.1183	80810525	95909.0	0.1187
UK	244661	63495088	45945.9	0.0724	64853393	46182.8	0.0712	66273576	46247.9	0.0698

The area weighted average meff varies significantly across the DEGURBA classes which confirms differences in landscape fragmentation over different urbanization levels (Figure 26). The mostly uninhabited areas show overall the highest meff values, indicating large, contiguous natural areas with minimal fragmentation. This result aligns with expectations given the sparse human presence in these regions, The average meff varies significantly across the DEGURBA classes which confirms differences in which allows for preserving vast, uninterrupted landscapes. Conversely, cities and towns exhibit much lower average meff values, indicating higher fragmentation levels due to intensive urban development. The Kruskal-Wallis test confirms that the overall difference across all DEGURBA classes is statistically significant. Results of pairwise Dunn’s posthoc test further reveal that the differences in meff are statistically significant between most pairs of DEGURBA classes (Figure 27). However, observed differences between suburbs and villages, are not statistically significant, surprisingly suggesting similar fragmentation characteristics in these classes.

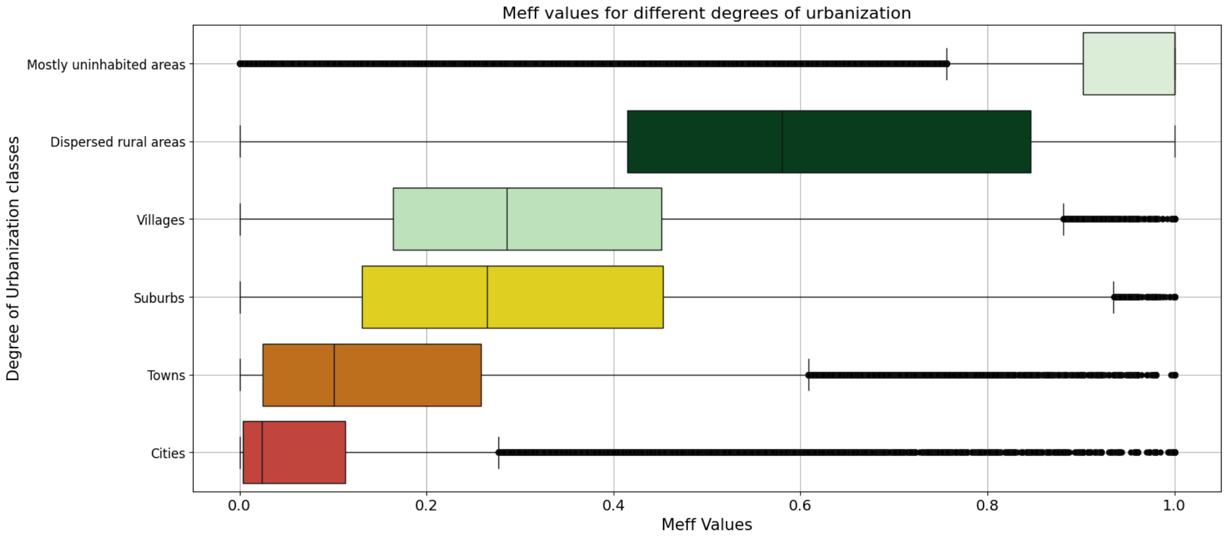

Figure 26: The box plots show significant differences in average meff values (2018) for different DEGURBA classes, generally confirmed by the Kruskal-Wallis test (p<0.5), although the observed difference between villages and suburbs is very small. –

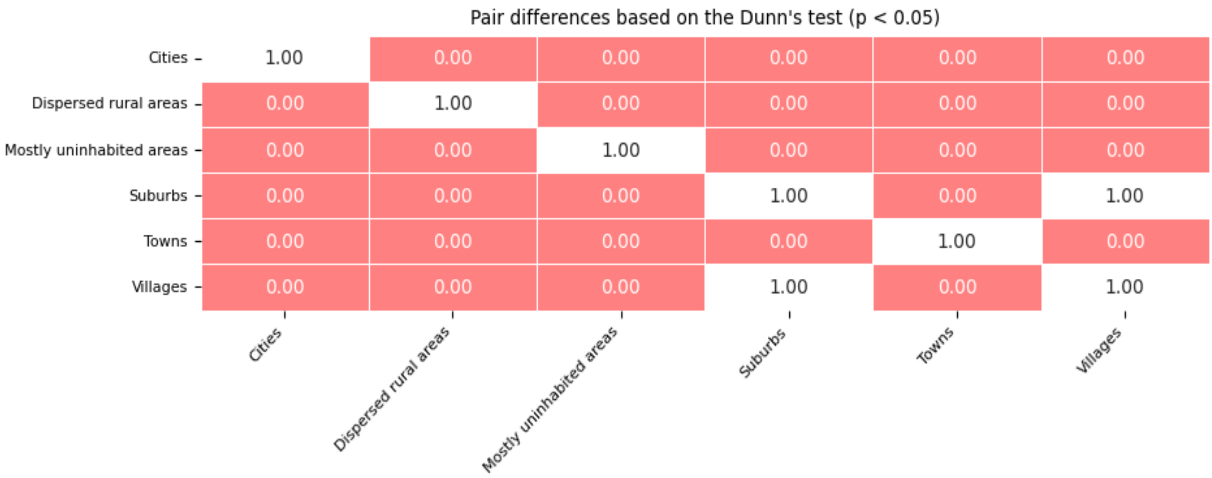

Figure 27: Dunn's test further confirms differences in mean meff values (2018) between all different pairs of DEGURBA classes (p-value is significantly lower than 0.05, highlighted by red) except villages and suburbs where the observed difference is not statistically significant.

The analysis of the average fragmentation per capita shows a reverse urban-rural gradient trend compared to the simple average meff (Figure 28). The box plots demonstrate that mostly uninhabited areas have much higher median fragmentation per capita compared to other classes. This is expected, given the low population density and extensive natural landscapes in these areas, which result in a higher fragmentation value when calculated on a per capita basis. In contrast, urbanized areas such as cities and towns display much lower median fragmentation per capita values, reflecting the concentrated population and more efficient land use in these regions. Unlike the average meff, the Dunns test confirms the differences in average fragmentation per capita between all pairs of DEGURBA classes.

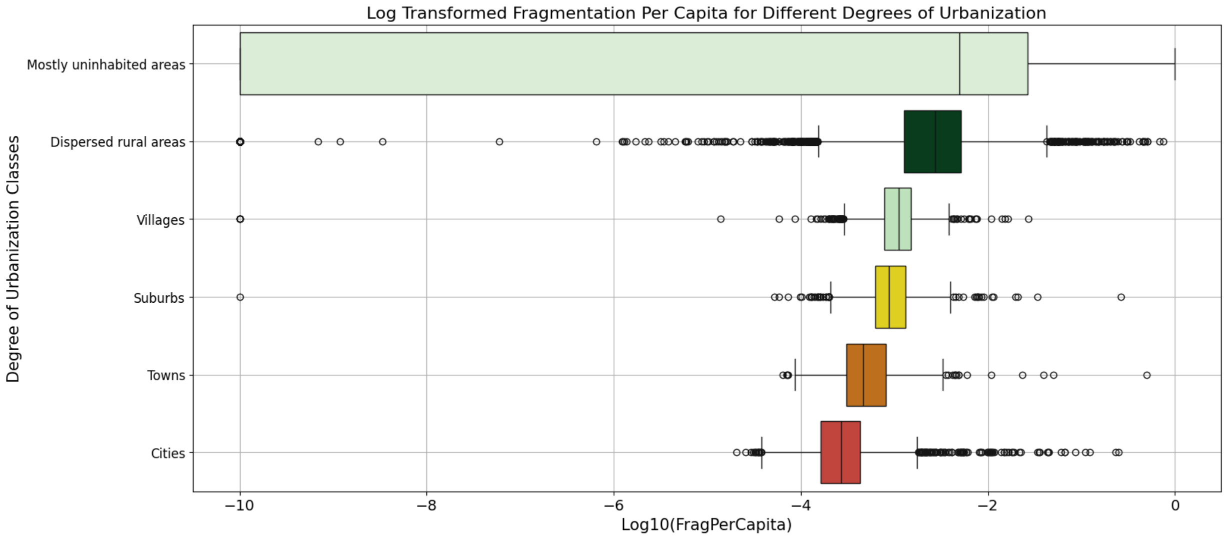

Figure 28: The box plots display significant differences in average fragmentation per capita values (log-transformed) for different DEGURBA classes. Values are expressed in a logarithmic scale to highlight differences between classes.

The observed relation of fragmentation per capita between different DEGURBA classes observed within European-wide analysis is also investigated across the countries (Figure 29) and various NUTS3 regions in Europe (Figure 30, Appendix L-Q).

The observed trend when the average fragmentation per capita decreases from the mostly uninhabited areas through villages and suburbs up to cities where it is the lowest is confirmed here. However, some interesting findings observed in the European-wide analysis can be further explored here in a closer look. This includes an explanation of why DEGURBA class of 'Mostly uninhabited areas' which is generally characterized by its high fragmentation per capita sometimes has extremely low values, even lower than those densely populated cities. The explanation of these observation is mainly related to the fragmentation in remote areas where significant fragmentation can still occur due to infrastructure like roads, railways, power lines, or other human activities and built-up areas without population. Examples of these cases include extensive long roads passing through the mostly uninhabited regions or at least regions with very low population density such as northern parts of Europe (e.g. Iceland or Norway). Although the northern European countries are typical by their low population density, similar exploration is observed also in those regions which have some extensive natural mountainous areas such as Scotland (the UK), Alps (e.g. Switzerland, Italy, or Balkan Dinaric (e.g. Croatia, Bosnia). Another possible explanation for these extremely low fragmentation per capita values includes an absence of analysed road classes in certain regions (e.g. Albania).

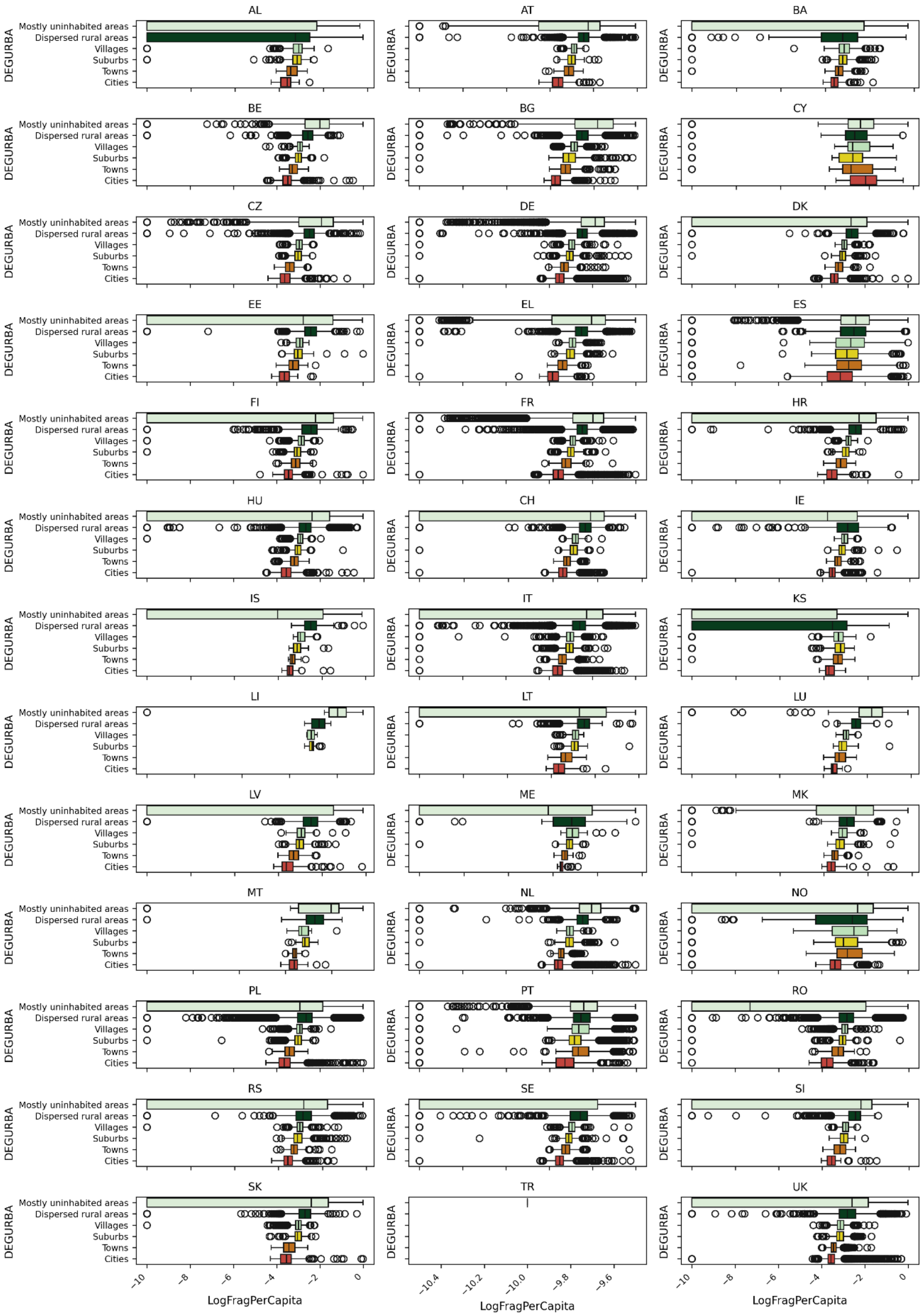

Figure 29: The combined box plots show significant differences in average fragmentation per capita values (in km^2, log-transformed) for different DEGURBA classes across NUTS0, usually in line with European-wide analysis. Values are expressed in a logarithmic scale to highlight differences between classes. DEGURBA is not available in Turkey.

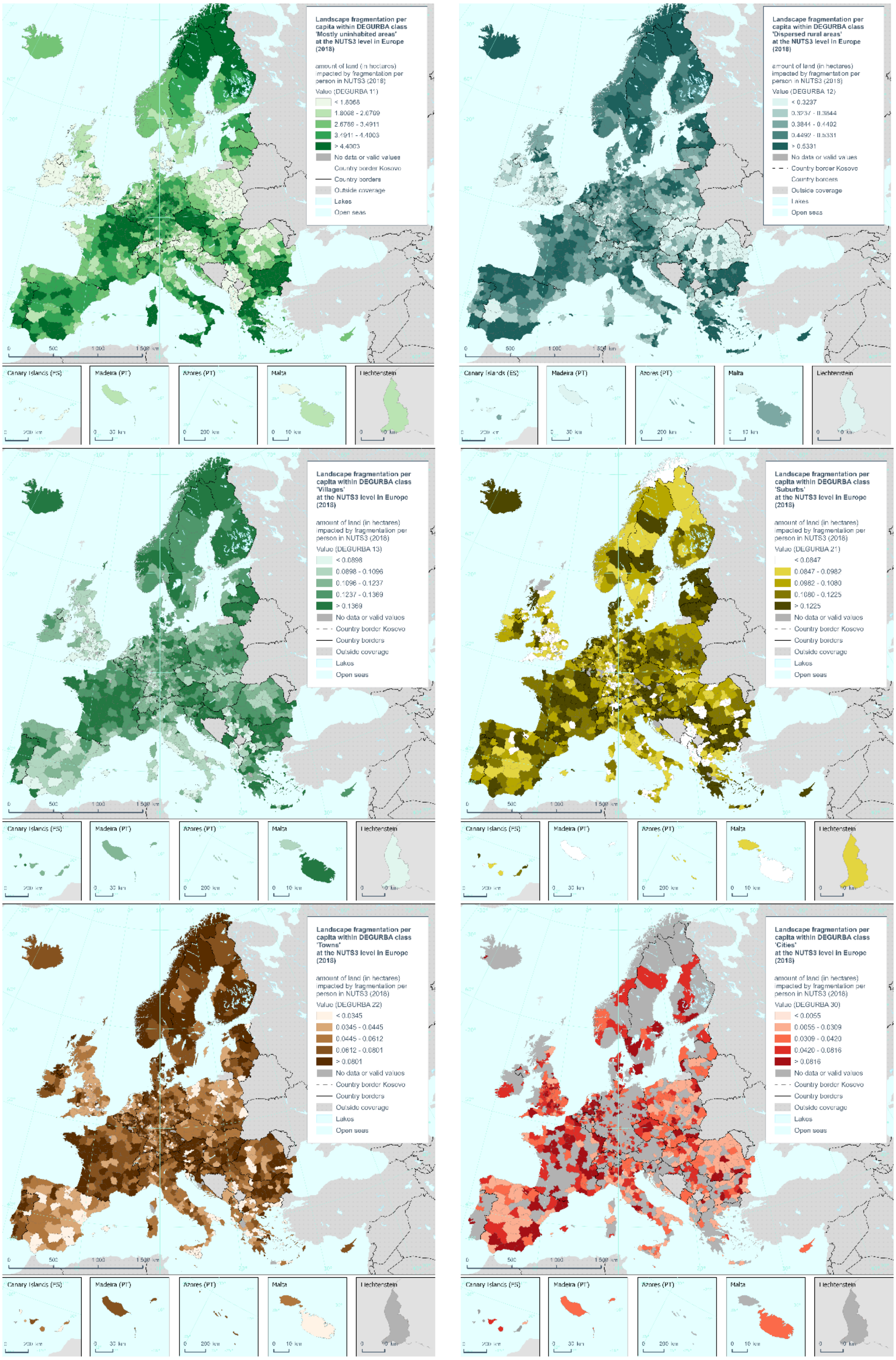

Figure 30: Mean fragmentation per capita according to DEGURBA in the NUTS3 across Europe (2018). Certain DEGURBA classes are missing in some regions. Full size maps are attached (Appendix L-Q).

Exploring average fragmentation per capita according to the DEGURBA classes at the NUTS3 level reveals the spatial heterogeneity within individual countries and identifies distinct patterns of settlement across Europe (Figure 30, Appendix L-Q).

The relatively low landscape fragmentation per capita in some NUTS3 regions can be attributed to compact settlement structures, where cities, towns, or villages are densely populated. In contrast, in more dispersed or sprawling areas with less compact settlements, where population density is lower and spread over a larger area, fragmentation per capita tends to be higher as fewer people share the fragmented landscape. This relationship explains why regions with concentrated populations often experience lower landscape fragmentation per person compared to more rural or dispersed regions.

The UK and the Benelux region serve as examples of countries with relatively low fragmentation per capita across almost all DEGURBA classes in their NUTS3 regions. These countries are characterized by high-density settlement clusters. When settlements are compact, and populations are concentrated within smaller areas, fragmentation per capita tends to be lower. This is because the fragmented land (infrastructure, roads, or built-up areas) is shared by a larger population within a confined space. In densely populated, compact urban areas, more individuals share the same fragmented landscape, reducing the amount of fragmentation per person. On the other hand, countries like France and Norway exhibit more dispersed settlement patterns, which results in higher fragmentation per capita. In such countries, populations are spread out over larger areas, which means that fewer people share the fragmented landscape, increasing the fragmentation per capita.

4.5 Spatial analysis and types of the observed changes in fragmentation

The changes in fragmentation are analysed mainly for 2015 and 2018 as a comparison of 2012 and 2015 reflects significant inconsistencies in TomTom MultiNet data found in some countries. Differences in average meff values are expressed at the NUTS3 level, where it is clear that there are some differences in weighted mean meff values between individual regions which are not in line with the expected evolution. Explanation of the unexpected evolution in meff values requires detailed analysis of the input data (Figure 32). When comparing changes in the transport network and infrastructure in a more detailed view at the pixel basis, it is obvious that especially newly constructed extensive transport infrastructure and extensive changes in built-up areas are best visible even at the continental scale in used spatial resolution while smaller changes related to increases of fragmentation are usually noticed by scattered change pixels (Figure 31).

Indeed, a good example of the extensive increase in the sealed area between 2015 and 2018 which is well captured in the fragmentation pattern is the newly constructed Istanbul Airport (Figure 31 Left). However, the difference raster also captures a new outer ring road or a sub-urban built-up area on the outskirts of the city. It is important to note, that observed changes in the European fragmentation are not often related to the core city because there is usually already a significantly fragmented landscape even at the beginning of the observed period in 2012 (or 2015). For this reason, changes in built-up areas are usually related to the outskirts of the cities and scattered across the rural landscape. However, when comparing changes in the transport network and built-up areas and their effect on fragmentation, the visual signal seems to be stronger for the increase in the transport network. This observation might be explained by the different impacts of both input data. Whereas every change within interested classes of the road network is reflected, new buildings might not have any influence on the values of the output meff index as this analysis works only with IMD values over 30%.

Concerning the observed changes in the transport infrastructure, it can be stated that especially large-scale changes in key elements of the transport infrastructure such as highways and railways, are visually captured even at the pan-European scale. A good example of this group of changes is the new high-speed railways in France or Germany which were constructed during the observed period. For example, the construction of the new railway Tour-Bordeaux started in mid-2012 and was completed in early 2017 and similarly high-speed railway between Le Mans and Rennes, which was opened also during 2017 or railway Erfurt-Leipzig finalized at the end of 2015 (Figure 31 Right).

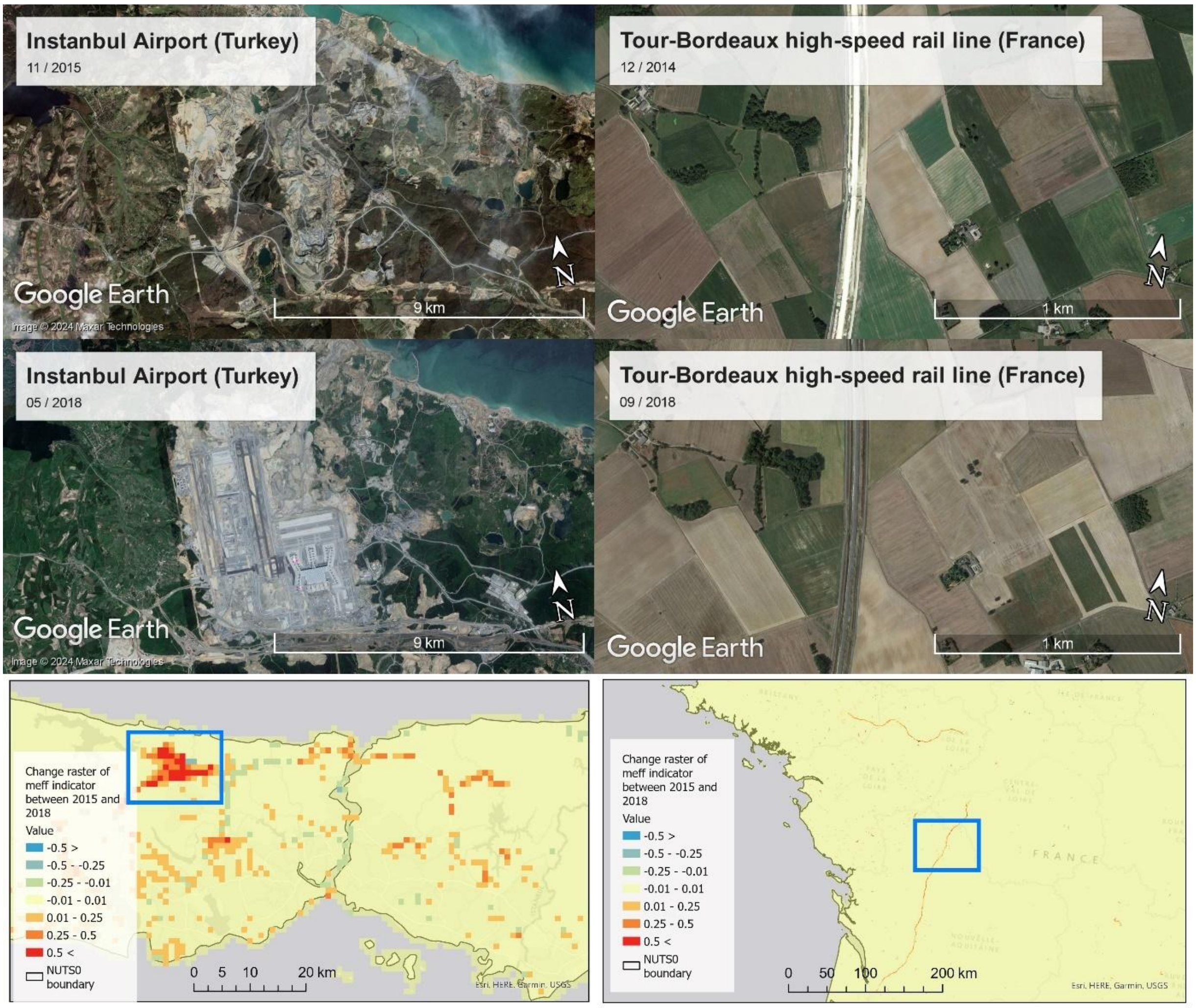

Figure 31: Left – one of the most extensive changes in fragmentation pattern observed in Europe related to the increase of IMD is the newly constructed Istanbul Airport, which was built between 2014–2018. Right – a section of the extensive newly built high-speed railway near Tours in France.

In the case of road networks, Western Europe generally boasts a dense and developed highway, reflecting its longer history of infrastructure investment and higher economic development levels. Countries like Germany, France, and the Netherlands have extensive, well-maintained highways facilitating efficient intra- and inter-country connectivity. The development of transport infrastructure in these countries focuses on modernization and efficiency improvements rather than extensive expansion. In contrast, Eastern Europe has been rapidly improving its transportation infrastructure post-1990s, which is also observed during the analysed period 2012-2018. A good example of the extensive increase in the highway network in Poland.

However, it is important to note that not all of the observed changes in transportation infrastructure must correspond with the real situation. This is because the input (TomTom MultiNet) data are gradually maintained and updated, which includes not only adding new roads but might include also changes due to improving or completing the representation of existing road networks in terms of their total length as well as road classification shifts between different road classes. This represents sometimes a problem in the homogeneity of some pan-European data, which can't be easily tackled and which compromises the interpretation of the results for affected regions not only related to this topic but in general. Thus, the observed status of the road network differs at the country level, but sometimes also within individual countries (e.g. Bosnia and Herzegovina). Therefore, it is not entirely unusual that the input road vectors can be missing in one year, while in the following year, they are supplemented. An explanation of observed changes and issues are described within next chapter.

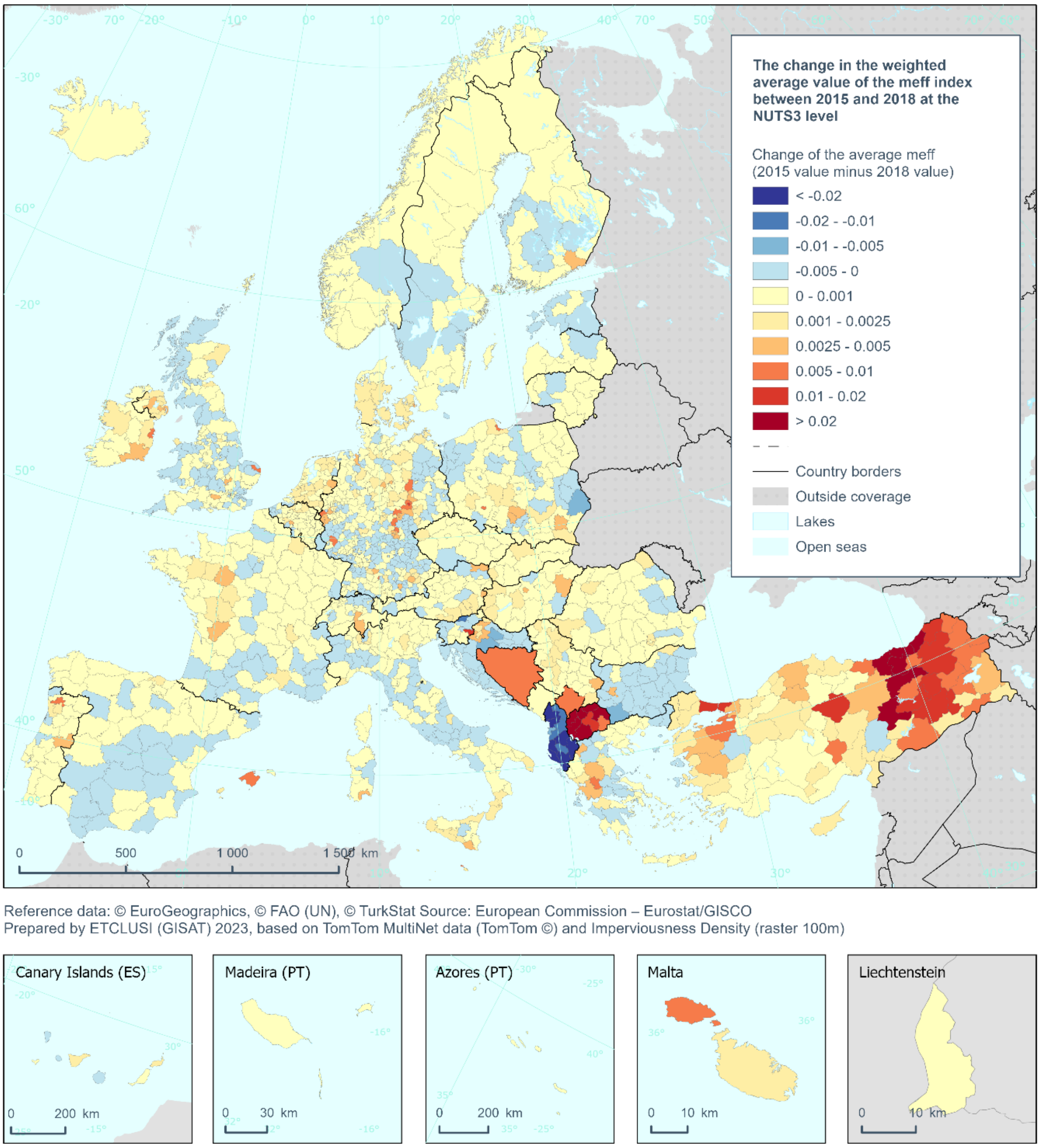

Figure 32: Change in the average meff value between 2015 and 2018 at the NUTS3 level (red = increase, max: 0.0351, Giresun, Turkey, blue = decrease, max: -0.0398, Korçë, Albania). The output of the difference raster shows that the highest increases in fragmentation based on used input data occurred mainly in east Turkey, Bosnia, Montenegro and Macedonia.

5 Discussion

In the overall context, based on the provided basic statistics and histograms, it might be confirmed that the area of the fragmented landscape is gradually increasing throughout the entire area and over almost all countries. However, as already shown in a previous chapter, a lot of observed differences are not entirely consistent with the expectation of the evolution of the meff index. This chapter provides an explanation of these findings.

In general, a newly fragmented landscape is indicated by a gradual decrease of the area within a class with meff values of 1.0-0.9. Thus, the decrease in the area in this category is suitable evidence of the increasing fragmentation over time. While the observed changes between 2015 and 2018 in the 100km grid are generally consistent with the expected landscape evolution (Figure 33), the spatial analysis of changes between 2012 and 2015 indicates strong outlier values in some countries (Figure 34).

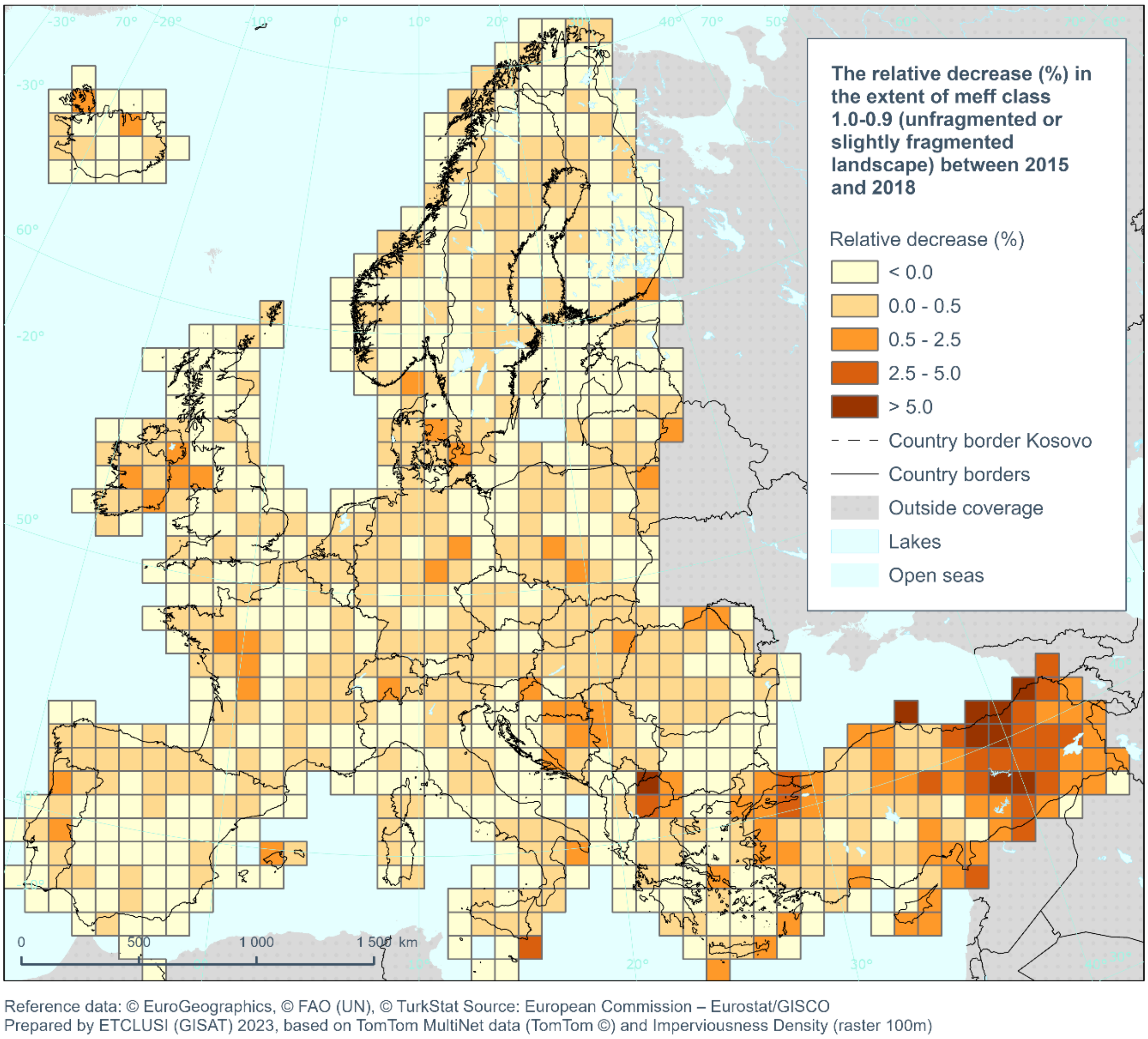

Figure 33: Relative decrease (%) in the extent of unfragmented or slightly fragmented landscape (including meff values within class 1.0 - 0.9) between 2015 and 2018. A slight increase in landscape fragmentation dominates, which corresponds to expectations.

These inconsistencies are detectable by a sharp increase in the extent of areas previously classified as unfragmented that cannot correspond with the real situation. Explanation of these inhomogeneities requires a detailed analysis of the input data, i.e. IMD and TomTom MultiNet. For that reason, the evolution of basic statistics in all countries and all administrative units at the NUTS3 level was compared for both variables (see the detailed comparison for all years attached in Appendix A-F).

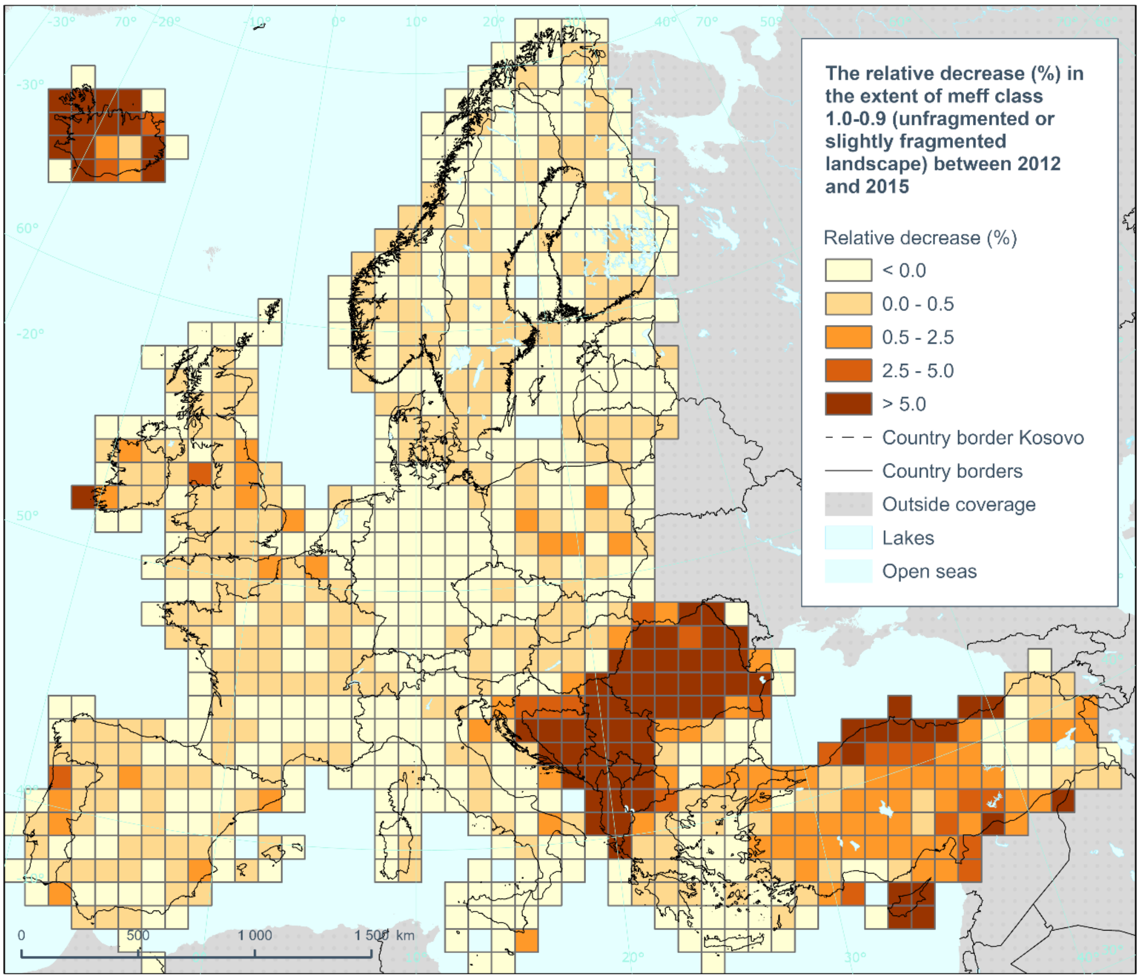

Reference data: © EuroGeographics, © FAO (UN), © TurkStat Source: European Commission – Eurostat/GISCO
Prepared by ETCLUSI (GISAT) 2023, based on TomTom MultiNet data (TomTom ©) and Imperviousness Density (raster 100m)

Figure 34: Relative decrease (%) in the extent of unfragmented or slightly fragmented landscape (meff class 1.0 - 0.9) between 2012 and 2015 highlights the most serious discrepancies indicated by dark brown.

While the evolution of average IMD throughout the entire EEA38+UK territory can be generally characterized by a gradual increase in the average value (Appendix A), the overall area of pixels with IMD over 30% within binary rasters does not have an increasing trend in all administrative units at NUTS3 level (Appendix B). Although the total extent of built-up areas defined within IMD above 30% increased from 202588.92 km^2 in 2012 through 204236.14 km^2 in 2015 up to 205160.78 km^2 in 2018, it slightly decreased in some regions (Figure 35). This decrease in the extent of IMD values over 30 is not significant, however it appears very often, and it is mostly observed in Great Britain, Italy, Spain, Greece or in the German Bavaria. Apart from the mentioned changes in extent, however, the spatial pattern is more interesting, which might be a remnant of the process during the creation of the original HRL IMD data (e.g. griding pattern in Germany).

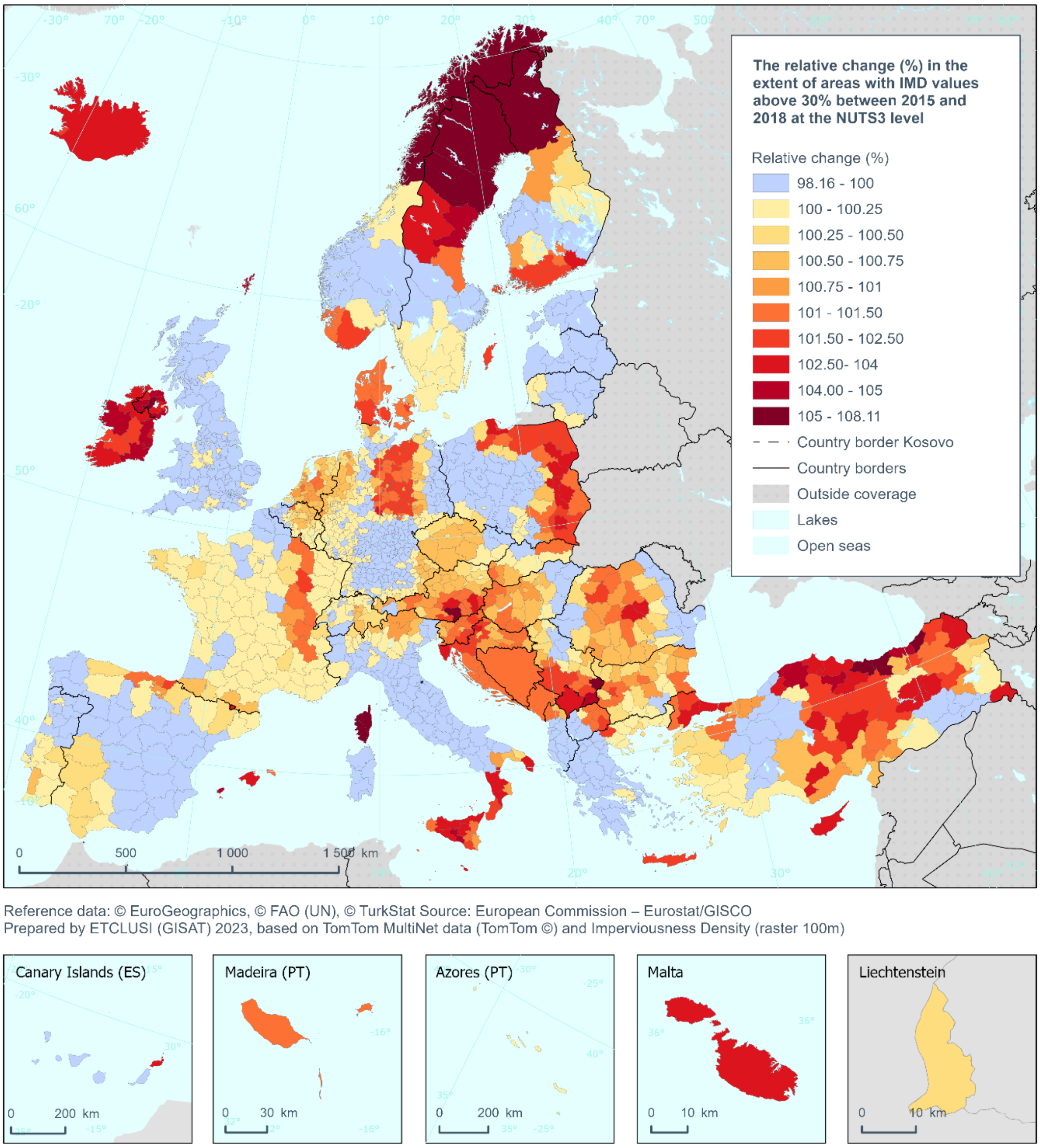

Figure 35: Relative change (%) in the area of IMD values above 30% between 2015 and 2018 at the NUTS3 level. Blue = decrease (min value: 98.16%), red = increase (max value: 108.11%). Artificial line patterns (e.g. East Germany, Bavaria) are similar to satellite tilling grids and might be related to the original process of creating the IMD data.

Regarding the second input data, the methodology of this work uses only classes 0 to 4 (i.e. highway, main road, other main roads, secondary and tertiary roads) and one rail class (rr) to calculate the meff index. The expected condition of consistency of input TomTom data is increasing the total length of transport infrastructure in time. Thus, the road lengths by individual classes and countries (NUTS0) were summarized for 2012, 2015 and 2018, and the observed findings can be divided into three groups considering the seriousness of the identified issue (Figure 36, Figure 39):

- The first group (green) represents countries where there were not any identified issues with summarized TomTom data. This means that the total length of the road has been gradually increasing over time. These differences are usually represented in relative values of hundredths to units of per cent as the average increase in length of road infrastructure (interested classes only) between 2012 and 2015 is by 1% and by 0.95% between 2015 and 2018 in these countries.
- The second group (yellow) are countries where some minor differences that do not correspond to the expected evolution were observed. As an example, the decrease in the length of roads over time (which is an unlikely situation). Observed decreases in this group of countries usually did not exceed 2%. In addition to missing data, another explanation could be the transfer of roads from one class to another that is out of the classes of interest.

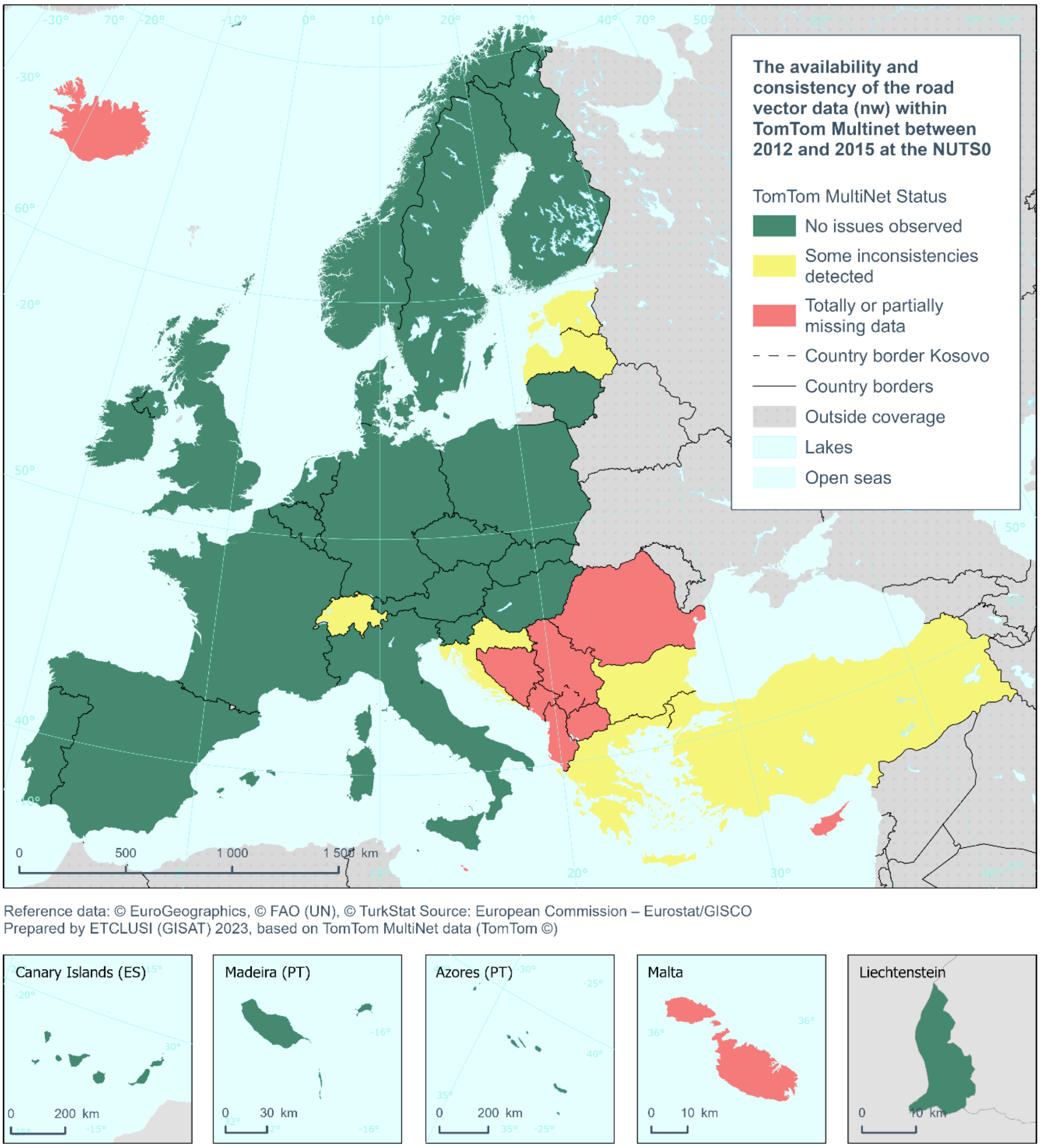

Figure 36: Availability and consistency status of road classes (0, 1, 2, 3 and 4) from the TomTom for 2012 and 2015.

- The third group (red) refers to countries in which more serious deficiencies are identified. In this case, there are no roads at all (Cyprus and Iceland) or a large part of roads (in Balkan countries like Romania, Albania, Macedonia, Serbia, Montenegro, Bosnia and Herzegovina and Kosovo). It is recommended, that the interpretation of the results is carried on only for countries without any observed problems with TomTom MultiNet data. In general, this applies for 2015-2018, but more caution is needed in the 2012-2015 interpretation as guided by Figure 36 and Figure 39.

Although input TomTom data inconsistencies are significantly less serios when comparing 2015 and 2018, some unexpected differences in the length of roads were recognized in south-eastern Europe (Figure 39). Serious inhomogeneities were found in Albania, Kosovo, Bosnia and Macedonia, where a major change between some road classes was observed (Albania, Macedonia) or a large part of roads available in 2018 are missing in the older data (Bosnia). Within Albania, a decrease in summarized length of almost 3000 km was observed, as a significant proportion of roads were moved from class 4 to class 7 (Figure 40, Table 12). Although considering the summary length of all roads (i.e. even those not used in the analysis) overall evolution shows an increase of 113 km from 46374 to 46487 km. Another example of incomplete data is from Bosnia, where large areas without fine patterns of road infrastructure are visible (Figure 37). In addition, the problem of the TomTom data homogeneity seems to also apply to the east Turkey region, as extreme increases in lengths between 2015 and 2018 are observed, up to almost 50% in some NUTS3 regions (Appendix C). Similar shifts might also be in other European countries. However, some observed shifts between road classes might be considered consequences of transportation policies. For example, in Czechia, the freeway class (nw class 1) was cancelled at the end of 2015 and all these roads were moved to highways (nw class 0). This describes the sharp increase in the length of highways from 1549km to 2635km between 2015 and 2018 (Appendix E-F). Shifts between road classes can lead to an increase or decrease in the area of buffer zones and this might affect the values of the meff index.

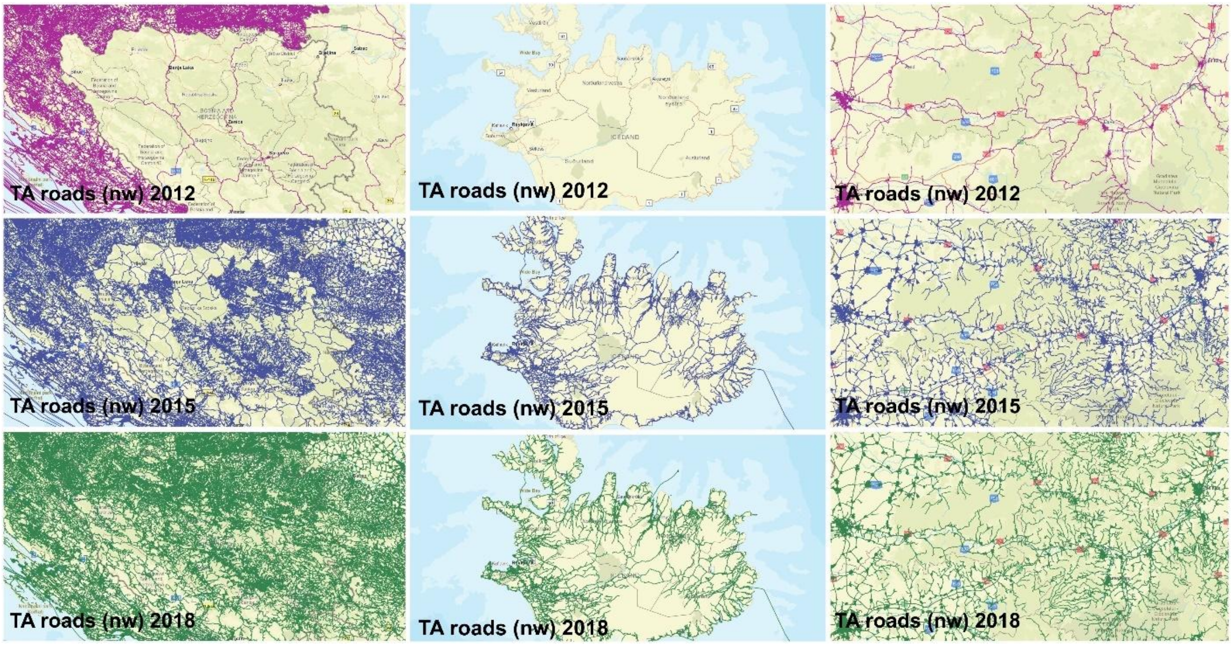

Figure 37: Incomplete TomTom data (all available road classes are visualized) in some countries (left - Bosnia, middle - Iceland, right - Romania).

It seems that the inconsistencies observed in the transportation infrastructures data, especially when comparing the year 2012 explain the observed unexpected trend in fragmentation as previously described by spatial patterns of differences in meff values at the NUTS3 level (Figure 32) as these meff changes closely reflect observed significant differences within the TomTom MultiNet (Figure 38). A detailed analysis at the NUTS 3 level reveals that, even in countries where the total summarized values point to the expected increasing of lenght of road infrastructure, within some regions the observed trend is the opposite.

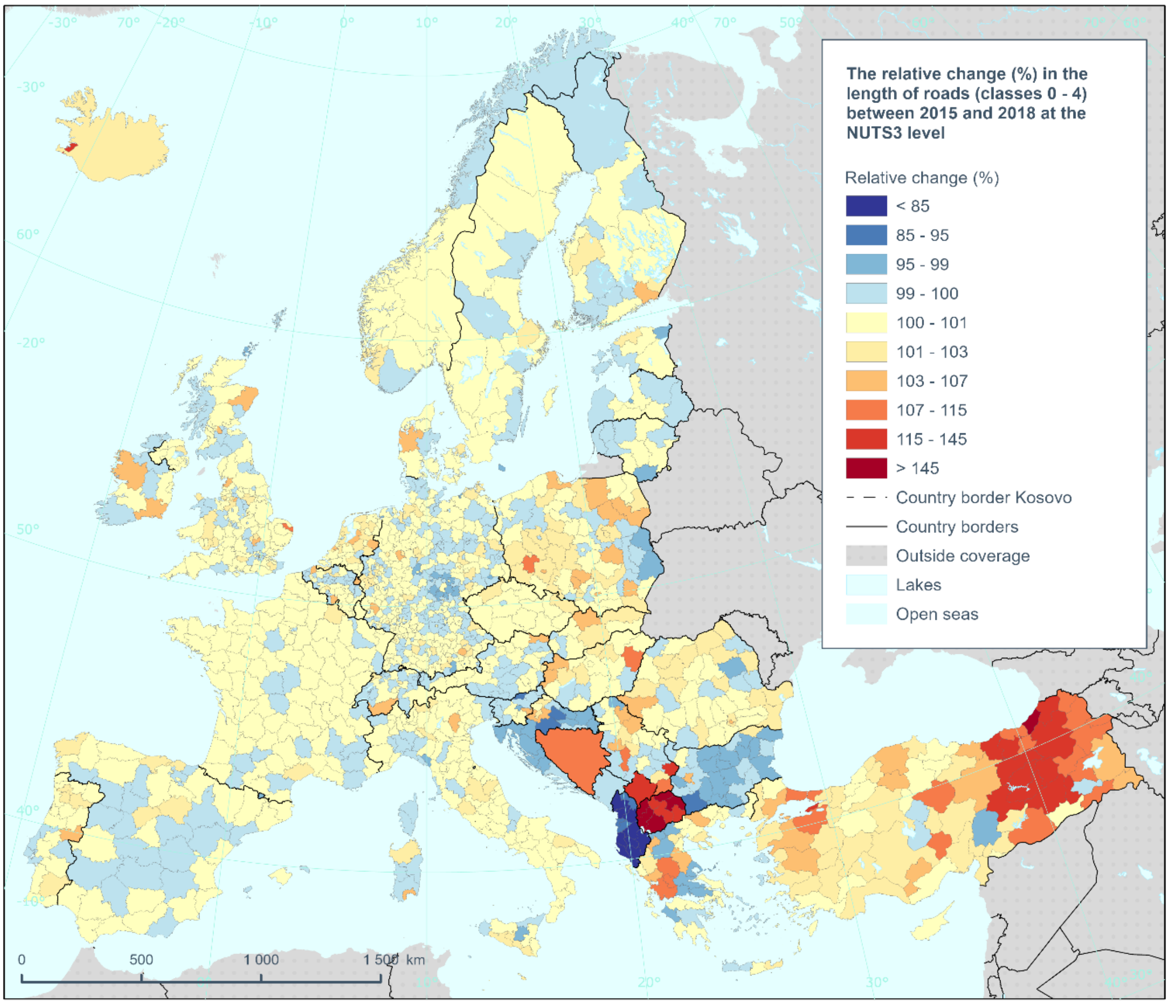

Reference data: © EuroGeographics, © FAO (UN), © TurkStat Source: European Commission – Eurostat/GISCO
Prepared by ETCLUSI (GISAT) 2023, based on TomTom MultiNet data (TomTom ©)

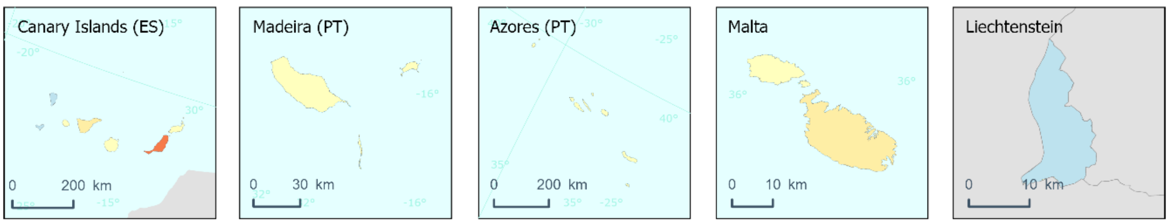

Figure 38: Relative change (%) in the summary length of the analysed road (nw) classes (class 0, 1, 2, 3 and 4) between 2015 and 2018 at the NUTS3 level. Values below 100% indicate a decrease in road length, while values above 100% indicate an increase. Blue = decrease (min value: 59.45%), red = increase (max value: 200.58%).

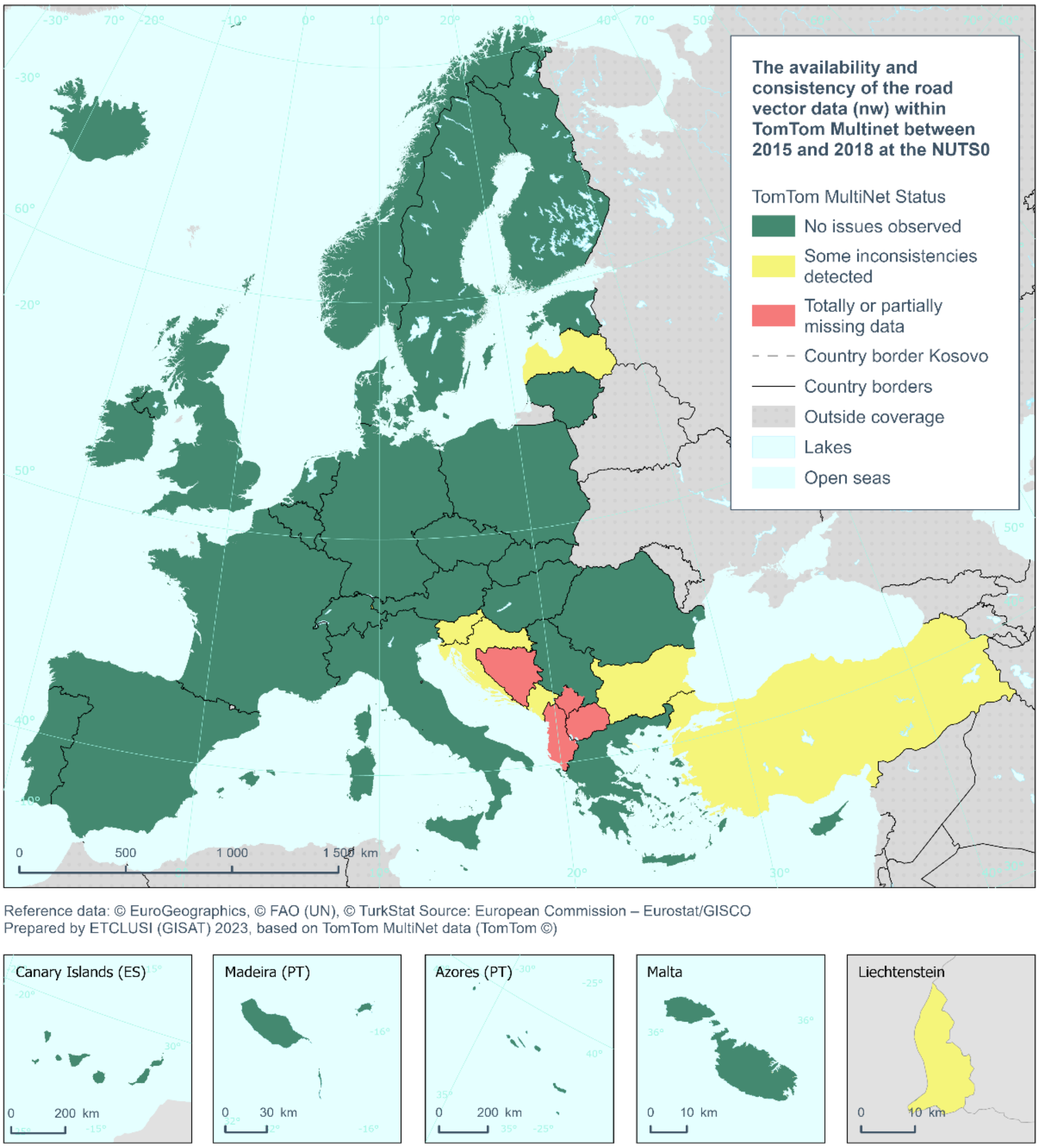

Figure 39: Availability and consistency status of road classes (0, 1, 2, 3 and 4) from the TomTom for 2015 and 2018.

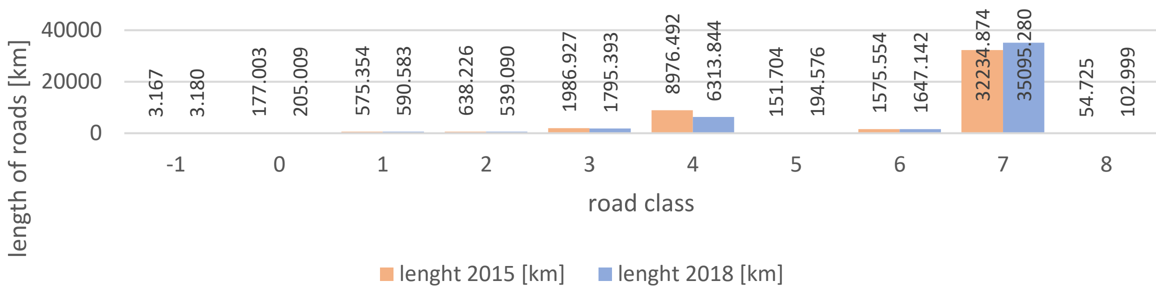

Figure 40: Part of the roads in Albania were shifted from classes 2, 3 and 4 (other main roads, secondary and local connecting roads in 2015) to class 7 which is out of the classes of interest in 2018.

Table 12: Comparison of road network length in Albania in 2015 and 2018 based on the TomTom MultiNet.

road class	length in 2015 [km]	length in 2018 [km]
-1	3.167	3.180
0	177.003	205.009
1	575.354	590.583
2	638.226	539.090
3	1986.927	1795.393
4	8976.492	6313.844
5	151.704	194.576
6	1575.554	1647.142
7	32234.874	35095.280
8	54.725	102.999
Sum of all classes	46374.027	46487.097
Sum of interested classes	12354.002	9443.919

Even inconsistencies in road vector shape might potentially lead to detectable observations. That is because the meff index with the non-CBC method takes into account not only the size of patches but also their shape, which may lead to small changes in the resulting meff values between two years and thus false detection of changes in the change raster, especially if the element of fragmentation geometry is moved to another tile of the grid or surrounding built-up areas (Figure 41). For longer line features through the many pixels, this can cause alternating rising and falling pixel values, even though no real changes have occurred. Therefore, these types of very small changes cannot be considered proof conclusive in terms of a real change.

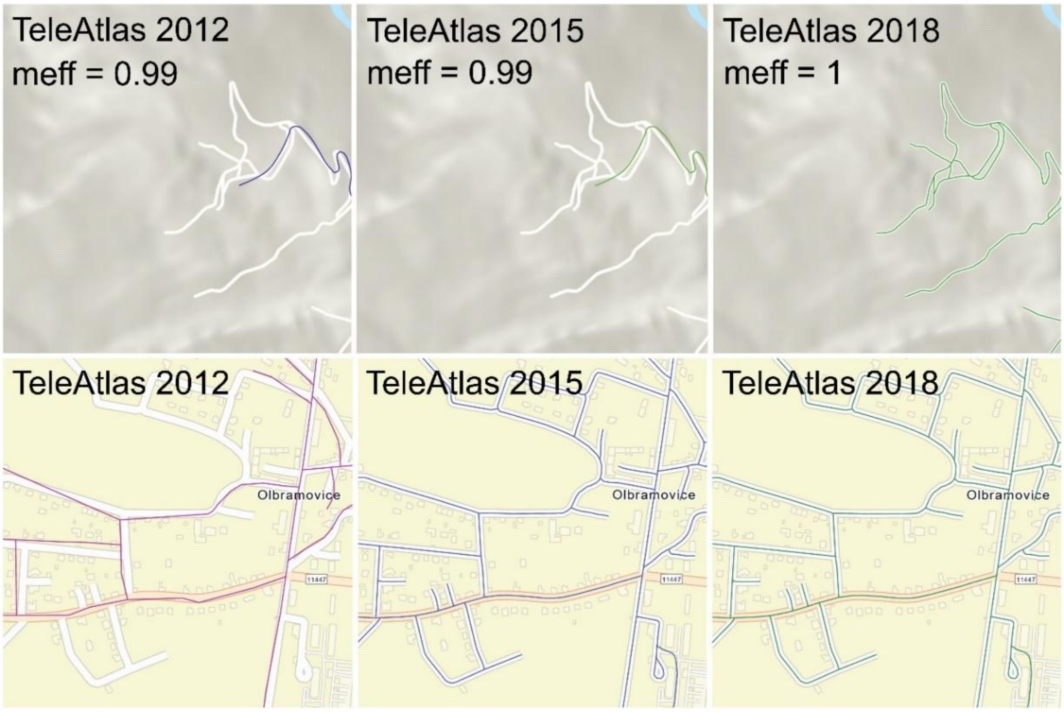

Figure 41: Other examples of the inconsistencies (EPSG:3035, upper images: XY= 6837500E, 2479500N m, lower images: XY=4644500E, 295500N m). The images above show a decrease in fragmentation despite the increasing length of the roads (movement of roads from class 4 to class 7). Similarly, the images below indicate the geometric discrepancy of TomTom 2012 as well as its incompleteness.

6 Conclusion

This study presents a comprehensive assessment of landscape fragmentation across Europe, focusing on the impacts of the expansion of built-up areas and transportation infrastructure. While these factors are significant drivers of fragmentation—leading to the division of large, contiguous natural habitats into smaller, isolated patches—it is important to acknowledge that they are not the sole contributors. Human activities such as agricultural expansion, deforestation, resource extraction, and climate change also play pivotal roles in altering land use and land cover. However, these elements were beyond the scope of this study, and their specific contributions to landscape fragmentation remain unexplored here.

The methodology employed in this study, particularly the non-cross boundary (non-CBC) approach, demonstrated several advantages, including its resilience to inconsistencies in transportation infrastructure data. However, it also presented limitations, such as the potential for scattered results and the overrepresentation of minor roads in some areas, like northern Finland, where even isolated roads are captured in continental-scale maps. These considerations underscore the complexity of landscape fragmentation analysis and highlight the importance of considering local context and data characteristics when interpreting results.

The study also addressed the challenges posed by regions with significantly heterogeneous borders, such as rugged coastlines and small islands. The non-CBC meff index has proven reliable in interpreting landscape fragmentation in these areas, despite inherent difficulties in calculation and interpretation. Moreover, the spatial resolution used was sufficient to capture the landscape's heterogeneity, even in complex coastal zones. The analysis of meff values across various NUTS3 units further illuminates the spatial heterogeneity of landscape fragmentation across Europe. The varying sizes of these units, coupled with the absence of detailed administrative divisions in certain regions, complicate the interpretation of fragmentation patterns. This observation suggests that future studies may benefit from the use of standardized spatial units to ensure consistency and comparability.

The findings across various administrative levels align with expected temporal trends, showing an overall increase in fragmentation, characterized by a decrease in unfragmented areas and an increase in moderately to highly fragmented landscapes. This trend reflects the growing impact of anthropogenic activities on natural habitats. Using the meff index, the study offers a detailed spatial-temporal analysis of habitat connectivity and fragmentation across Europe from 2012 to 2018. Fragmentation levels vary significantly between regions, with Western European countries like Belgium, the Netherlands, and Luxembourg exhibiting higher levels of fragmentation, while lower levels are observed in Northern Europe and certain Balkan countries.

One of the key dimensions explored was the relationship between fragmentation per capita and the DEGURBA classes. Areas classified as 'Cities' (DEGURBA 30) generally exhibited lower fragmentation per capita, driven by concentrated infrastructure and built-up areas. In contrast, 'Mostly Uninhabited Areas' (DEGURBA 11) showed high fragmentation per capita, though with higher variance. This variance can be attributed to isolated infrastructure, such as roads and railways in large, sparsely populated natural areas. Regions classified as 'Villages' (DEGURBA 13) and 'Towns' (DEGURBA 22) exhibited moderate levels of fragmentation, influenced by the density and distribution of settlements. More compact settlements tend to have lower fragmentation per capita than more sprawling ones. These findings emphasize that urbanization patterns, population density, and spatial distribution are crucial in determining the degree of fragmentation experienced by different regions.

The reliability of this fragmentation analysis is closely tied to the quality of the underlying data. While TomTom MultiNet data provided comprehensive coverage, inconsistencies and gaps in the archived data posed challenges to the analysis. As a result, the meff index outputs do not always reflect the real situation. These issues highlight the need for accurate and consistent data sources to improve the validity of future studies' conclusions.

In conclusion, this study offers valuable insights into the dynamics of European landscape fragmentation, driven by built-up area expansion and transportation infrastructure development. The analysis also highlights spatial patterns linked to urbanization, as demonstrated by the fragmentation trends observed across different DEGURBA classes. Despite some inconsistencies in the TomTom MultiNet data, the overall consistency of the input data is sufficient for a Europe-wide interpretation. The study shows how Copernicus data can be effectively combined with other European datasets to deliver comprehensive spatial-temporal assessments. Nevertheless, areas with inconsistent data require careful consideration, and the report provides guidance for assessing such areas.

References

EEA. European Environment Agency (EEA) and Swiss Federal Office for the Environment (FOEN) (eds.) (2011): Landscape fragmentation in Europe. Joint EEA-FOEN report. EEA Report No 2/2011. Authors: Jochen A. G. Jaeger. Tomáš Soukup. Luis F. Madriñán. Christian Schwick and Felix Kienast. ISBN 978-92-9213-215-6ISSN 1725-9177doi:10.2800/78322.

Gustafson E. J. (1998): Quantifying landscape spatial pattern: What is the state of the art? Ecosystems. 1(2): 143-156.

Hanski I. (1999): Metapopulation Ecology. Oxford Series in Ecology and. Evolution, Oxford University Press, Oxford, U.K., 313 pp.

Jaeger J. A. G. (2000): Landscape division. splitting index. and effective mesh size: New measures of landscape fragmentation. Landscape Ecology 15(2): 115–130.

MacArthur R.H., Wilson E.O. (1967): The Theory of island biogeography. Princeton Univ. Press, U.S., 203 pp.

Maucha G., Kerékgyártó É., Turos V., Sannier C., Dufek J., Soukup T., Ivits E. (2024). Analysis of Usability of Imperviousness and CLC Backbone Data for Mapping Sealed Areas (ETC/DI Report 2024/3). European Topic Centre on Data Integration (ETC/DI). Available at: https://www.eionet.europa.eu/etcs/etc-di/products/etc-di-report-2024-3-analysis-of-usability-of-imperviousness-and-clc-backbone-data-for-mapping-sealed-areas

Moser B., Jaeger J. A. G., Tappeiner U., Tasser E., Eiselt B. (2007): Modification of the effective mesh size for measuring landscape fragmentation to solve the boundary problem. Landscape Ecology 22(3): 447-459.

Sannier C., Ivits E., Maucha G., Maes J., Dijkstra L. (2024): Harmonized Pan-European Time Series for Monitoring Soil Sealing. Land. 13(7): 1087.

Appendices

Appendix A: General descriptive statistics of harmonized IMD in EEA38+UK countries (NUTS0 level).

		2012		2015		2018	
NUTS0	area [km^2]	mean	std	mean	std	mean	std
AL	28780	1.5229	8.6585	1.5306	8.6810	1.5373	8.7221
AT	83929	3.9379	13.3457	3.9439	13.3622	3.9809	13.4679
BA	51221	1.4443	7.6754	1.4565	7.7256	1.4680	7.7809
BE	30652	11.6003	23.2307	11.6417	23.2909	11.7264	23.4395
BG	110999	1.9337	9.9522	1.9447	9.9809	1.9582	10.0272
CY	9249	5.1312	16.4421	5.2888	16.7825	5.4409	17.1557
CZ	78886	4.3252	14.9401	4.3374	14.9674	4.3670	15.0571
DE	357656	7.1471	19.7021	7.1734	19.7539	7.2154	19.8450
DK	43139	5.7499	16.3094	5.7611	16.3321	5.8267	16.4718
EE	45328	1.4802	6.8834	1.4887	6.9373	1.4914	6.9624
EL	131685	2.3459	10.6667	2.3561	10.6911	2.3737	10.7849
ES	505997	2.3434	11.5446	2.3562	11.5898	2.3694	11.6583
FI	337529	0.9732	5.7886	0.9766	5.8135	0.9851	5.8734
FR	548901	4.5688	14.7931	4.5911	14.8558	4.6185	14.9437
HR	56547	2.3334	10.2782	2.3438	10.3093	2.3719	10.4051
HU	93020	3.4429	13.3701	3.4686	13.4282	3.4892	13.4856
CH	41289	5.3647	17.1116	5.3732	17.1360	5.3932	17.2002
IE	69949	2.4229	9.8557	2.4270	9.8721	2.4802	10.0195
IS	102689	0.1908	2.9850	0.1928	3.0081	0.1957	3.0499
IT	300622	5.4679	17.0507	5.4789	17.0766	5.5079	17.1547
KS	10910	2.8068	10.9562	2.9127	11.2869	2.9686	11.4263
LI	161	8.0945	20.1058	8.0962	20.1107	8.1337	20.1797
LT	64893	1.8387	8.2075	1.8457	8.2378	1.8504	8.2705
LU	2594	7.7074	20.1575	7.7298	20.2052	7.7854	20.3458
LV	64578	1.3734	6.4501	1.3819	6.5014	1.3842	6.5230
ME	13877	0.8787	6.4665	0.8790	6.4679	0.8873	6.5244
MK	25442	1.4071	8.9761	1.4204	9.0176	1.4285	9.0579
MT	321	22.3272	33.7354	22.3347	33.7368	23.1904	34.3593
NL	37407	12.0064	25.3709	12.0278	25.4010	12.1695	25.6341
NO	323388	0.6916	5.3553	0.6952	5.3847	0.7037	5.4618
PL	311940	3.1965	11.9617	3.2432	12.0912	3.2664	12.1645
PT	91885	4.0540	13.9876	4.0836	14.0659	4.1058	14.1578
RO	238367	2.0600	10.1107	2.0793	10.1661	2.0922	10.2114
RS	77477	2.3754	11.0669	2.3923	11.1168	2.4082	11.1658
SE	449675	0.9393	6.2649	0.9418	6.2831	0.9514	6.3497
SI	20273	3.3909	11.8910	3.3932	11.8985	3.4270	11.9833
SK	49023	3.1274	12.8424	3.1532	12.9071	3.1728	12.9625
TR	780121	1.3029	8.4890	1.3463	8.6914	1.3629	8.7814
UK	244661	6.0605	18.9822	6.0749	19.0142	6.0985	19.0749

Appendix B: Upper half: 18 regions with the highest relative increase in areas with IMD > 30% between 2012 and 2018 at the NUTS3 level. Lower half: 18 regions with the highest relative decrease in areas with IMD > 30% between 2012 and 2018 at the NUTS3 level.

NUTS3 CODE	NUTS3 NAME	2012 abs (km^2)	2012 rel (%)	2015 abs (km^2)	2015 rel (%)	2018 abs (km^2)	2018 rel (%)
RS226	Pirotska oblast	25.850	100	28.250	109.284	30.540	118.143
TR821	Kastamonu	72.150	100	80.990	112.252	84.400	116.979
TR721	Kayseri	229.720	100	252.410	109.877	259.500	112.964
TR211	Tekirdağ	192.510	100	206.010	107.013	213.680	110.997
TR522	Karaman	56.520	100	60.290	106.670	62.390	110.386
TR831	Samsun	145.780	100	154.940	106.283	160.260	109.933
TR711	Kırıkkale	58.830	100	63.900	108.618	64.620	109.842
TR823	Sinop	28.430	100	30.420	107.000	31.200	109.743
TRC21	Şanlıurfa	273.030	100	299.400	109.658	299.450	109.677
PL823	Rzeszowski	192.470	100	204.480	106.240	210.630	109.435
PL814	Lubelski	171.060	100	181.610	106.167	187.190	109.429
TR834	Amasya	81.640	100	85.120	104.263	89.250	109.321
TR812	Karabük	40.230	100	42.570	105.817	43.880	109.073
PL619	Włocławski	91.720	100	100.090	109.126	100.040	109.071
TR715	Kırşehir	52.640	100	55.950	106.288	57.410	109.062
TR902	Ordu	53.210	100	54.320	102.086	57.950	108.908
TRB24	Hakkari	21.990	100	23.260	105.775	23.940	108.868
ES704	Fuerteventura	39.670	100	43.150	108.772	43.150	108.772
ES640	Melilla	8.710	100	8.710	100.000	8.660	99.426
ES706	La Gomera	5.410	100	5.400	99.815	5.390	99.630
ITI34	Ascoli Piceno	57.140	100	57.160	100.035	57.000	99.755
ITF12	Teramo	102.340	100	102.470	100.127	102.120	99.785
ES414	Palencia	122.750	100	122.960	100.171	122.500	99.796
DE24D	Wunsiedel i. Fich.	40.800	100	40.800	100.000	40.730	99.828
ITF13	Pescara	75.350	100	75.400	100.066	75.240	99.854
ITF35	Salerno	395.850	100	396.710	100.217	395.320	99.866
DE125	Heidelberg. Stadtkreis	30.340	100	30.340	100.000	30.310	99.901
DE231	Amberg. Kr. Stadt	15.430	100	15.430	100.000	15.420	99.935
UKI32	Westminster	17.690	100	17.690	100.000	17.680	99.943
ITF14	Chieti	129.440	100	129.550	100.085	129.370	99.946
AT334	Tiroler Oberland	56.480	100	56.490	100.018	56.450	99.947
UKJ41	Medway	60.180	100	60.180	100.000	60.150	99.950
UKJ46	West Kent	101.060	100	101.060	100.000	101.010	99.951
EL633	Ηλεία	68.290	100	68.320	100.044	68.260	99.956
UKL12	Gwynedd	46.980	100	46.980	100.000	46.960	99.957
CH012	Valais	165.250	100	165.440	100.115	165.180	99.958

Appendix C: Upper half: 18 regions with the highest relative increase in the length of roads (summarized by classes 0, 1, 2, 3 and 4) between 2015 and 2018 at the NUTS3 level. Lower half: 18 regions with the highest relative decrease in the length of roads (summarized by classes 0, 1, 2, 3 and 4) between 2015 and 2018 at the NUTS3 level.

		2015		2018	
NUTS3 CODE	NUTS3 NAME	abs (km)	rel (%)	abs (km)	rel (%)
MK006	Pološki	401.979	100	806.282	200.578
MK003	Jugozapaden	564.455	100	1090.517	193.198
MK007	Severoistočen	338.910	100	624.461	184.255
MK002	Istočen	473.369	100	870.260	183.844
MK005	Pelagoniski	724.910	100	1225.305	169.029
TR904	Rize	1439.001	100	2125.421	147.701
TR906	Gümüşhane	2116.103	100	3056.692	144.449
MK008	Skopski	567.510	100	799.155	140.818
TR905	Artvin	1967.859	100	2680.423	136.210
TRA12	Erzincan	3086.918	100	4185.504	135.588
MK001	Vardarski	702.154	100	939.907	133.861
RS226	Pirotska oblast	384.855	100	511.146	132.815
TR903	Giresun	4145.793	100	5352.963	129.118
TRB11	Malatya	4618.971	100	5699.117	123.385
MK004	Jugoistočen	624.132	100	753.245	120.687
TRB13	Bingöl	2483.438	100	2972.480	119.692
KS	Kosovo	2068.117	100	2456.095	118.760
TRC32	Batman	2019.135	100	2377.318	117.739

AL034	Korçë	1499.924	100	891.754	59.453
AL033	Gjirokastër	1173.170	100	718.004	61.202
AL015	Shkodër	1181.765	100	841.640	71.219
AL021	Elbasan	1216.615	100	881.263	72.436
AL032	Fier	1091.284	100	826.834	75.767
AL035	Vlorë	1286.354	100	1031.024	80.151
AL031	Berat	828.456	100	680.766	82.173
AL011	Dibër	1035.133	100	860.807	83.159
AL014	Lezhë	1037.470	100	863.485	83.230
AL013	Kukës	962.278	100	834.877	86.760
SI033	Koroška	801.615	100	727.606	90.767
BG413	Благоевград	1951.346	100	1795.614	92.019
HR021	Bjelovarsko-b. ž.	1131.563	100	1051.640	92.937
AL022	Tiranë	712.690	100	667.141	93.609
AL012	Durrës	548.110	100	515.386	94.030
DE213	RKreisfreie Stadt	48.755	100	45.902	94.149
HR028	Sisačko-mos. žup.	1798.415	100	1705.158	94.815
HR026	Vukovarsko-s. ž.	902.778	100	862.051	95.489

Appendix D: Summary statistics of length (km) of all road classes (nw) according to TomTom 2012 in EEA38+UK. Used classes are motorways (0), major roads (1), other major r. (2), secondary (3) and tertiary roads (4).

NUTS0	-1	0	1	2	3	4	5	6	7	8
AL	0.0	0.0	291.6	398.3	189.7	59.5	6.4	0.0	3.0	3.5
AT	43.4	4087.1	1615.0	7646.2	6340.6	35786.8	1453.8	17208.6	138981.8	1276.3
BA	0.0	39.8	478.6	849.0	11.5	48.7	0.0	0.7	89.2	5.1
BE	18.4	3662.5	1927.8	5341.7	6613.5	17737.1	2432.6	33655.2	43538.8	1479.6
BG	0.0	1043.9	2877.5	4376.9	11598.2	20799.6	270.6	1730.0	21762.3	198.3
CY	0.0	0.0	0.0	0.0	0.0	0.0	0.0	0.0	0.0	0.0
CZ	2.0	1500.0	3474.6	6825.5	13060.3	33817.5	802.5	2676.7	71263.5	22221.7
DE	646.8	27032.7	48988.0	22549.1	66472.4	177625.9	5259.5	59830.7	803507.9	74056.1
DK	58.3	2511.5	193.0	2574.1	5958.6	9483.3	1279.0	24554.6	70952.2	1751.7
EE	0.0	0.0	715.6	1578.5	2494.7	12451.5	1426.4	924.1	57941.1	417.6
EL	0.0	3009.7	1258.5	4626.2	6569.2	65072.2	557.3	7111.2	141318.3	358.9
ES	1610.5	26630.0	2640.8	15344.1	40501.0	156252.8	10493.4	46607.7	753943.8	2996.3
FI	1.8	1605.1	4057.9	9561.5	14222.8	50051.6	4382.8	27633.1	305466.7	2921.4
FR	755.8	23446.8	31323.2	45568.6	95355.4	261783.4	8164.5	255173.3	820278.9	7631.6
HR	0.2	2233.9	548.2	1998.3	5403.6	18699.0	372.3	720.8	112467.5	1913.5
HU	0.3	2302.8	1163.6	4332.9	3437.8	21233.8	3577.1	3332.6	72451.9	1936.6
CH	119.1	3189.4	808.2	4925.6	3034.9	17933.0	486.7	7193.7	60855.6	4391.1
IE	0.4	1795.7	1894.9	3167.1	811.5	12134.1	8013.7	13622.4	61731.5	295.9
IS	0.0	0.0	0.0	0.0	0.0	0.0	0.0	0.0	0.0	0.0
IT	944.8	14169.6	9446.1	16114.8	29064.0	143107.9	11233.4	132495.7	613602.2	7475.5
KS	0.0	0.0	161.4	0.0	0.0	0.0	0.0	0.0	0.0	0.3
LI	0.6	0.0	7.0	25.2	0.0	62.7	0.0	41.6	301.1	4.4
LT	0.0	636.8	1456.8	574.8	5169.2	16086.2	1021.6	1102.2	45115.1	184.7
LU	5.3	302.3	207.1	232.0	539.4	2162.5	69.6	796.0	5193.5	102.5
LV	3.6	0.0	1398.4	673.7	5748.8	12760.3	1455.2	1246.6	57655.0	125.6
ME	0.0	0.0	165.2	313.2	0.0	29.2	0.0	2.5	13.7	1.2
MK	0.0	508.8	230.0	242.3	3.1	0.0	0.0	1.9	1.7	2.3
MT	0.2	0.0	0.0	111.2	208.9	363.2	45.4	227.7	2596.9	1.4
NL	1.5	5391.2	477.1	5379.3	7699.5	19705.9	4794.5	44481.8	62270.8	8013.2
NO	8.9	810.9	6108.6	10305.2	11374.7	24316.6	370.5	6400.9	159742.6	294.1
PL	113.9	3222.0	10885.2	11362.0	28475.4	96409.1	21292.6	8815.4	335724.5	817.6
PT	26.9	5639.6	83.8	4870.7	8990.0	43870.3	3605.6	12245.6	174117.9	475.6
RO	0.0	939.3	6467.8	5223.8	2991.9	1804.5	209.9	913.7	26850.6	49.7
RS	0.0	945.6	892.9	267.4	7.5	7.3	30.5	46.1	35.9	5.1
SE	69.8	4191.6	4690.2	13017.0	13849.5	41611.6	2540.2	42076.7	459285.2	6541.3
SI	0.0	1133.6	495.4	1958.0	2741.2	10568.1	193.1	572.0	86870.7	954.1
SK	0.0	822.5	1346.5	2845.1	3652.1	10361.8	854.3	1004.8	44867.8	15071.3
TR	10.2	3795.5	15268.8	17901.2	24737.3	234518.1	9974.4	19818.6	152650.2	3192.0
UK	24.8	7445.5	9647.2	20619.8	30358.1	34742.9	76368.4	68657.7	329160.7	8908.5
SUM	4467.5	154045.8	173692.6	253700.5	457686.2	1603458.2	183037.9	842922.9	6092610.3	176075.6

Appendix E: Summary statistics of length (km) of all road classes (nw) according to TomTom 2015 in EEA38+UK. Used classes are motorways (0), major roads (1), other major r. (2), secondary (3) and tertiary roads (4).

NUTS0	-1	0	1	2	3	4	5	6	7	8
AL	3.2	176.7	576.3	644.6	2092.4	8985.2	151.7	1575.7	32234.6	54.7
AT	42.2	4131.2	1601.3	7710.6	6397.1	35815.8	1463.0	17223.5	141361.5	1753.2
BA	0.0	234.9	821.9	2946.2	813.6	4393.4	145.8	216.1	43937.5	72.8
BE	18.3	3672.7	1093.7	6286.7	6621.9	17775.4	2469.9	33359.3	45282.1	1633.4
BG	0.0	1392.2	2854.2	4474.9	11281.4	20488.0	324.7	1770.7	40914.9	227.6
CY	2.1	487.8	0.0	1052.5	714.5	3488.7	314.6	904.4	29163.9	124.4
CZ	2.0	1548.8	3426.2	6959.6	13078.1	33963.6	821.0	2810.1	81335.3	23671.1
DE	642.4	27287.4	48665.0	23144.8	67137.5	176689.3	5251.5	59446.7	812813.4	78320.8
DK	64.8	2569.2	178.3	2514.6	6076.6	9519.2	1266.3	24516.7	74879.5	7279.7
EE	0.0	0.0	726.5	1616.7	2518.4	12408.3	1482.0	947.8	58156.6	488.4
EL	31.4	3250.4	1165.5	4698.0	6607.9	64408.9	867.1	7726.0	142943.8	366.7
ES	1637.4	27768.3	2493.1	14959.2	41495.4	156694.2	10667.7	46961.3	762220.0	3746.8
FI	1.7	1744.9	4029.5	9592.0	14304.2	50065.7	4402.0	27518.5	307837.8	4719.8
FR	776.4	23605.9	31483.1	45755.9	95593.0	261712.3	8195.0	254477.3	836804.6	14121.7
HR	0.2	2448.8	475.5	2699.7	5027.0	17206.8	540.6	804.5	116552.9	5552.1
HU	0.3	2379.4	1238.7	4415.1	3459.8	21373.5	3376.3	3585.6	78154.2	2828.0
CH	119.2	3246.0	779.4	4958.6	3044.0	17798.3	488.8	7178.4	66198.8	6669.2
IE	0.4	1835.8	1877.7	3161.3	866.6	12321.5	7910.8	13600.1	71724.1	345.6
IS	0.0	0.0	1381.3	2600.9	581.0	2724.5	34.5	408.5	24755.5	1.4
IT	944.8	14648.4	9497.6	16379.9	29542.7	142132.3	11388.8	131530.0	623380.0	8091.8
KS	0.0	147.2	271.2	400.2	450.7	798.7	59.1	24.1	20622.8	3.1
LI	0.6	0.0	7.0	25.2	0.0	63.8	0.0	41.6	328.9	9.6
LT	0.0	636.7	1502.6	587.8	5202.4	16095.4	1045.2	1107.2	49201.0	216.0
LU	5.3	319.5	186.7	256.2	542.0	2164.8	65.1	800.1	5263.1	106.4
LV	3.7	0.0	1406.0	685.2	5785.5	12693.5	1537.2	1472.9	58658.7	183.0
ME	0.0	0.0	383.9	713.7	179.5	1003.9	95.0	8.7	6017.5	34.0
MK	0.0	507.4	251.1	659.5	1090.9	1862.7	273.6	465.2	45784.1	113.6
MT	0.2	0.0	0.0	104.3	159.8	328.0	45.8	228.2	2533.2	2.6
NL	1.4	5470.5	564.0	5441.1	7900.2	19742.3	4817.1	44133.1	67423.5	10137.4
NO	9.9	900.3	6166.1	10348.5	10702.4	25408.5	373.6	6370.0	164260.3	451.6
PL	113.3	3314.0	11307.3	11671.3	29310.9	96742.8	22744.3	9555.5	367627.6	859.1
PT	29.6	6065.4	85.5	4136.9	9900.7	44590.8	3773.1	12461.1	174156.7	489.4
RO	0.0	1446.9	6906.1	4903.9	4995.8	32468.7	648.8	2028.9	166337.0	5316.2
RS	0.0	1261.3	1264.5	3318.3	5423.4	7812.0	771.2	250.2	63835.4	419.9
SE	70.2	4411.3	4710.2	13424.7	13700.6	41765.7	2572.3	42002.1	483509.6	9840.7
SI	0.0	1130.8	502.8	1984.6	2714.5	10673.5	201.6	588.4	87100.9	957.9
SK	0.0	870.2	1339.2	2944.7	3660.1	10355.9	873.5	1060.9	49897.9	15064.0
TR	13.9	3957.0	16405.9	20420.1	30247.3	246568.0	14803.3	31128.2	279437.8	3526.8
UK	33.4	7479.3	9682.7	20743.8	30424.3	34809.5	76229.3	68080.0	340891.9	12150.1
SUM	4568.4	160346.7	177307.4	269341.8	479644.3	1675913.1	192491.0	858367.3	6823538.9	219950.4

Appendix F: Summary statistics of length (km) of all road classes (nw) according to TomTom 2018 in EEA38+UK. Used classes are motorways (0), major roads (1), other major r. (2), secondary (3) and tertiary roads (4).

NUTS0	-1	0	1	2	3	4	5	6	7	8
AL	3.2	204.8	591.6	540.0	1900.9	6322.4	194.5	1647.4	35095.2	103.0
AT	42.0	4183.8	1610.3	7792.4	6390.0	35853.8	1463.8	17221.8	180277.0	6784.8
BA	0.0	409.2	816.1	2939.2	2230.9	3999.2	515.4	459.2	72852.4	148.4
BE	18.0	3683.4	1055.0	6314.0	6814.0	17721.0	2447.2	33298.0	60886.0	5676.1
BG	0.0	1490.5	2774.8	4980.4	10486.9	20207.0	356.8	1811.6	71480.5	538.9
CY	2.1	487.6	0.0	1069.9	828.6	3396.6	375.6	916.3	28425.5	122.7
CZ	2.0	2634.8	2599.7	6951.2	13062.3	34039.4	835.7	2910.9	92056.3	29585.1
DE	638.8	27538.5	48417.4	23752.8	67574.2	176783.3	5233.1	59042.7	921660.1	87632.3
DK	65.2	2653.0	180.2	2512.6	6195.9	9487.1	1259.9	24513.6	95333.7	10188.1
EE	0.0	0.0	731.2	1635.3	2565.8	12338.4	1454.5	941.1	59248.5	869.2
EL	31.4	4406.6	892.8	5083.4	7846.2	62772.5	965.6	7937.7	145315.0	525.8
ES	1649.5	28100.2	2545.7	15103.5	41808.6	156893.3	10718.7	46962.4	1115060.4	15166.4
FI	1.7	1808.8	4059.7	9624.2	14406.8	50096.1	4390.0	27543.9	430632.4	8362.1
FR	776.7	23783.3	31498.0	45803.8	95956.1	261818.0	8238.9	254174.6	882201.3	16060.3
HR	0.2	2469.9	478.2	2753.7	5256.5	16444.7	610.7	907.3	117181.3	6885.7
HU	0.4	2484.4	1509.9	4364.9	3515.6	21500.9	3351.4	3628.3	80571.8	3485.9
CH	119.4	3350.9	719.9	5047.7	3056.4	17803.7	499.6	7161.0	71481.6	7916.3
IE	0.4	2003.9	1813.0	3286.0	853.8	12352.4	7924.8	13593.8	80297.1	938.3
IS	0.0	0.0	1409.6	2886.3	523.9	2701.0	25.4	359.5	25088.7	63.7
IT	941.1	14760.5	9589.3	16460.7	29922.3	142471.7	11460.7	130815.7	680492.3	15875.8
KS	0.0	244.4	287.1	419.3	483.4	1021.8	138.1	139.5	20362.0	6.9
LI	0.6	0.0	7.0	25.2	0.0	63.8	0.0	39.5	341.6	13.0
LT	0.0	627.6	1465.2	617.2	5232.7	16121.0	1037.6	1119.0	72556.7	849.3
LU	5.0	322.5	183.2	237.2	610.6	2123.0	67.0	799.0	5572.5	170.5
LV	3.7	0.0	1385.9	670.5	5754.3	12708.2	1548.3	1485.8	59459.8	1105.5
ME	0.0	0.0	383.2	705.8	181.3	1009.7	122.4	16.3	7484.6	37.2
MK	0.0	562.5	217.4	692.6	1220.1	4370.4	874.4	1052.7	35403.6	199.0
MT	0.2	0.0	0.0	122.0	151.6	325.0	56.3	227.8	2512.6	6.9
NL	1.4	5505.9	631.6	4887.1	8728.0	19880.1	4873.7	43922.8	74059.0	12184.3
NO	10.0	1004.3	6066.7	10397.9	10798.6	25459.8	374.7	6433.6	188471.5	1876.9
PL	112.9	3432.0	11950.2	11863.6	29969.1	96962.6	23134.3	9593.0	381737.0	4055.8
PT	29.7	6150.5	83.4	4143.3	9903.0	44869.4	3785.1	12467.8	176826.7	1943.2
RO	0.0	1569.6	6935.3	4932.9	5067.3	32667.3	767.5	2283.2	168158.5	5650.7
RS	0.0	1541.1	1216.0	3390.2	5467.9	7899.3	837.5	257.2	64232.8	418.1
SE	70.1	4442.5	4705.6	13590.7	13788.2	41837.2	2607.3	41953.9	509640.8	12036.2
SI	0.0	1157.6	489.1	1996.9	2703.1	10605.4	202.1	605.4	87102.8	1089.6
SK	0.0	974.2	1359.1	3002.9	3684.2	10371.1	894.5	1061.2	52630.2	18200.6
TR	13.8	5084.3	16338.3	22536.4	31580.4	262305.0	16464.3	34604.1	434906.7	4187.4
UK	33.4	7542.1	9926.2	20748.1	30541.1	34957.6	76315.6	68004.5	396585.6	17553.2
SUM	4573.1	166615.2	176922.8	273881.6	487060.3	1690560.2	196422.9	861913.1	7983682.4	298513.2

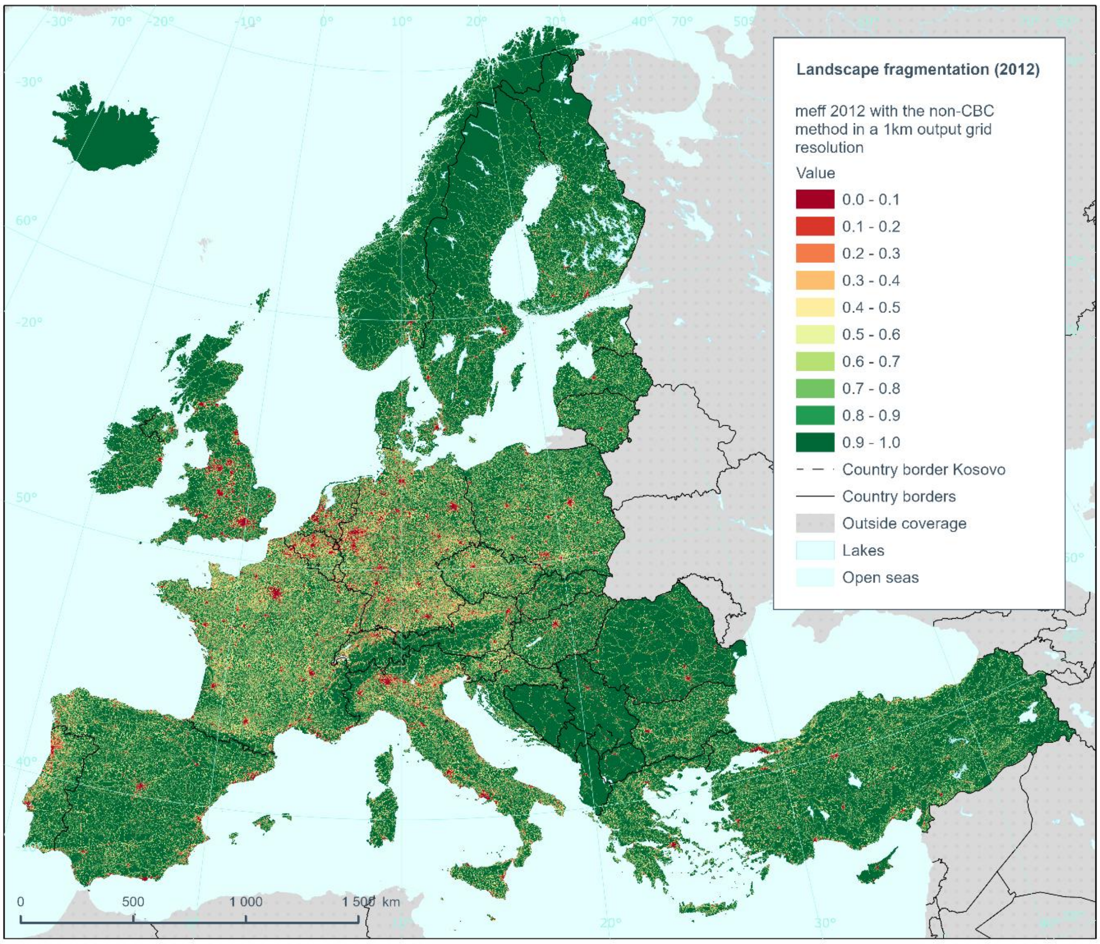

Reference data: © EuroGeographics, © FAO (UN), © TurkStat Source: European Commission – Eurostat/GISCO
Prepared by ETCLUSI (GISAT) 2023, based on TomTom MultiNet data (TomTom ©) and Imperviousness Density (raster 100m)

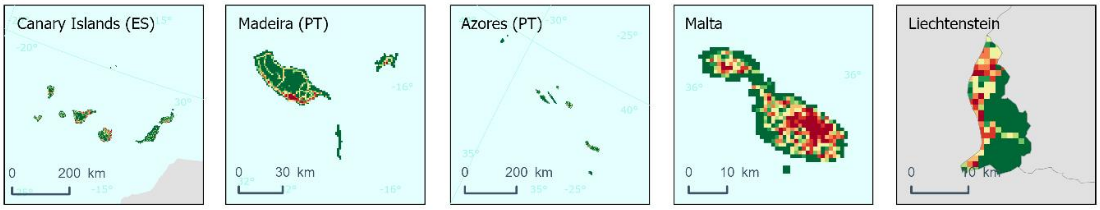

Appendix G: Landscape fragmentation represented by meff index in EEA38+UK in 2012.

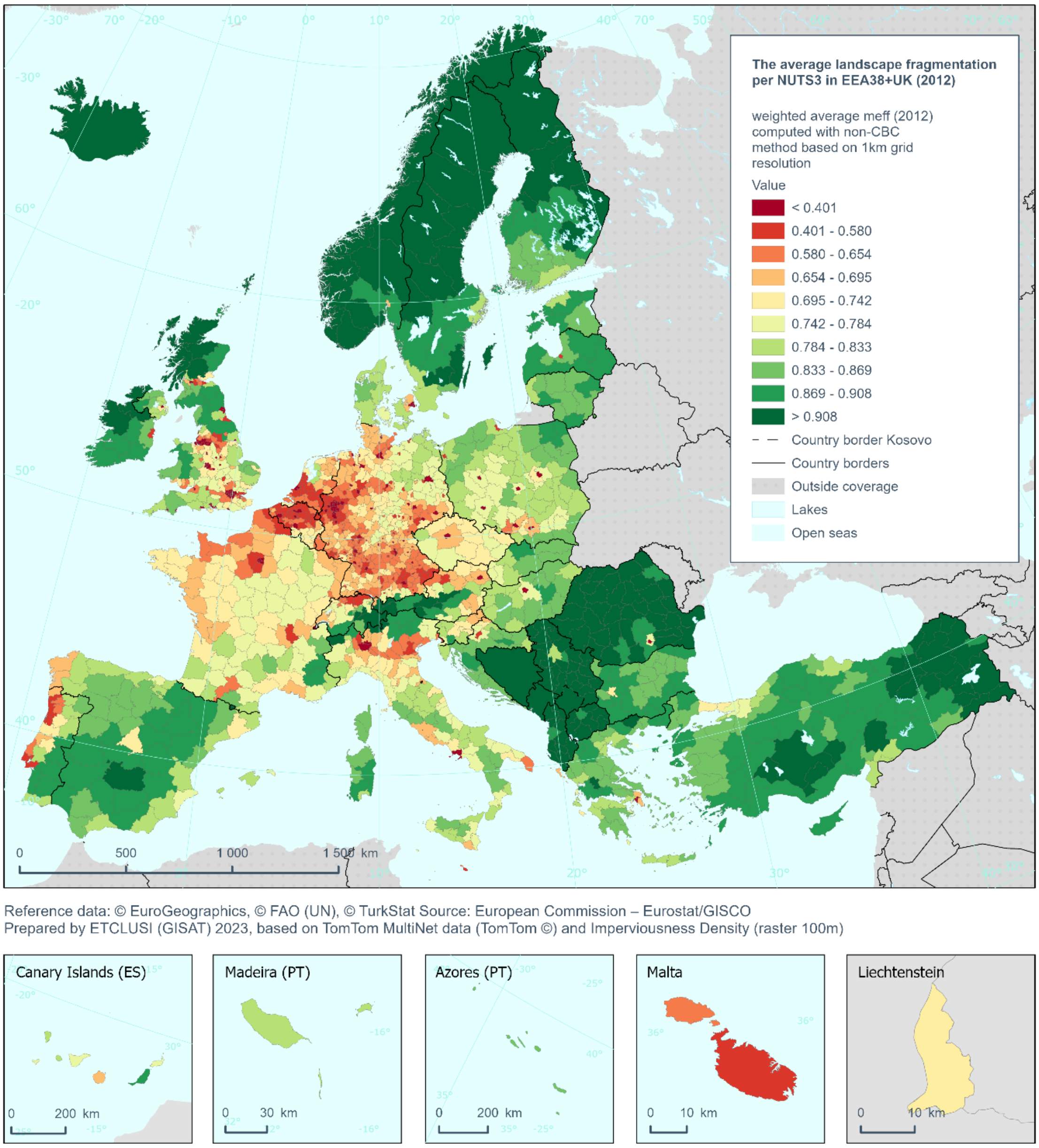

Reference data: © EuroGeographics, © FAO (UN), © TurkStat Source: European Commission – Eurostat/GISCO
Prepared by ETCLUSI (GISAT) 2023, based on TomTom MultiNet data (TomTom ©) and Imperviousness Density (raster 100m)

Appendix H: Average meff per NUTS3 in EEA38+UK in 2012. The map legend is classified according to the Quantile method to better distinguish the differences between individual regions and harmonised with other years.

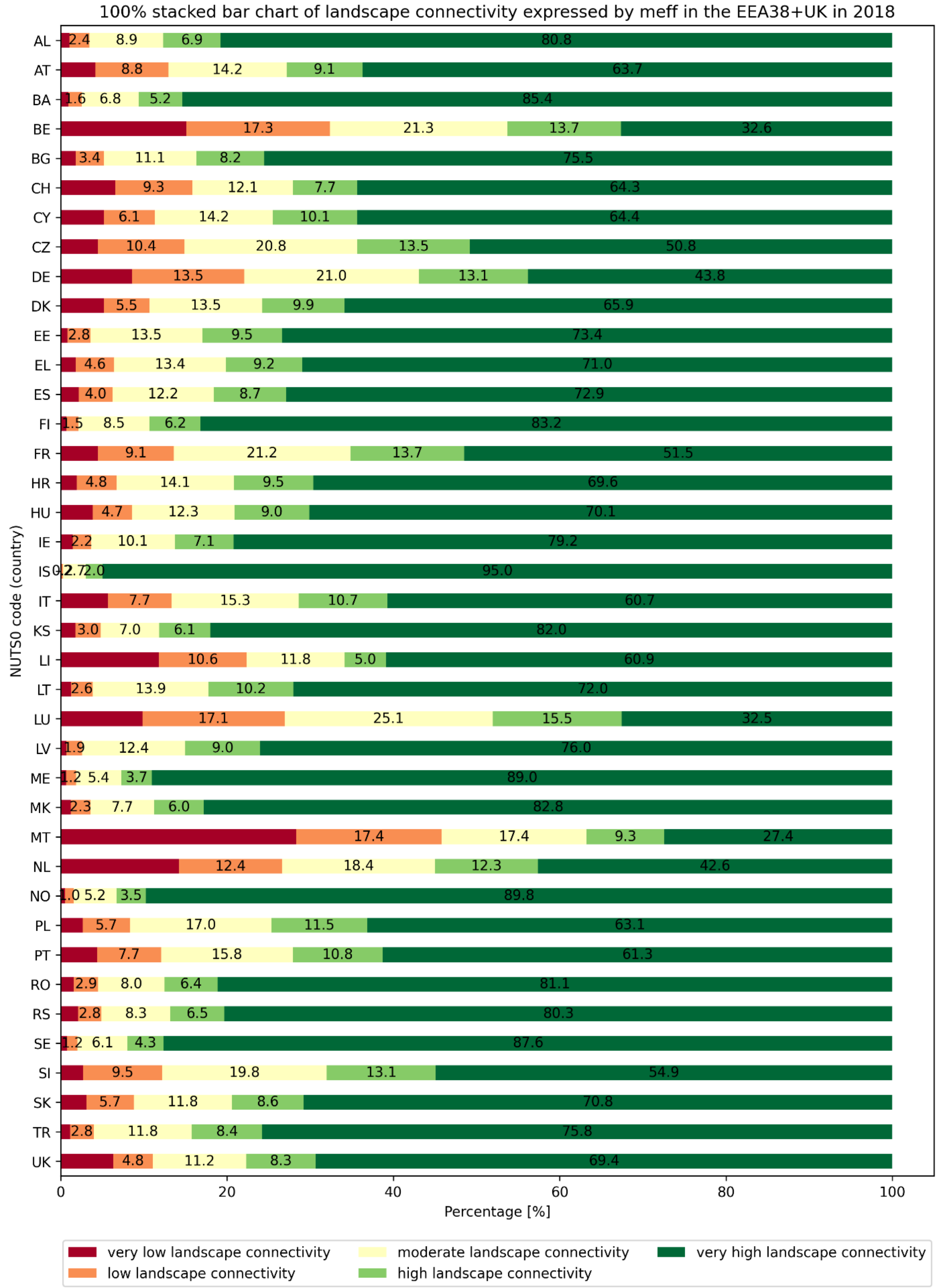

Appendix I: A 100% stacked bar chart shows landscape connectivity per EEA38+UK NUTS0 units expressed by meff indicator in 2018. Landscape connectivity is the opposite information to landscape fragmentation as high meff values indicate weak fragmentation and strong connectivity.

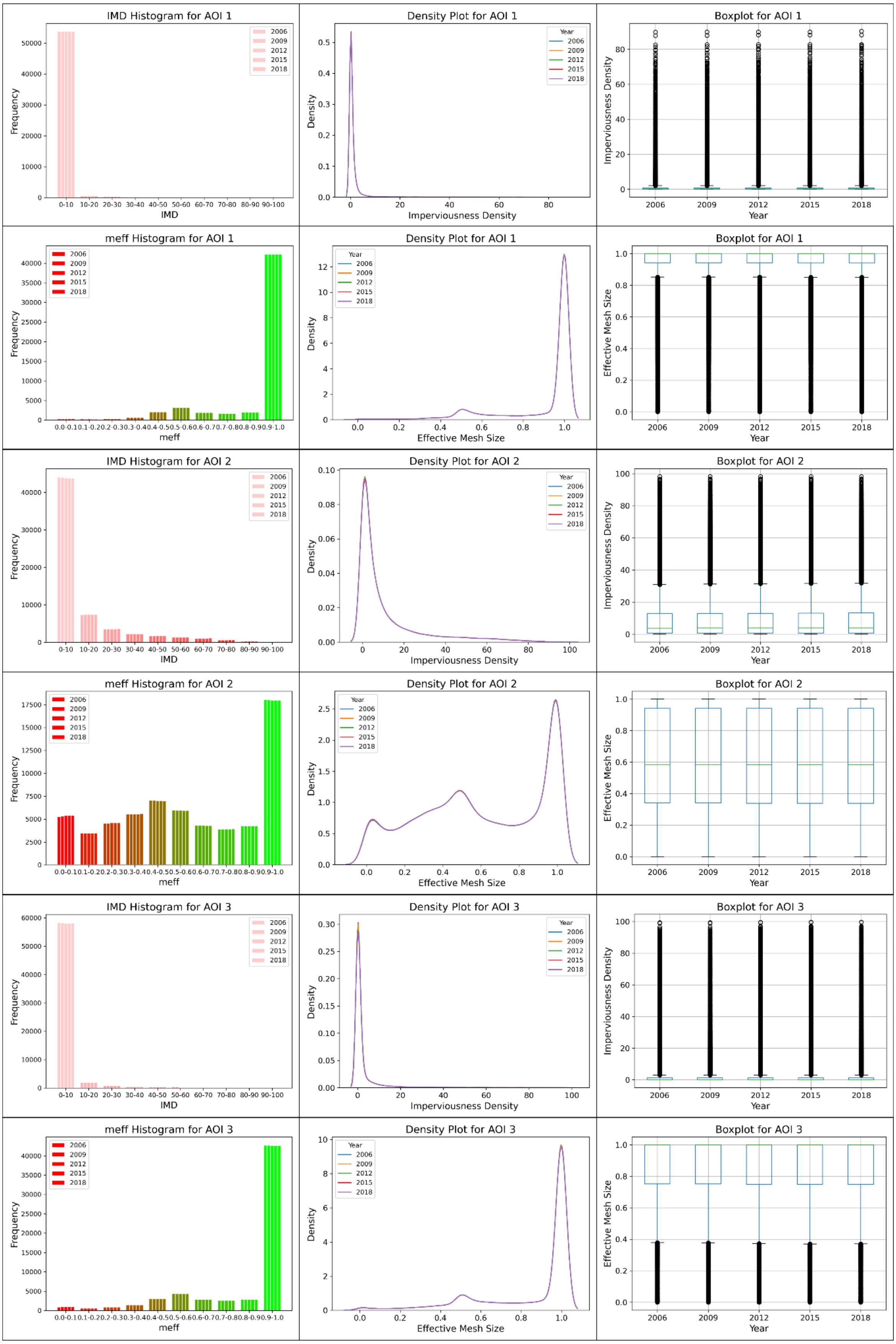

Appendix J: Statistical distribution of meff and IMD values within the test areas (AOI1 = South Sweden, AOI2 = West Germany, AOI3 = Central Spain).

Appendix K: Statistical distribution of meff and IMD values within three test areas for years 2006-2018. A consistent increase in IMD values while decrease in meff is found in all selected areas.

South Sweden	**AOI1**	**year**	**frequency**	**weighted avg**	**min**	**max**	**stdv**
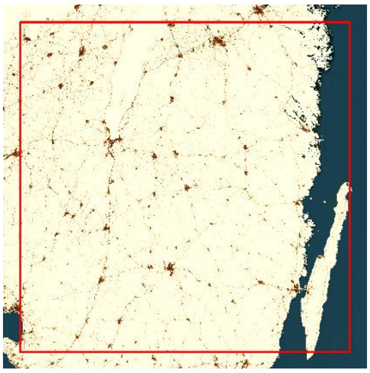	**output: meff 1km**	2006	55902	0.902309	0	1	0.194701
		2009	55902	0.902189	0	1	0.194883
		2012	55902	0.902046	0	1	0.195134
		2015	55902	0.901984	0	1	0.195237
		2018	55902	0.901980	0	1	0.195244
	input: IMD 100m	2006	5611977	1.232017	0	100	6.930034
		2009	5611977	1.239667	0	100	6.964166
		2012	5611977	1.249164	0	100	7.017672
		2015	5611977	1.253103	0	100	7.041481
		2018	5611977	1.263966	0	100	7.128372
West Germany	**AOI2**	**year**	**frequency**	**weighted avg**	**min**	**max**	**stdv**
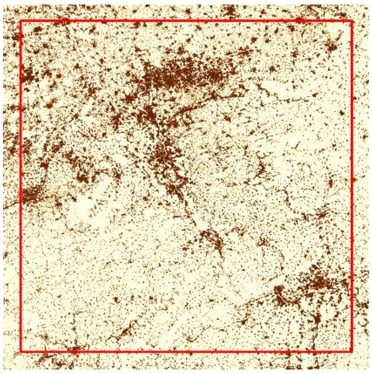	**output: meff 1km**	2006	62500	0.597954	0	1	0.322264
		2009	62500	0.597338	0	1	0.322479
		2012	62500	0.596535	0	1	0.322885
		2015	62500	0.596291	0	1	0.323027
		2018	62500	0.596108	0	1	0.323097
	input: IMD 100m	2006	6250000	10.908168	0	100	24.185731
		2009	6250000	10.976743	0	100	24.287197
		2012	6250000	11.073580	0	100	24.436494
		2015	6250000	11.102038	0	100	24.479884
		2018	6250000	11.167621	0	100	24.601376
Central Spain	**AOI3**	**year**	**frequency**	**weighted avg**	**min**	**max**	**stdv**
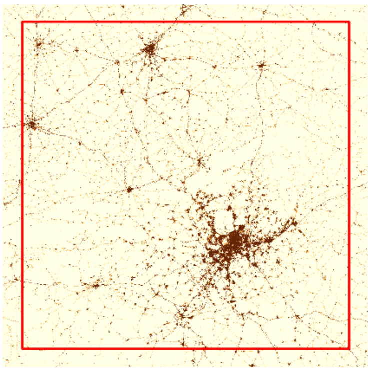	**output: meff 1km**	2006	62500	0.855727	0	1	0.237341
		2009	62500	0.855299	0	1	0.237926
		2012	62500	0.854315	0	1	0.239461
		2015	62500	0.854029	0	1	0.239882
		2018	62500	0.854061	0	1	0.239828
	input: IMD 100m	2006	6250000	2.712940	0	100	12.664190
		2009	6250000	2.746386	0	100	12.768146
		2012	6250000	2.843549	0	100	13.072586
		2015	6250000	2.869094	0	100	13.155627
		2018	6250000	2.879828	0	100	13.214830

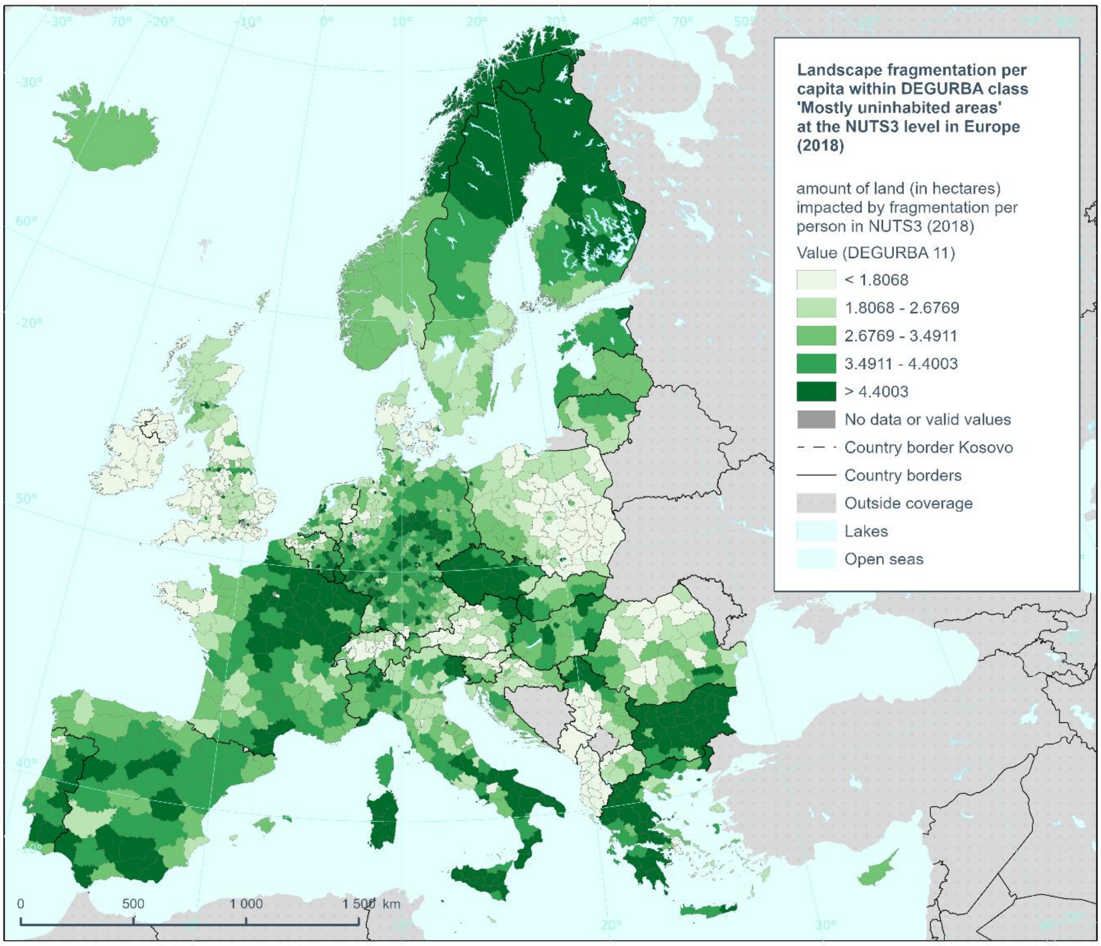

Reference data: © EuroGeographics, © FAO (UN), © TurkStat Source: European Commission – Eurostat/GISCO
Prepared by ETCLUSI (GISAT) 2023, based on TomTom MultiNet data (TomTom ©) and Imperviousness Density (raster 100m)

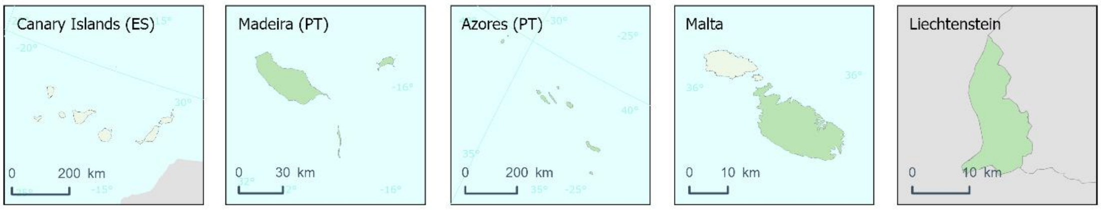

Appendix L: Average fragmentation per capita according to DEGURBA class 'Mostly uninhabited areas' in the NUTS3 across Europe (2018). Selected DEGURBA class might be missed in some regions. The map legend is classified according to the Quantile method to better distinguish the differences.

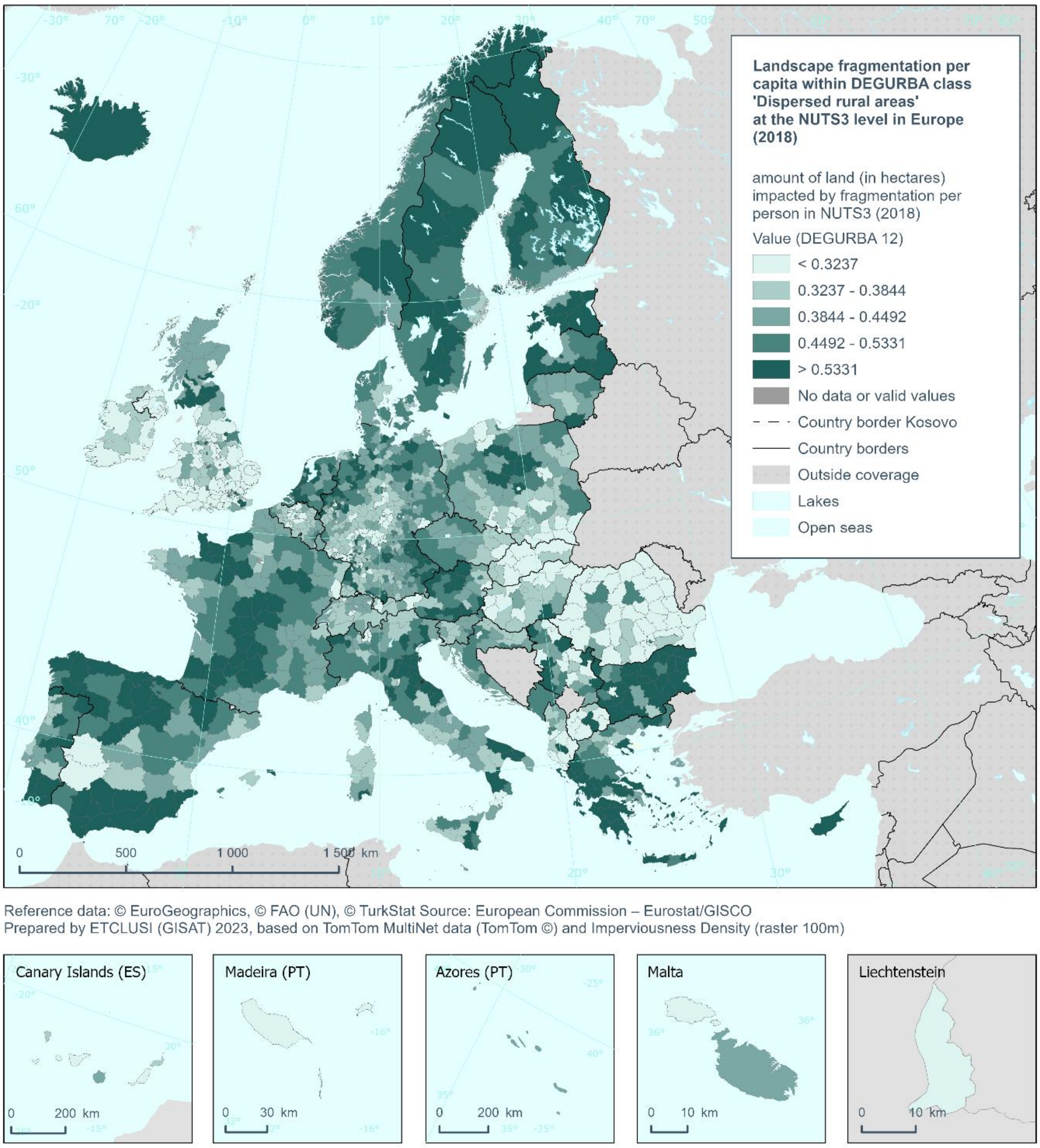

Appendix M: Average fragmentation per capita according to DEGURBA class 'Dispersed rural areas' in the NUTS3 across Europe (2018). Selected DEGURBA class might be missed in some regions. The map legend is classified according to the Quantile method to better distinguish the differences.

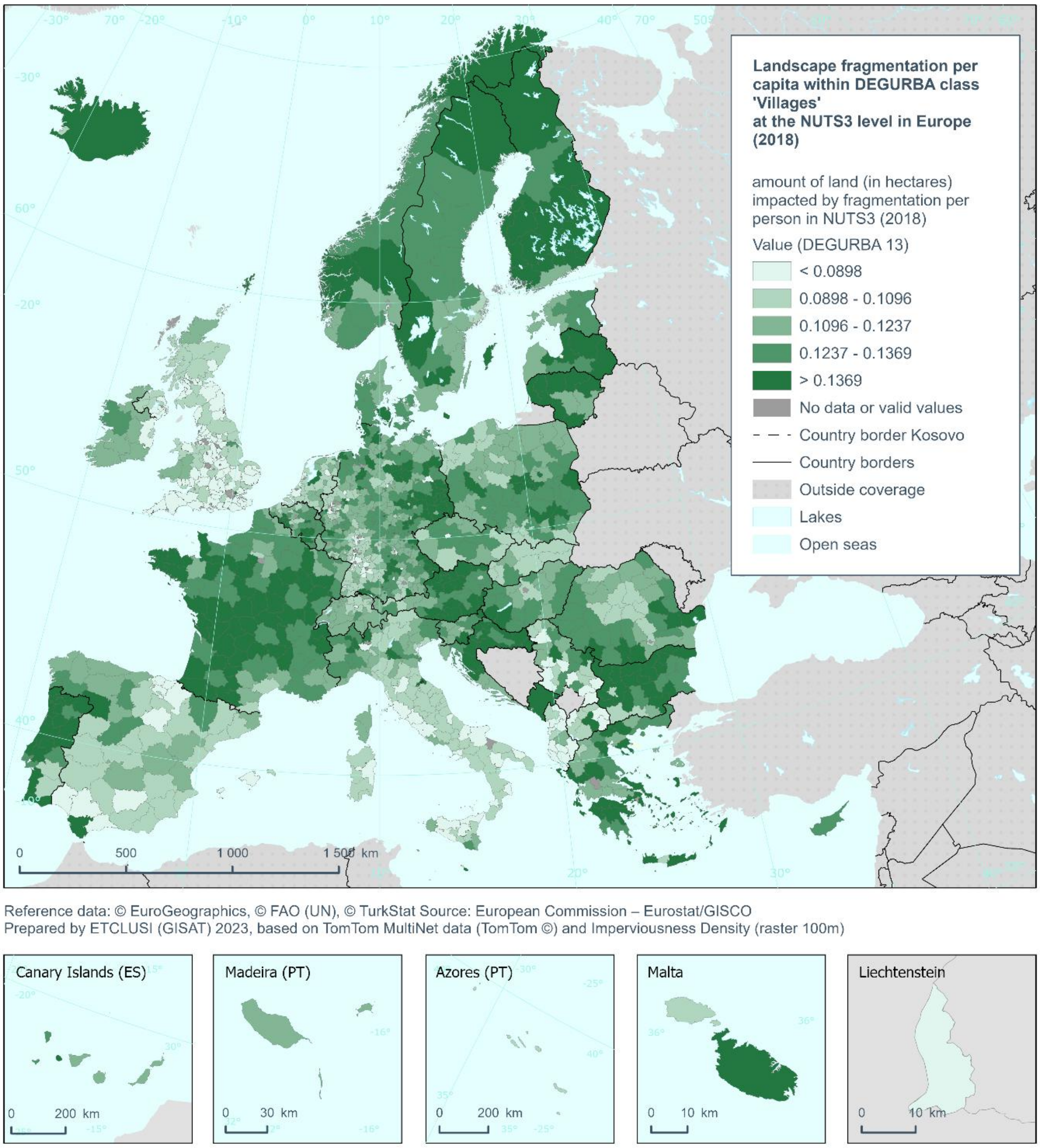

Reference data: © EuroGeographics, © FAO (UN), © TurkStat Source: European Commission – Eurostat/GISCO
Prepared by ETCLUSI (GISAT) 2023, based on TomTom MultiNet data (TomTom ©) and Imperviousness Density (raster 100m)

Appendix N: Average fragmentation per capita according to DEGURBA class 'Villages' in the NUTS3 across Europe (2018). Selected DEGURBA class might be missed in some regions. The map legend is classified according to the Quantile method to better distinguish the differences.

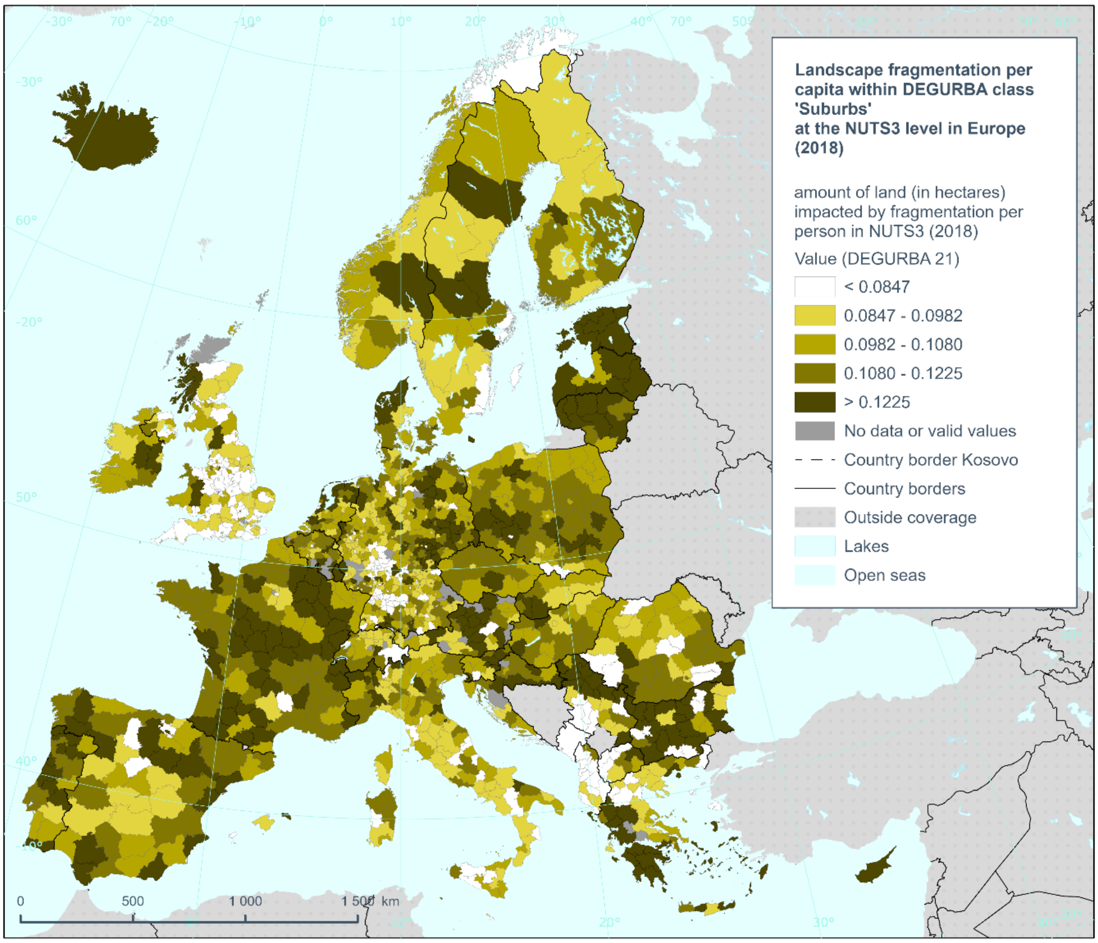

Reference data: © EuroGeographics, © FAO (UN), © TurkStat Source: European Commission – Eurostat/GISCO
Prepared by ETCLUSI (GISAT) 2023, based on TomTom MultiNet data (TomTom ©) and Imperviousness Density (raster 100m)

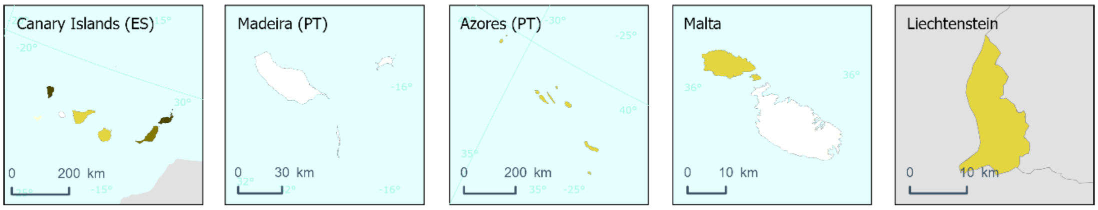

Appendix O: Average fragmentation per capita according to DEGURBA class 'Suburbs' in the NUTS3 across Europe (2018). Selected DEGURBA class might be missed in some regions. The map legend is classified according to the Quantile method to better distinguish the differences.

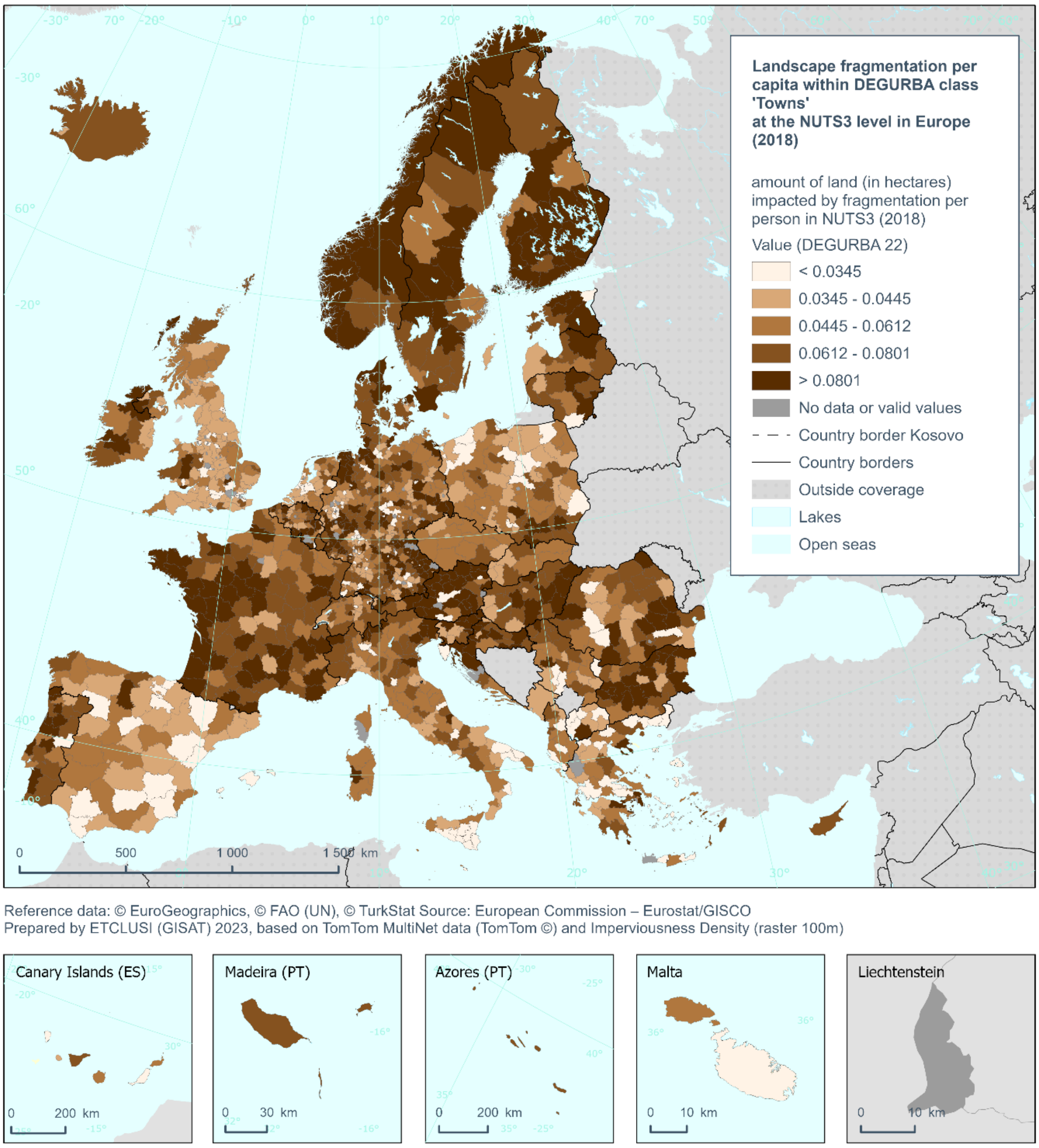

Appendix P: Average fragmentation per capita according to DEGURBA class 'Towns' in the NUTS3 across Europe (2018). Selected DEGURBA class might be missed in some regions. The map legend is classified according to the Quantile method to better distinguish the differences.

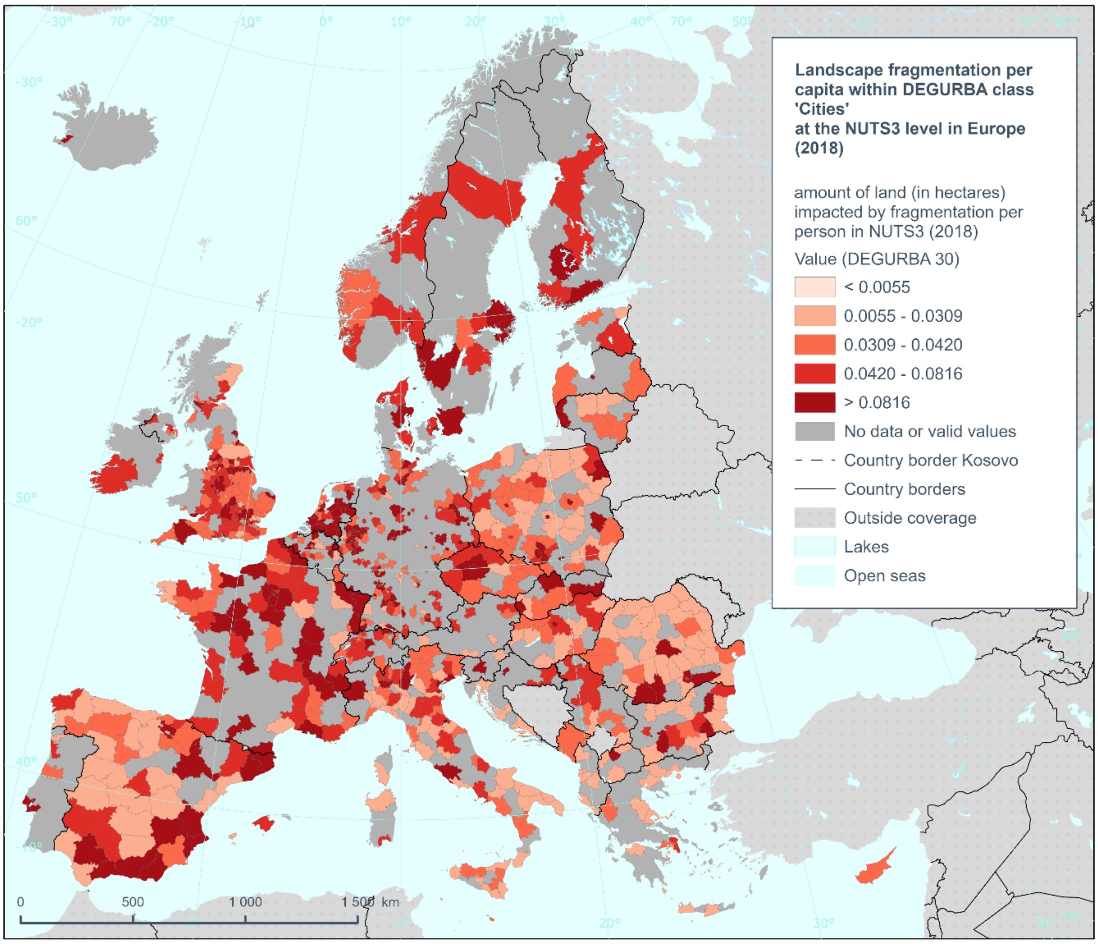

Reference data: © EuroGeographics, © FAO (UN), © TurkStat Source: European Commission – Eurostat/GISCO
Prepared by ETCLUSI (GISAT) 2023, based on TomTom MultiNet data (TomTom ©) and Imperviousness Density (raster 100m)

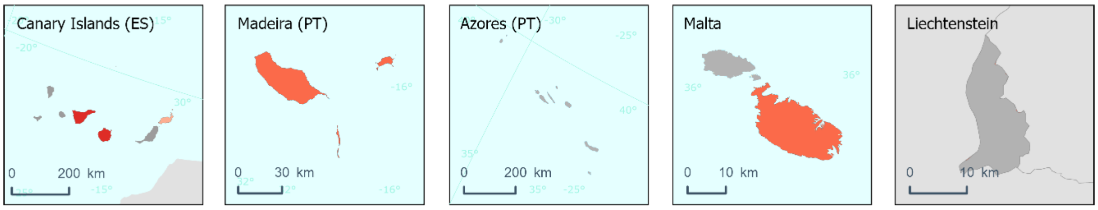

Appendix Q: Average fragmentation per capita according to DEGURBA class 'Cities' in the NUTS3 across Europe (2018). Selected DEGURBA class is missing in lot of regions. The map legend is classified according to the Quantile method to better distinguish the differences.

European Topic Centre on

Data integration and digitalisation

https://www.eionet.europa.eu/etcs/etc-di

The European Topic Centre on Data integration and digitalisation (ETC-DI) is a consortium of European institutes under contract of the European Environment Agency.

European Environment Agency
European Topic Centre
Data integration and digitalisation